2018-02-13

RUNX1 Is an Oncogenic Transcription Factor that Regulates MYB and MYC Enhancer Activity in T-ALL

AHyun Choi
University of Massachusetts Medical School

RUNX1 IS AN ONCOGENIC TRANSCRIPTION FACTOR THAT REGULATES MYB AND MYC ENHANCER ACTIVITY IN T-ALL

A Dissertation Presented

By

AHYUN CHOI

Submitted to the Faculties of the

University of Massachusetts Graduate School of Biomedical Sciences, Worcester
in partial fulfillment of the requirements for the degree of

DOCTOR OF PHILOSOPHY

FEBRUARY 13, 2018

CANCER BIOLOGY

RUNX1 IS AN ONCOGENIC TRANSCRIPTION FACTOR THAT REGULATES MYB AND MYC ENHANCER ACTIVITY IN T-ALL

A Dissertation Presented

By

AHYUN CHOI

This work was undertaken in the Graduate School of Biomedical Sciences

Cancer Biology

Under the mentorship of

Michelle Kelliher, Ph.D., Thesis Advisor

The signatures of the Dissertation Defense Committee signify completion and approval as to style and content of the Dissertation

_____

Lucio H. Castilla, Ph.D., Member of Committee

_____

Glen Raffel, MD., Ph.D., Member of Committee

_____

Thomas Fazzio, Ph.D., Member of Committee

_____

Alan B. Cantor, M.D., Ph.D., External Member of Committee

_____

Merav Socolovsky, MBBS., Ph.D., Chair of Committee

_____

Anthony Carruthers, Ph.D.,

Dean of the Graduate School of Biomedical Sciences

February 13, 2018

ACKNOWLEDGEMENTS

These works could not be done without support and help from lots of people. First of all, I would like to thank my mentor, Dr. Michelle Kelliher, for her support and guidance. I have learned from her a way of thinking and handling the science. I also thank the lab member of the Kelliher lab, past and present, for their help and making the enjoyable lab life. Their advice and achievement have inspired me and kept me moving forward.

I appreciate the advice and support from my committees, Dr. Lucio Castilla, Dr. Merav Socolovsky, Dr. Glen Raffel, and Dr. Thomas Fazzio. Additionally, I thank Dr. Alan Cantor for serving as an external examiner of my dissertation defense. I also appreciate Dr. John Pulikkan in the Castilla's lab for his friendship and guidance.

I would like to thank my friends and family. Their support and advice help me going through this long journey. I also really enjoyed the adventures I have had with friends for years. Lastly, I cannot appreciate enough the understanding and support of my parents and husband, Hwanjong. They make me not to get lost, follow what I want, and smile every day.

Thank you.

ABSTRACT

RUNX1, a transcription factor required for hematopoiesis and lymphocyte differentiation, is one of the most commonly targeted genes in hematopoietic malignancies. Mutations in the *RUNX1* gene are associated with a poor prognosis in a subset of T cell acute lymphoblastic leukemia (T-ALL) and RUNX1 has been proposed as a tumor suppressor in TLX1/3-transformed human T-ALL. Recent ChIP-seq studies in human T-ALL cell lines demonstrated that a large portion of TAL1- and NOTCH1- bound regions contain RUNX binding sites in promoter or enhancer regions, suggesting oncogenic roles for RUNX1 in T-ALL. To interrogate RUNX1 functions in leukemogenesis, we depleted RUNX1 in a T-ALL mouse model and in human T-ALL cell lines. We found that RUNX1 is required for the maintenance of mouse T-ALL growth *in vivo* and the survival of human T-ALL cell lines *in vitro*. In addition, inhibition of the RUNX1 activity with a small molecule inhibitor impairs the growth of human T-ALL cell lines and primary patient samples. RUNX1 depletion reduces the expression of a subset of TAL1- and NOTCH1-regulated genes including the *MYB* and *MYC* oncogenes, respectively. We demonstrate that RUNX1 regulates transcription factor binding and acetylation of H3K27 at the *Myb* and *Myc* enhancer loci. These studies provide genetic and pharmacological evidences that RUNX1 supports T-ALL cell survival and suggest RUNX1 inhibitor as a therapeutic strategy in T-ALL treatment.

TABLE OF CONTENTS

List of Tables

List of Figures

Copyrighted Materials Produced by the Author

Some data and analysis in this thesis have been submitted as manuscripts not yet in print. All submitted data and analysis presented in this thesis were originally obtained and analyzed by the author. Final analysis included contributions from co-authors listed.

Chapter II and Chapter III have been published in

AHyun Choi, Anuradha Illendula, John A. Pulikkan, Justine E. Roderick, Jessica Tesell, Jun Yu, Nicole Hermance, Lihua Julie Zhu, Lucio H. Castilla, John H. Bushweller and Michelle A. Kelliher. RUNX1 is required for oncogenic *Myb* and *Myc* enhancer activity in T cell acute lymphoblastic *Blood* (2017) 12;130(15):1722-1733

Chapter I

Introduction

T cell acute lymphoblastic leukemia (T-ALL) is a disease of immature transformed lymphoid cells expressing T-cell linage markers. T-ALL accounts for about 20% of ALL cases and an estimated 6590 new cases of ALL were diagnosed in 2016 (American Cancer Society). Although intensive chemotherapy regimens have significantly improved outcomes of the patients, they often suffer from side effects of the therapies, such as learning disorder, cardiovascular impairment, and nervous system toxicity. Those patients who relapse have a poor prognosis, with less than 25% rate of survival (1,2). Therefore, understanding the molecular basis for T-ALL initiation and maintenance is fundamental for the development of improved treatment strategies. Since T-ALL is derived from abnormal T-cells, it is important to understand the normal process and molecular basis of hematopoiesis and T-cell development in comparison with T-ALL pathogenesis.

Hematopoiesis and T-cell development

Hematopoiesis is a hierarchical process that generates all of the cellular components of blood from more immature cells. Advances in research techniques have made it possible to stratify hematopoietic cell lineages and to study the roles of each cell type. By using flow cytometry, blood cell lineages have been grouped according to the expression of cell surface markers (3). The function of each lineage has been determined by reconstitution of mice with sorted cells and by *in vitro* colony forming assays. Recently, combined

transcriptome, epigenome, and proteome analyses at the single cell level have been employed in order to refine the understanding of hematopoietic progression (4). Murine hematopoiesis is the best understood system at this time and evidence suggests that human hematopoiesis is similar to that of mice.

All blood lineages arise from hematopoietic stem cells (HSCs) that reside in bone marrow medulla and have the ability to self-renew (5–7). HSCs consist of two populations that differ in their degree of self-renewal capacity and life span: long-term HSCs (LT-HSCs) and short-term HSCs (ST-HSCs) (6,8–10). LT-HSCs can divide without losing their self-renewal ability and can differentiate into any blood cell (6). LT-HSCs have been defined by a cell surface profile of $Lin^{-}Sca1^{+}c\text{-}Kit^{+}CD34^{-}Flt3^{-}$ (6,11,12) or alternatively by $CD150^{+}CD48^{-}CD224^{-}$ SLAM markers (13,14). ST-HSCs have limited self-renewal capacity but are still able to differentiate to all blood lineages. The immunophenotype of ST-HSCs is similar with LT-HSCs except increased expression of CD34 ($CD34^{hi}$). ST-HSCs differentiate into multipotent progenitor cells (MPPs), which have multilineage potential but are not able to self-renew. This population is distinguished from HSCs by expression of Flt3 ($Flt3^{hi}$) (11).

According to the classic model of hematopoiesis hierarchy, MPPs give rise to two populations that are restricted to myeloid progenitors (common myeloid progenitors [CMPs], $Lin^{-}IL\text{-}7R\alpha^{-}Sca\text{-}1^{-}c\text{-}Kit^{+}Fc\gamma R^{lo}CD34^{+}$) or lymphoid progenitors (common lymphoid progenitors [CLPs], $Lin^{-}IL\text{-}7R\alpha^{+}Thy\text{-}1^{-}Sca\text{-}1^{lo}c\text{-}Kit^{lo}$) (15,16).

CMPs then differentiate into granulocyte-macrophage progenitors (GMPs, Lin^-IL-$7R\alpha^-Sca\text{-}1^-c\text{-}Kit^+Fc\gamma R^{hi}CD34^+$) and megakaryocyte-erythrocyte progenitors (MEPs, Lin^-IL-$7R\alpha^-Sca\text{-}1^-c\text{-}Kit^+Fc\gamma R^{lo}CD34^-$) (15). GMPs finally give rise to monocytes, granulocytes, and dendritic cells while MEPs differentiate into erythrocytes and megakaryocytes. CLPs give rise to all lymphoid lineages including T-, B-, and natural killer (NK) cells (16,17).

Recently, a population of cells derived from ST-HSCs that sustains potential for lymphoid lineages as well as GMPs but not for erythrocyte and megakaryocyte lineages has been identifed (18,19). This population, named as lymphoid-primed multipotent progenitors (LMPPs) is the major progenitor cells migrating to the thymus and differentiate into T-cell lineages while losing potential for other lineages (20). The first progenitors seeded in the thymus are designated as early thymic progenitor cells (ETP; $Lin^-Sca1^+c\text{-}Kit^+CD24^{lo/+}CD25^-CD44^+$IL-$7R\alpha^{lo/-}$) that are found in double negative 1 (DN1; $CD4^-CD8^-CD25^-CD44^+$) fraction (21,22). Intrathymic signals, such as the NOTCH signal, instruct the progenitor cells to commit to T-cell lineages (20,23). Thymocytes physically travel through the thymus as they differentiate where they encounter various microenvironments and receive different signals from thymic stroma or epithelium cells of the thymus (24,25). DN1 cells give rise to DN2 cells that begin to express CD25 ($CD25^+CD44^+$). It has been demonstrated that DN2 cells can then be divided into two subgroups DN2a and DN2b, based on c-Kit expression; DN2b

cells that lose c-Kit expression are no longer able to differentiate into dendritic cells (26).

As DN2b cells transition to the DN3 stage ($CD25^+CD44^-$), where the thymocytes fully commit to the T-cell lineage and stop proliferating while simultaneously initiating rearrangement of *T-cell receptor (TCR)* β, δ, and γ gene loci, catalyzed by recombinase activating gene 1 (RAG1) and RAG2 (27). Rearranged TCRβ chains pair with the invariant pre-TCRα and CD3 molecules to form pre-TCR complexes on the cell surface (28). Only thymocytes that successfully rearrange the *TCR*β gene and produce the functional pre-TCR undergo β-selection and receive signals to proliferate and differentiate into DN4 cells, to initiate the *TCR*α gene rearrangement, and to express CD4 and CD8 molecules (29). If DN3 cells successfully rearrange the *TCR*δ or *TCR*γ gene instead of β gene, these cells are selected as $\gamma\delta$ T-cells (30). Thymocytes will undergo apoptosis if they fail to rearrange one of these loci. According to CD27 expression, cell size, and the completion of β-selection, the DN3 population can also be subtyped into DN3a and DN3b (before and after the β-selection, respectively) (29,31).

Thymocytes that survive β-selection give rise to immature single positive CD8 cells (ISP $CD8^+$), and subsequently to $CD4^+CD8^+$ double positive (DP) cells that acquire cell surface TCR$\alpha\beta$ complexes. Then they undergo both positive and

negative selection to become either mature $CD4^+$ or $CD8^+$ single positive cells and leave thymus to enter the circulation (32).

RUNX1 regulates hematopoiesis

The RUNX proteins, Runt-related transcription factors, are DNA-binding α subunits of the heterodimeric transcriptional complex core binding factor (CBF) which regulates various developmental processes including cell proliferation, differentiation, apoptosis, and lineage specification (33). In mammals, there are three RUNX gene family members of: RUNX1, RUNX2, and RUNX3. The RUNX genes share a highly-conserved DNA binding RUNT-homology domain (RHD), transactivation domain (TAD), and a C-terminal VWRPY motif, which is required for the interaction with the co-repressor Groucho (also known as TLE1 (transducing-like enhancer split) in mammals) (Figure 1.2) (34). All three *RUNX* genes are expressed from two alternative promoters (distal P1 and proximal P2) encoding isoforms with distinct N-terminal sequences (33). The formation of heterodimers with CBF subunit β (CBFβ) increases the binding affinity of RUNX proteins to DNA binding motif 5'-PuACCPuCA-3' and also increases the stability of the complexes (35,36). RUNX proteins bind with diverse types of proteins including co-activators and co-repressors, thus functioning as both activators and repressors of transcription (37–39). They have also been reported to interact with several chromatin modifiers, such as polycomb repressive complex1 (PRC1) (40), histone deacetylases (HDACs) (41), H3K4 methyltransferase mixed lineage

leukemia (MLL) (42), and SWI/SNF chromatin remodeling complex (43). The activity and stability of the RUNX proteins are modulated at the post-translational level by phosphorylation and acetylation (44–47).

The different RUNX family proteins have divergent roles in the development process, which was demonstrated using mouse knock out models. The RUNX1-null mouse is embryonic lethal at E11.5-12.5 due to central nervous system hemorrhage and fetal liver anemia (48,49). The RUNX2-deficient mouse presents with major defects in osteoblast development resulting in postnatal lethality (50,51). Abnormal thymopoiesis, neurogenesis, and gastric epithelial hyperplasia were reported in RUNX3-deficient mice (52–55). These different diverse phenotypes are due to the distinct tissue specific expression patterns of each gene. Hematopoiesis can be rescued by the knock-in of chimeric genes expressing the *Runx1* N-terminus with the C-terminus of *Runx2* or *Runx3* in *Runx1* deficient mice; this provides evidence of partial functional redundancy between RUNX proteins (34).

While RUNX1 is required for definitive embryonic hematopoiesis, it is dispensable for adult hematopoiesis, though significant defects in the lymphoid and megakaryocyte lineages were observed (56,57). Conditional deletion of *Runx1* using *Mx1-Cre* in adult mice demonstrated fully maintained, even expanded hematopoietic stem cells (HSC, $Lin^{-}Sca\text{-}1^{+}c\text{-}Kit^{+}$ population) in BM (56–58). BM cells from the *Runx1* targeted mice reconstituted all hematopoietic

lineages when transplanted into irradiated recipient mice (56,57). However, the effects of *Runx1* deficiency on the long-term repopulation capability are still controversial. Ichikawa *et al*. (56) demonstrated increased frequency of LT-HSCs in *Runx1* deleted bone marrow cells while Growney *et al.* (57) and *Cai et al.* (58) showed decreased or unchanged number of LT-HSCs upon *Runx1* deletion, depending on which cells were used to assess the repopulation. Whether these discrepancies can be explained by differences in experimental methods or deletion strategies, remains to be elucidated.

The numbers of red blood cells and neutrophils in the peripheral blood of *Runx1* deleted adult mice were normal, suggesting that the development of erythrocytes and granulocytes does not require RUNX1 activity (56,57). In contrast, remarkably reduced platelet counts were observed in the peripheral blood of *Runx1*-deficient mice, due to defective megakaryocyte maturation (56,57). This appears to be correlated with the expression pattern of *Runx1*, which is maintained during megakaryocyte development but is significantly decreased in the erythrocytes lineage (59,60). *Runx1* targeted mice also presented with a mild expansion of the myeloid lineage in the BM and spleen, suggesting a myeloproliferative phenotype in these mice (56,57,61).

RUNX1 directs T-cell maturation

Conditional *Runx1* deletion in adult mice display significantly reduced T- and B-lymphocytes in peripheral blood and reduced cellularity of the thymus,

which indicates a critical role of RUNX1 in lymphocyte development (56,57,62). *Runx1* is highly expressed in double negative thymocytes and downregulated when cells undergo thymic maturation (63). Conditional targeting of *Runx1* in bone marrow using *Mx1-cre* and in thymocytes using *Lck-cre* resulted in differentiation blocks at DN2 and DN3 stages, respectively, and thereby prevented the emergence of DP cells (56,64). *Runx1*-deficient DN4 cells are less proliferative, suggesting defective β-selection, which might be due to decreased TCRβ expression (64). This is supported by RUNX1 binding to the *Tcrb* enhancer (Eβ), which promotes the transcription of the complete *Tcrb* gene (65,66). In human thymocytes, RUNX1 regulates TCRδ rearrangement by directing RAG1 binding to recombination signal sequences through physical interaction (67). In addition, positive selection and maturation of CD4SP were impaired in *Cd4-cre Runx1f/f mice* (62,64), indicating that RUNX1 is an essential transcription factor for thymocyte differentiation.

RUNX1 also directly represses CD4 expression by binding to the CD4 silencer, which restricts CD4 expression to appropriate thymocyte populations (62,68,69). Mutations in RUNX binding sites in the CD4 silencer region induced de-repression of CD4 expression in DN cells and CD8SP cells (62). While RUNX1 is required for CD4 repression in DN cells, it is dispensable for maintenance of CD4 silencing in mature $CD8^+$ cells (62).

RUNX3 regulates the development of CD8$^+$ cells

Runx3 expression is high in CD8SP thymocytes and cytotoxic T-cells and is critical for the specification of CD8SP cells (62–64). *Cd4-cre* mediated *Runx3* deletion resulted in a reduction of CD8SP thymocytes and cytotoxic T-cells in the periphery (64). RUNX3 binds to the *Cd8* enhancer regions to activate *Cd8* expression while silencing CD4 expression through binding to the silencer in CD8$^+$ cells (62,63). Accordingly, the absence of RUNX3 in CD8 T-cells de-repressed CD4 expression and slightly reduced CD8 expression (62,64).

In addition to silencing CD4 expression directly, RUNX3 represses *T-helper inducing POZ-Kruppel factor* (*Thpok),* a determinant factor of the CD4 lineage (70). RUNX3 also directly modulates T-cell factor-1 (TCF-1) and lymphoid enhancer-binding factor-1 (LEF-1), the upstream regulators of *Thpok* to ensure the specification of CD8$^+$ cells from DP thymocytes (71).

TAL1/SCL controls hematopoietic lineage specification and development

TAL1/SCL (T-cell acute lymphoblastic leukemia 1/stem cell leukemia) was first cloned from a T-ALL patient derived cell line as a gene translocated in the TCRδ locus where it was constitutively expressed (72) and was later found to be a crucial gene for hematopoiesis. Disruption of the *Tal1* gene in mice resulted in growth retardation and embryonic lethality around E8.5 to E10.5 due to the absence of yolk sac primitive erythropoiesis (73,74). The absence of all

hematopoietic cells from *Tal1*-null ES cells in adult chimera mice supports the theory that TAL1 is required for the specification of hematopoietic lineages (75,76). In contrast, conditional deletion of *Tal1* in adult mice using *Mx1-cre* displayed only moderate anemia and thrombocytopenia, indicating that continuous *Tal1* expression is not necessary for the maintenance of HSCs (77). In addition, *Tal1*-deleted HSCs were capable of self-renewing and competing with wild type BM cells to reconstitute hematopoiesis in lethally irradiated recipients (77,78).

TAL1 is a class II basic helix-loop-helix (bHLH) family transcription factor and binds to the E-box DNA binding motif (CANNTG) as a obligate heterodimer with class I bHLH transcription factor E-proteins including E12/E47, HEB, and E2-2 (79). TAL1 can either activate or repress target gene expression through integration with cofactors such as P300/CBP histone acetyltransferase and pCAF (P300/CBP-associated factor) for activation, or mSIN3A for repression (80–82). TAL1 also forms regulatory complexes with non-DNA binding proteins such as LIM-only domain proteins LMO1/2 and LIM domain-binding protein 1 (LDB1), which bridge the TAL1:E-protein heterodimer with other transcription factors, including GATA proteins and SP1, to influence its downstream targets (83,84). DNA binding activity of TAL1 is not always required for its functions (85–87). In normal hematopoiesis, mice carrying mutant *Tal1* that cannot bind to DNA developed primitive hematopoietic cells, in contrast to the complete absence of hematopoiesis in *Tal1*-null mice (76,85).

TAL1/SCL is required for erythrocyte development and is silenced in lymphoid lineages

Tal1 is expressed in hematopoietic stem cells, multipotent progenitor cells, erythrocyte and megakaryocyte lineages, but is silenced during lymphocyte development (88–90). *In vitro* colony forming assays with *Tal1*-depleted BM cells revealed that TAL1 is required for erythroid and megakaryocytic cell differentiation, but not for lymphoid and myeloid development (77). Forced TAL1 expression induced differentiation of hematopoietic progenitor cells toward the erythroid lineage (91). ChIP-seq studies combined with gene expression analysis in immature erythroid progenitor cells revealed that TAL1 regulates the expression of genes involved in erythrocyte development, including *β-globin* (*HBB),* Krueppel-like factor 1 (*KLF1*), and glycophorin A (*GPA),* suggesting a pivotal role of TAL1 in erythrocyte differentiation (92–94). In addition, direct DNA binding of TAL1 is required for the terminal differentiation of erythrocytes (85,92). *Tal1* expression in thymocytes is restricted to the DN2 stage; ectopic expression of TAL1 with LMO1 in thymocytes resulted in the differentiation arrest at the DN stage and subsequently leukemogenesis, as described below (89,95).

NOTCH1 signaling is essential for T-cell development

NOTCH1 is a class I transmembrane protein receptor that functions as a ligand-activating transcription factor, transducing extracellular signals directly to the nucleus. NOTCH1 anchors in the cell membrane as a heterodimer composed

of an N-terminal extracellular subunit, a C-terminal transmembrane subunit, and C-terminal intracellular subunit, which are non-covalently linked through the heterodimerization (HD) domain in each subunit (96). These subunits are encoded by a single gene and processed into two polypeptides during maturation. NOTCH1 interacts with its ligands expressed on adjacent thymic stromal cells, such as Delta-like ligand 1 (DLL1), DLL3, DLL4, Jagged1, and Jagged2, through 36 epidermal growth factor (EGF)-like repeats in the extracellular subunit. Ligand binding initiates signaling, first by inducing a conformational change in a negative regulatory region (NRR), which allows the cleavage of the HD domain by the ADAM10 and ADMA17 metalloproteases at the cell surface (97–100). The second cleavage by the γ-secretase complex in the transmembrane region releases the intracellular domain of NOTCH1 (ICN1) from the membrane and leads to its translocation into the nucleus (97,98). In the nucleus, ICN1 associates with a transcriptional factor RBPJ/CSL, which is bound to DNA with corepressors in the absence of NOTCH1, and recruits coactivator proteins such as mastermind 1 (MAML1) and p300/CBP to activate its target genes (96). The activated signaling is terminated through the C-terminal PEST (proline [P], glutamic acid [E], serine [S], and threonine [T] rich) domain of NOTCH1. Polyubiquitination of the PEST domain by FBXW7/SCF (F-box and WD repeat domain containing 7/SKP1-Cullin-1-F-box protein) ubiquitin ligase complex results in proteasomal degradation of ICN1 (96).

T-cell development within the thymus is directed by signals from thymocytes themselves and from interactions between thymocytes and thymus stroma (101). NOTCH-mediated signaling is one of the pathways pivotal for T-cell development (101). There are four family members of NOTCH in mammals, which are named NOTCH1-4, and perform variety roles in normal cellular processes such as lineage commitment, proliferation, apoptosis, and differentiation, as well as in human malignancies (96). In lymphoid cells, all four NOTCH proteins are expressed at different levels (102,103). NOTCH1 is expressed in thymocytes and has been known to be critical for T-cell development (discussed below) (96,102–104). The expression of NOTCH2 is high in B-cells and NOTCH2 deficiency in BM cells impairs B-cell maturation but not T-cell development (105). NOTCH3 is expressed in the T-cell lineage, in similar patterns as NOTCH1 expression, but targeting NOTCH3 showed only mild effects on T-cell development (106), suggesting that NOTCH1 plays the dominant role in T-cell development. Lastly, NOTCH4 is expressed weakly in immature DP cells, but the role of NOTCH4 in T-cell development has not been determined (103).

NOTCH determines the fate of committed T-cells between $\alpha\beta$ and $\gamma\delta$ T-cell lineages (107–109). The fraction of thymocytes at the DN3a stage that successfully rearranges the *TCRβ* gene, assembles the pre-TCR composed of TCRβ, pre-TCRα and CD3 protein, and commits to the $\alpha\beta$ T-cell lineage. Signaling through the pre-TCR induces $\alpha\beta$ T-cells to proliferate extensively and

to differentiate into DN3b, DN4, and DP cells (109). Deletion of NOTCH1 or RBPJ/CSL in immature thymocytes using *Lck-Cre* results in a differentiation block of αβ T-cells at DN3 stage due to impaired V-DJβ rearrangement, and consequently, the significantly reduced number of DP cells (107,108). In addition, NOTCH signaling regulates pre-Tα gene expression in association with E47 (110,111). Interestingly, the number of γδ T-cells was increased in RBPJ/CSL-deficient mice, but not in mice deficient for NOTCH1 (107,108). These data imply that other NOTCH receptors may contribute to T-cell fate decisions, and that the role of NOTCH1 may be restricted to the generation and maintenance of αβ T-cells.

In vitro T-cell differentiation studies demonstrated that NOTCH signaling is required for the survival and proliferation of immature thymocytes (112–114). Expression of DLL1 in OP9 stroma cells has been shown to be sufficient to maintain hematopoietic progenitor cells and to induce DP thymocyte differentiation in cell culture systems (115). In the absence of the interaction between the NOTCH receptor and its ligand, however, DN3 cells rapidly undergo apoptosis due to the lack of glucose metabolism associated with PI3K (phosphatidylinositol 3-kinase)-AKT (serine-threonine kinase) pathway (114). Proliferation of DN3 thymocytes upon CD3 induction was also impaired by withdrawal of NOTCH1 signaling (113).

T-cell acute lymphoblastic leukemia and current therapies for patients with T-ALL

T-ALL is a disease characterized by the uncontrolled proliferation of immature T lymphocytes. T-ALL accounts for 10-15% of pediatric and 20-25% of adult ALL cases and is associated with anemia, thrombocytopenia, neutropenia, and high white cell counts with atypical blasts in the blood. Patients with T-ALL frequently present with a mediastinal thymic mass and leukemic infiltration of the central nervous system at diagnosis (1,116).

The main therapeutic approach for T-ALL is repeated cycles of chemotherapy, regardless of genetic abnormalities. Rigorous therapeutic regimens have improved the outcome of the disease with five-year disease-free survival rates of over 80% in pediatric T-ALL patients, which is still inferior to that of pediatric B-ALL patients (117). The outcome of adult patients with T-ALL is poor, with about a 50% 5-year survival rate (118,119). When disease relapse occurs, the prognosis is even worse, less than 25% of patients survive long term (120,121).

Chemotherapy regimens for patients with T-ALL consist of several phases including induction, consolidation, and maintenance. Induction therapy is given for 4 to 6 weeks and is a combination of glucocorticoids (prednisone or dexamethasone), vincristine, and L-asparaginase. The high-risk group of patients will also receive an anthracycline class drug such as doxorubicin, epirubicin, and

valrubicin. More than 90% of patients attain remission, though additional treatments are required for preventing relapse. To consolidate the remission and prevent development of CNS leukemia, intensive chemotherapy composed of methotrexate and 6-mercaptopurine or 6-thioguanine will be used for 1 to 2 months. Vincristine, L-asparaginase, doxorubicin, and etoposide may be added. If children stay in remission after the consolidation phase, maintenance therapy may begin. Daily 6-mercaptopurine and weekly methotrexate, often with vincristine and glococorticoid will be given for 18 to 30 months as maintenance therapy (1)(American cancer society).

Approximately 1% to 2% of children die from toxic effects of therapy during remission, mostly due to infection (122,123). Intensive chemotherapy results in several side effects as well, the most prominent being osteonecrosis, which occurs in 5-10 % of pediatric ALL patients (124,125). Additional side effects include metabolism syndrome, obesity, cardiovascular impairment, and CNS toxicity, and peripheral nervous system toxicity (1). In addition, children who survive ALL have been shown to suffer from learning disorders and secondary malignancies such as brain cancer and non-Hodgkin lymphoma (126,127). Therefore, targeted therapies have been the focus of pharmaceutical development in order to reduce adverse side effects while improving remission rates.

Genetic alterations in oncogenes and tumor suppressors drive T-ALL leukemogenesis

T-cell transformation results from the accumulation of multiple genetic abnormalities. Mutations that disrupt the functions of oncogenes, tumor suppressors, and genes involved in cell cycle, proliferation, survival, and differentiation of normal thymocyte development have been identified in T-ALL (128). T-ALL is subgrouped into early T cell precursor T-ALL (ETP-ALL), and early or late cortical T-ALL based on the immunophenotype reflecting the stage of thymic maturation arrest (129). Each subgroup exhibits a distinct gene expression profile defined by altered expression of transcription factors (129). The immunophenotype and gene expression profile of ETP-ALL resemble that of ETP cells (130). In addition, ETP-ALL harbors mutations commonly found in myeloid leukemias, including *FLT3*, *ETV6*, and *NRAS* (131). T-ALL cells with the early cortical thymocyte immunophenotype ($CD1a^+CD4^+CD8^+$) are associated with activation of TLX1/3 and NKX2-1/2 transcription factors (129). Late cortical T-ALL cells express CD3, CD4, and CD8, an immunophenotype corresponding to the late stage of cortical thymocyte maturation and typically misexpress TAL1 (129). Among the subgroups, ETP-ALL is a high-risk subtype while early cortical T-ALL subtype shows a favorable prognosis (132,133,130).

Despite the infrequency of cytogenetic abnormalities, about 35% of T-ALL exhibits chromosomal translocations involving TCR genes and T-cell specific

transcription factors (134,135). The rearrangements place strong regulatory elements of *TCR*β or *TCR*α/δ genes near transcription factors including *TAL1* (72,136,137), *TAL2* (138), *LYL1* (139), *BHLHB1* (140), *TLX1/HOX11* (141,142), *TLX3/HOX11L2* (143), *LMO1* (144), *LMO2* (145), *MYB* (146), and *MYC* (147,148), which result in aberrant activation of the affected transcription factors leading to transformation of T-cells.

Chromosomal deletions leading to loss of tumor suppressors also occur in T-ALL. Over 70% of T-ALL exhibits deletion of cyclin-dependent kinase inhibitor 2A (*CDKN2A*) locus at chromosome 9p21, which encodes $p16^{INK4A}$ and $p14^{ARF}$, resulting in uncontrolled cell proliferation (149,150). Broad deletions of chromosome 6q14-23 were observed in 19.3% of pediatric T-ALL cases, although the related tumor suppressors have not yet been identified (150).

Other activating and loss of function mutations in *NOTCH1*, *NRAS*, *FLT3, NF1,* and *PTEN,* were identified in T-ALL (131,151–154). Among them, activation of the NOTCH1 pathway is one of the most frequent genetic mutations in T-ALL and will be discussed below. Recent sequencing studies have demonstrated that epigenetic regulators such as *PHF6*, *EED*, *EZH2*, *SUZ12*, and *KDM6A* are also deleted or mutated in T-ALL (131,155–158). Genome-wide studies combined with integrated analyses have identified genetic alterations and the associations between mutations defining the genomic landscapes of T-ALL (150). Functional studies have provided additional rationale for new therapeutic approaches.

Activating mutations in NOTCH1 is prevalent in T-ALL

NOTCH1 mutations resulting in abnormal activation of downstream signaling pathways have been observed in more than 60% of T-ALL patient samples regardless of the subtype of T-ALL, though the highest association is found in the early cortical TLX1/3 positive T-ALL subtype (151,159). Aberrant activation of NOTCH1 in T-ALL was first identified in rare cases carrying a chromosomal translocation t(7;9)(q34;q34.3), generating a truncated constitutively active NOTCH1 allele (160). A subsequent experiment that reconstituted mice with bone marrow progenitor cells expressing activated forms of NOTCH1 resulted in the development of T-ALL, providing direct evidence that NOTCH1 is oncogenic in T-ALL (161).

Most NOTCH1 activating mutations localize to the HD or PEST domains (151,159). Mutations in the HD domain, which account for about 40% of T-ALL cases, result in ligand-independent NOTCH1 activation or ligand hypersensitivity (162). Nonsense or truncating mutations in the PEST domain have been observed in approximately 15% of T-ALL patients. The result of these mutations is the loss of the recognition sequences by FBWX7/SCF complex and consequentially impaired degradation of activated ICN1 (151,163–165). In rare cases, NOTCH1 is activated in a ligand-independent manner by in-frame insertions at the extracellular juxtamembrane region (juxtamembrane expansion, JME), which reposition the HD domain away from the membrane (166). In

addition to the mutations found in NOTCH1 genes, about 15% of T-ALLs carry FBXW7 mutations (167,168). These mutations typically reside in key residues responsible for the recognition of phosphorylated NOTCH1 PEST domain thus failing to degrade the activated ICN1 (167,168). Since FBXW7 targets other oncoproteins such as MYC, JUN, Cyclin E, and mTOR (169–171) for degradation, FBWX7 mutations might augment tumorigenesis. Interestingly, majority of T-ALL patients harbor either double mutations in the HD and PEST domain of NOTCH1 (~20%) or mutations in NOTCH1 HD domain and FBXW7 mutation together (~60%). The combined mutations synergistically activate NOTCH1 signaling due to ligand-independent activation combined with ICN1 degradation (151,168).

Activating NOTCH1 mutations were also found in T-ALL mouse models. First, in T-ALL developed using $MMTV^{D}$(mouse mammalian tumor virus)/Myc transgenic mice, more than 50% of provirus insertions took place in the *Notch1* gene, resulting in constitutive NOTCH1 activation (172) and 74% of leukemic cells from *Lck-Tal1* driven T-ALL mouse model harbored spontaneous mutations in *Notch1* (173). Deletions of 5' region of the *Notch1* gene were the majority of mutations identified in mouse T-ALL cells (174). These deletions resulted in ligand-independent activation of NOTCH11 signaling, which mimicked HD domain mutations in human T-ALL cells (174). In addition, NOTCH1 mutations were observed in pre-leukemic cells from *Lck-Tal1/Lmo2* or *pSil-TSCL/Lck-LMO1* bitransgenic mice (175,176), indicating that NOTCH1 activation is important at the early stage of transformation.

The activation level of each NOTCH1 mutation is not equivalent, thus results of the overexpression of individual NOTCH1 mutant alleles or combinations of them in mouse hematopoietic progenitor cells yield differing results (177). Typically mutations in the PEST domain are considered to be weak alleles and require other oncogenes such as *K-ras* to initiate T-ALL in mouse models (177). However, most of the *Notch1* mutations found in *Tal1*-induced murine leukemic cells were mapped to the PEST domain (173). Collectively, while strong NOTCH1-activating mutations, including rare truncated *NOTCH1* alleles resulted from the chromosomal translocation (<1%) and double mutant alleles (HD with PEST or HD with FBXW7 mutations), may play a role as driving oncogenes, others mutations might contribute to the progression of T-ALL pathogenesis. The inhibition of tumor growth upon treatment with γ-secretase complex inhibitors (GSIs) in T-ALL engrafted mice models (175,178) underscores the important roles of NOTCH1 in T-ALL maintenance.

NOTCH1 directly regulates MYC expression in T-ALL

Understanding the role of aberrant NOTCH1 activation in T-ALL led to extensive efforts to reveal downstream pathways and target genes of NOTCH1. ChIP-seq and gene expression analyses revealed that NOTCH1 directly regulates the expression of genes involved in cell metabolism and anabolic pathways, including ribosome biosynthesis, protein translation, and nucleotide and amino acid metabolism (179), supporting the role of NOTCH1 in the control

of cell growth. Consistent with this, NOTCH1 inhibition by GSI treatment reduced cell size (179).

Among the list of NOTCH1 target genes, *MYC,* the central regulator of cell metabolism and required for entry into S-phase, was identified as one of the top responsive genes upon NOTCH1 inhibition by GSI treatment or silencing (179). Several independent studies confirmed that *MYC* is a direct target gene of NOTCH1 in T-ALL, as well as in breast cancer (180–182). NOTCH1 binding to the *Myc* promoter region was validated using chromatin immunoprecipitation (ChIP) (180–182). Moreover, *Myc* overexpression rescued the apoptosis and G1 cell cycle arrest induced by NOTCH1 inhibition, while inhibition of MYC impeded the NOTCH1-medited growth (180,181). It has been reported that MYC target genes were enriched in NOTCH1-regulated genes (179) and that MYC binds to the majority of NOTCH1-bound promoter regions (183), indicating that MYC is an essential mediator and collaborator of the NOTCH1 pathway.

MYC is a basic helix-loop-helix leucine zipper transcription factor, controlling the expression of genes mediated in various cellular growth processes including DNA replication, cell cycle regulation, cell metabolism, and ribosome biogenesis (184–186). The expression pattern of *Myc* during thymocyte development mimics that of *Notch1*, and is increased at DN3/4 stages while silenced in the transition to DP cells (102,187), consistent with the finding of MYC as a NOTCH1 target gene. Pre-TCR signaling also contributes to the increase in

MYC protein levels at the DN3 stage, leading to proliferation of DN3 cells (188). Without *Myc* expression, the number of thymocytes was remarkably reduced while thymocyte differentiation was not impaired (188).

The overexpression of *MYC* was first discovered in Burkitt's lymphoma which results from chromosomal translocation t(8;14)(q23;q32) (189), and has subsequently been found deregulated in several hem-malignancies, including T-ALL (190–192). In addition to chromosomal rearrangement, mutations and gene amplification can lead to the MYC overexpression (190,191). Diverse oncogenic pathways including NOTCH1, MAP kinase, and WNT signaling induce MYC activity by upregulation of transcription or increase in the protein stability (179–181,193,194). It has been shown that overexpression of MYC contributes to tumor initiation, malignant cell proliferation, and survival (192).

Before becoming known as a direct target of NOTCH1, the contribution of MYC in T-ALL pathogenesis was implicated from the recurrent observation of chromosomal translocation t(8;14)(q24;q11) affecting *MYC* expression (147,148,195). As result of the translocation, *MYC* gene expression is under control of the strong regulatory element of *TCRA/TCRD* genes (195). The MYC protein half-life is controlled by FBXW7-mediated proteasomal degradation (196). Thus, loss-of-function mutations on *FBXW7* in T-ALL increase the protein stability of ICN1 and MYC. In addition, the increased MYC level in primary T-ALL patient samples without the NOTCH1/FBXW7 mutations was observed,

indicating NOTCH1 independent mechanisms of MYC deregulation in T-ALL (197). Phosphorylation of MYC by GSK3B enhances proteasomal degradation of MYC (198). Inhibition of GSK3B by AKT activation resulted from *PTEN* loss has been suggested as one additional mechanism of MYC regulation (197).

Targeting the NOTCH1-MYC pathway inhibits T-ALL leukemogenesis

In accordance with the prevalence of NOTCH1 aberrant activation and the importance of MYC activity in T-ALL, inhibiting NOTCH1 signaling has been shown to effectively interfere with T-ALL development. The effect of NOTCH pathway suppression has been tested with treatment of GSI in *in vitro* and *in vivo* systems. The γ-secretase complex cleaves all NOTCH family members and their ligands (199,200). It also targets growth hormone receptor and cell adherence molecules such as E- and N-cadherin (201,202). In T-ALL, enforced expression of ICN1 sufficiently overcame the phenotype induced by GSI treatment, suggesting that NOTCH1 is the major substrate of γ-secretase complex in this cell type (180,181). GSI treatment of T-ALL cells resulted in clearance of ICN1 and downregulated the expression of NOTCH1 target genes (151,179,180). NOTCH1 inhibition in human T-ALL cell lines resulted in G1 cell cycle arrest, decreased cell growth and proliferation, and reduced cell size (179,180). Our lab first demonstrated that murine T-ALL cells undergo apoptosis upon GSI treatment (167,178,203). We also showed that administration of GSI to leukemic mice extends or prolongs disease latency (175,178). In addition, engraftment of

leukemic cells pre-treated with GSI was impaired, confirming that inhibition of NOTCH1 signaling suppresses initiation as well as maintenance of T-ALL (175,204).

Targeting MYC in T-ALL is attractive since we showed that Myc inhibition or silencing eliminating leukemia-initiating cells (LICs), which are responsible for the disease initiation in recipient mice, self-renew, and relapse of the disease in patients. In a NOTCH1-activated background, mutation of *FBXW7* enhanced MYC protein stability and as a result, increased the number of LICs (196). On the other hand, depletion or inhibition of MYC by genetic ablation, shRNA expression, or pharmacologic treatment interfered with T-ALL development and decreased the number of LICs (196,205). MYC expression is highly sensitive to JQ1, an inhibitor of BRD4 (BET bromodomain-containing protein 4), which is a chromatin reader protein binding to acetylated histone, especially in hematopoietic cells (206). The effect of MYC inhibition on the induction of leukemic cell death was superior to NOTCH1 inhibition by GSI treatment in both mouse and human primary T-ALL cells (205). This was in agreement with the idea that MYC activity is controlled by other pathways other than NOTCH1 (193,197), and suggested that targeting MYC may be more successful for the inhibition of T-ALL pathogenesis.

The importance of targeting MYC to induce suppression of T-ALL also came from efforts to find a mechanism for how T-ALL cells acquire resistance to

GSI (207,208). It was reported that GSI-sensitive human T-ALL cell lines could become GSI resistant following prolonged culture with GSI (persister cells) (207). Persister cells expressed undetectable levels of ICN1 but moderate levels of MYC (207). In addition, BRD4 was found to be required for the maintenance of persister cells specifically, and binding loci of BRD4 and H3K27ac in persister cells were distinct from those in treatment-naïve cells, indicating that the epigenetic changes were involved in the acquisition of GSI resistance (207). Treatment with JQ1 or rapamycin, an inhibitor of mTOR, reduced MYC expression to a very low level and inhibited the proliferation of persister cells (207). Our lab demonstrated that treating NOD-*scid* IL2R$\gamma^{-/-}$ (NSG) mice engrafted with relapsed T-ALL patient cells with NOTCH1 inhibitor DBZ and JQ1 together also prolonged the survival of leukemic mice (207). These results stress the importance of MYC expression on T-ALL maintenance, and therefore the effectiveness of MYC targeting for T-ALL inhibition.

NOTCH1 downstream pathways can be therapeutic targets for T-ALL

Other than MYC, NOTCH1 has been found to control the PI3K-AKT-mTOR signaling pathway in T-ALL; this pathway is one of critical regulators of cell growth and metabolism. The upregulation of the PI3K-AKT-mTOR pathway was detected in over 85% of pediatric T-ALL patients resulting from various mechanisms, including mutations in *PI3K*, *AKT*, and loss of function mutations or inactivation of *PTEN* (154,209,210). In particular, loss of *PTEN* was reported in

17% of patient cases and resulted in GSI resistance (154). NOTCH1 activation and PTEN loss appeared to cooperate in T-ALL pathogenesis (178,211). NOTCH1 inhibition in T-ALL seems to be able to suppress this pathway at several levels. HES1, a direct target of NOTCH1, is a well-known transcriptional repressor and was shown to downregulate *PTEN* gene expression by binding at the promoter sequences (154). PTEN negatively regulates the PI3K-AKT-mTOR pathway by removing the 3-phosphate from phosphoinositide 3,4,5 triphosphate (PIP3) and destabilizing PI3K-mediated membrane recruitment of AKT required for activation. PTEN is also post-translationally inactivated by phosphorylation by casein kinase 2 (CK2) (209). Consistent with this, combined treatment with CK2 inhibitors and GSI was more effective for T-ALL inhibition compared with each of the single reagent treatments (212).

Additional NOTCH1 target genes, including Interleukin receptor 7 alpha chain (IL7Rα), *PTCRA* , and insulin-like growth factor 1 receptor (*IGF1R*), are important factors for T-ALL proliferation and are also upstream PI3K regulators (111,213,214). The LCK tyrosine kinase expressed in T cells can activate AKT downstream of NOTCH1 signaling (215). Targeting each gene with inhibitors such as BMS-526924 and NAC against IGF1R and IL7R, respectively, inhibited cell proliferation (214,216). In addition, combinational therapies targeting PI3K and mTOR with NOTCH1 inhibition have shown efficacy in pre-clinical models (178,217,218). A recent report that NOTCH1 regulates PP2A dephosphorylation of AKT suggested modulation of PP2A activity as a potential T-ALL therapy (219).

NOTCH1 activation has also been shown to stimulate NF-κB activity (220). Mechanistically, NOTCH1 directly regulates the expression of NF-κB factors *RelB* and *Nfkb2* and induces their nuclear localization (220). In addition, HES1, a direct target of NOTCH1, represses deubiquitinase *CYLD* expression, which results in activation of the IκB kinase (IKK) complex and upregulation of NF-κB target genes, including intercellular adhesion molecule 1 (*ICAM1*) and BCL2 related protein A1 (*BCL-2A1*) (220,221). Consistent with these data, targeting NF-κB using a small molecule inhibitor significantly induced apoptosis of T-ALL cells which synergized with GSI treatment (220).

It has been discovered that NOTCH1 signaling promotes G1/S cell cycle progression by transcriptionally activating cell cycle regulators such as cyclin D3 (*CCND3*), cyclin dependent kinase 4 (*CDK4*), and *CDK6* (222,223). CCND3 was required for NOTCH1-induced T-ALL development (224). A negative regulator of CCND3, *CDKN2A* ($p16^{INK4a}$) is inactivated in T-ALL by mutation, deletion, or silencing in approximately 90% of T-ALL cases (149,225,226). In contrast, the expression of other negative regulators of CDK, *CDKN2D* ($p19^{INK4d}$) and *CDKN1B* ($p27^{Kip1}$), was upregulated in GSI-treated cells to exit cell cycle (223). Consistent with this, blocking CDK4/6 activities by inhibitor treatment, with or without NOTCH1 inhibition, effectively interferes with T-ALL progression (223,227,228).

NOTCH1 as a candidate for targeted T-ALL therapy

NOTCH1 inhibition is a promising option, due to the prevalence of NOTCH1 pathway mutations, and has been extensively studied. The effects of NOTCH1 inhibition by GSI treatment in T-ALL cell lines and mouse models were encouraging, with rapid regression of leukemic cells observed. However, a clinical trial with MK-0752, an oral GSI developed by Merck was not successful (229). Patients who participated in the trial showed continued disease progression and severe drug-related toxicities, including diarrhea due to inhibition of NOTCH signaling in the gut (229). Our lab demonstrated that an intermittent dosing regimen reduced gastrointestinal toxicity while suppressed leukemia progression in T-ALL mice model (178). This dosing regimen in patients with melanoma was well-tolerated but showed minimal activity against the disease in a clinical trial, possibly due to insufficient exposure to the drug (230). Therefore, alternative strategies may need for successful administration of GSIs.

Combination treatment of GSIs and other molecularly targeted inhibitors has been investigated in order to improve the safety and efficacy of NOTCH1 inhibition. As discussed earlier, in combination with GSIs, treatment with inhibitors of CDK4/6, the PI3K-AKT-mTOR pathway, and NF-κB signaling have shown to be effective in T-ALL inhibition(154,178,220,223).

A driving oncogenic factor, TAL1 is misexpressed in T-ALL

Misexpression of TAL1 has been reported in approximately 60% of pediatric and 40% of adult T-ALL and is associated with a poor prognosis (231). The activation of *TAL1* occurs by interchromosomal translocation with *TCR*α/δ (t(1;14)(p33;q11)) (72,136) or *TCR*β (t(1;7)(p32;q35)) (137) genes or by ~90kb of interstitial deletion that places undamaged *TAL1* coding regions under the promoter of *SIL* (*SCL/TAL1* interrupting locus) gene (232,233). Recently, heterozygous somatic mutations were identified at a specific site upstream of the *TAL1* gene (234). These mutations create an enhancer site containing new MYB binding motifs that promote aberrant monoallelic *TAL1* activation in T-ALL (234).

The initial studies of the abnormal TAL1 regulations in T-ALL focused on TAL1 interference with E-protein functions, which are important for normal T-cell development. Under normal conditions, TAL1 expression is downregulated at the early stages of lymphoid development whereas the levels of HEB and E2A are increased up to the DP stage of T-cell development (89). The aberrant expression of TAL1 has been suggested to deplete HEB and E47 tumor suppressors by sequestering them from their target loci (89,235). TAL1 then recruits corepressor mSIN3A to the target genes, such as CD4 and pre-TCRα, resulting in decreased transcription, and consequently, a differentiation block and transformation of the thymocytes (235). In line with this, TAL1 overexpression accelerated T-ALL pathogenesis in HEB or E2A heterozygote mice (235).

Several genomic occupancy studies revealed that TAL1 shares binding loci with HEB and/or E47 (236,237). Combined global gene expression analyses identified direct target genes of TAL1 that are activated by TAL1, including *TRAF3* (TNF receptor associated factor 3, required for T cell effector functions)*, CDK6* (cyclin dependent kinase 6, regulates cell cycle and is downregulated during T cells differentiation), as well as genes involved in cell differentiation and apoptosis (93,236,237). In addition, TAL1 silencing using shRNA induced leukemic cell apoptosis, suggesting that TAL1 is required for leukemic cell maintenance (93,237).

Thymic expression of TAL1, in cooperation with other genetic mutations, results in T-ALL in mice

Efforts to verify the oncogenic activity of TAL1 and to establish a mouse model for T-ALL have been made. Unfortunately, the first few attempts with *Tal1* overexpression by the *CD2* enhancer failed to develop leukemia or lymphoma in mice despite the high expression of TAL1 in thymocytes (238,239). Reconstituted mice with bone marrow cells transduced with *TAL1* expressing retrovirus did not develop T-ALL (240). Other trials overexpressing *TAL1* under *SIL* promoter were not successful either (241,242). Finally, when *Tal1* was mis-expressed in developing thymocytes under the promoter of T-cell specific protein kinase *LCK*, 28% of mice was able to develop T-ALL after a long latency (243). Mice that

developed T-ALL presented with infiltration of lymphoblastic cells into the thymus, liver, spleen, and kidney, which was similar to human T-ALL (243).

The pathogenesis of TAL1-induced leukemia was significantly enhanced by co-overexpression of other oncogenes such as *LMO1/2*, a TAL1 activity modulator Casein Kinase IIα (*CKIIα*), or by loss of the *CDKN2A* locus (241,243–245). In addition, transgenic expression of $p16^{INK4A}$ prolonged the survival of TAL1 and LMO1 bitransgenic leukemic mice, and tumors from diseased mice had silenced $p16^{INK4A}$ expression (246).

LMO1/2 is misexpressed in T-ALL and collaborates with TAL1 to cause leukemia in mice

Overexpression of *LMO1/2* has been observed in approximately 45% of patients with T-ALL and is highly associated with cases of *TAL1* misexpression (129,145,247). LMO1/2 are also targets of chromosomal rearrangements involving *TCR* genes and *LMO2* can be overexpressed by deletion of a cis-negative regulator of the *LMO2* gene in T-ALL (144,145,248). The oncogenic function of LMO2 was discovered from studies using retrovirus-based gene therapy for X-linked severe combined immunodeficiency syndrome (SCID-X1) (249–251) where 25% of patients who participated in the trials developed T-ALL due to LMO2 activation by virus insertion upstream of the *LMO2* locus (249–251). In addition, enforced expression of *LMO1* or *LMO2* transgenes in thymocytes resulted in the development of T-ALL in mice (252–255).

In *Tal1*-transgenic mice, additional ectopic expression of *Lmo1* or *Lmo2* significantly enhanced the penetrance and accelerated the onset of T-ALL (87,238,241). All mice expressing *Tal1* and *Lmo2* transgenes under the *Lck* promoter developed T-ALL with a median survival of about 100 days (87). The double transgenic mice with *Tal1* and *Lmo1* or *Lmo2* exhibited abnormalities in thymocyte development at the pre-leukemic stage, such as differentiation block, reduced thymocyte cellularity, increased cell proliferation, and apoptosis (87,244).

In normal hematopoiesis, TAL1 and LMO2 share expression patterns and the phenotype of *Lmo2*-null mice is comparable to that of *Tal1*-null mice (76,256). In erythroid cells, LMO1/2 cannot bind to DNA directly but instead forms a regulatory complex with the TAL1:E-protein heterodimer and LDB1 through the LIM domain, to regulate expression of genes important for erythropoiesis (92,238). It is suggested that LMO1/2 may be a critical factor for the function of TAL1 and that LMO1/2 and TAL1 share common oncogenic pathways in T-ALL.

It has also been suggested that aberrant expression of TAL1 and LMO2 inhibits the functions of E-protein homodimers essential for normal T cell maturation, leading to differentiation block of T cells (89). The phenotype of *Heb*-null mice resembled that of *Tal1* and *Lmo2* transgenic mice during the pre-leukemic stage (89). Structural studies revealed that TAL1:E47 heterodimer is more stable than E47 homodimer and that LMO2 binding to the heterodimer strengthens the interaction between TAL1 and E47 even more (257), supporting

the idea of HEB/E47 sequestration by TAL1 and LMO1/2. Interestingly, LMO2 recruitment to the heterodimer weakened the affinity of protein binding to DNA (257). Thus other transcription factors would be critical for TAL1:E47:LMO1/2:LDB1 to form a regulatory complex and to stably occupy the target genomic loci. In fact, a DNA binding mutant of TAL1 was able to develop T-ALL in cooperation with LMO2 overexpression (87).

TAL1 is a part of a transcriptional auto-regulatory circuit with RUNX1 and GATA3, activating the MYB oncogene in T-ALL

Formation of transcriptional regulatory circuits has been suggested in several cell types including embryonic stem cells and normal hematopoietic cells (258,259). In human T-ALL cell lines and patient samples, ChIP-seq studies followed by binding motif analyses found the ETS and RUNX binding motifs were highly enriched at TAL1 binding sites, in addition to the GATA binding motif, which is also found in erythroid cells (93,237). Consistently, ChIP-seq analyses for TAL1, HEB, E2A, GATA2, LMO1/2, and RUNX1 demonstrated that a large portion of genomic sites occupied by TAL1 are also bound by multiple transcription factors (237). The combined gene expression profiles of cells in which *TAL1*, *RUNX1*, or *GATA3* are suppressed uncovered that the expression of direct target genes of TAL1, such as *MYB,* were also altered by GATA3 and RUNX1 depletion (237). Furthermore, it was observed that these transcription factors were bound to each other's and their own regulatory regions suggesting

that the complex is autoregulated (237). Therefore, it appears that TAL1 is part of a large interconnected regulatory complex in T-ALL cells to reinforce the oncogenic downstream pathways.

MYB is a transcription factor, essential for normal and malignant hematopoiesis (260) found highly expressed in hematopoietic stem and progenitor cells (HSPCs), and decreased during differentiation (261). Studies targeting *Myb* at different stages of T-cell development revealed that MYB is required for pre-TCR rearrangement at the DN stage, for the survival of DP cells, and for the differentiation of DP cells into SP cells (262). MYB was initially identified as a common retrovirus insertion site, associated with myeloid leukemia (263,264). In T-ALL, chromosomal translocation with the *TCR*β enhancer or Alu element-mediated duplication resulted in aberrant expression of *MYB* (146,265,266). In addition, overexpression of *v-Myb* induced T-ALL in mice (267) while *MYB* silencing released the differentiation block and impeded the growth of T-ALL cell lines (266), suggesting an oncogenic role of MYB in human T-ALL.

ChIP-seq and gene expression studies showed that *MYB* is a direct target gene of the TAL1 regulatory complex and that MYB contributes to the oncogenic gene expression program of TAL1 in T-ALL (237). The recent finding of mutations in the upstream region of *TAL1* allowing MYB binding indicated that

MYB is also a component of the TAL1 interconnected auto-regulatory complex (234).

Controversial roles of RUNX1 in leukemogenesis

RUNX1 is one of the most commonly mutated genes in hematopoietic malignancies (33). Most genes associated with tumorigenesis are classified as oncogenes or tumor suppressors; however, RUNX1 has been found to perform both functions depending on the cell type. The involvement of RUNX1 in leukemia was first discovered by identification of chromosomal translocation t(8;21) creating *RUNX1-RUNX1T1/EPT* gene, encoding AML1/RUNX1-ETO, which is the most frequent mutation in AML (268). Subsequently, several types of translocations and somatic point mutations affecting the *RUNX1* gene have been identified in AML, myelodysplastic syndrome (MDS), and ALL (33,269–273). AML1/RUNX1-ETO functions as a dominant negative inhibitor against the normal RUNX1 protein or reduces its activity, suggesting that loss of function of RUNX1 is associated with hematopoietic malignancy (270,273–276). The tumor suppressor roles of RUNX1 have been supported by findings of germline monoallelic *RUNX1* mutations in familiar platelet disorder (FPD) with predisposition to AML (277–279). On the other hand, overexpression of *RUNX1* in leukemic cells has suggested that RUNX1 can function as an oncogene. First, the promoter region of the *RUNX1* gene was a frequent site of retroviral insertion in lymphoid leukemias in mice (280–283) and as result, the expression of the

whole intact gene was increased in leukemic cells (283). In addition, the overexpression of *RUNX1* resulting from the amplification of a large region of chromosome 21 has been observed in a subset of B-ALL associated with a poor-prognosis and in few AML cases (284–288). A remarkable number of B-ALL patients exhibit upregulated *RUNX1* even in the absence of chromosomal amplifications (289).

The ability of RUNX1 to either activate or repress the transcription of critical regulators of cell differentiation and growth can explain the contrasting roles of RUNX1 in leukemogenesis. In addition, the fact that the deregulation of RUNX1 can result in different cell lineages argues for cell-type dependent roles of RUNX1. Indeed, the enforced expression of *RUNX1-ETO* in stem cells resulted in expansion of myeloid cell lineage and myeloproliferative disorder (290,291). However, expression of the transgene was not detected in lymphoid cells, probably due to the adverse effects of the fusion protein on lymphoid cell survival and development (290). Furthermore, administration of DNA-alkylating mutagen *N*-ethyl-*N*-nitrosourea (ENU) resulted in AML development in RUNX1-ETO expressing mice, in contrast to ALL development in wild type RUNX1 expressing mice (292).

RUNX1 deregulation results in the development of myeloid malignancy

In addition to the t(8;21) translocation, more than 50 cases of chromosomal translocation including t(3;21)(q26;q22), which results in *RUNX1-*

MECOM (MDS1-EVI1), have been found in malignant hematopoietic cells (269,293). Most of the translocations affecting the *RUNX1* gene have been observed in AML or MDS (33,269). One of the predominant translocations t(12;21) prevalent in B-progenitor ALL (B-ALL), creates a TEL1-RUNX1 fusion protein (294–296). The resulting fusion protein contains the RUNT domain with or without other domains of RUNX1 and parts of or entire other proteins (33,268,293,296). These fusion proteins can bind to RUNX binding sites while interacting with coactivators such as p300 and protein arginine methyltransferase 1 (PRMT1) (297,298), or corepressors such as NCOR1, HDAC1, and SIN3A (275,276,299), in different ways than normal RUNX1 (274), resulting in altered gene regulation. In addition, the fusion proteins interfere with the function of other transcription factors by direct interaction. For example, RUNX1-ETO binds with and inhibits CCAAT/enhancer binding protein alpha (CEBPA) and PU.1, which are critical transcription factors for myeloid development, leading to myeloid leukemia development (300–302).

Besides the abnormal chromosome rearrangements, monoallelic or biallelic somatic mutations of the RUNX1 gene have been identified in AML and MDS (270,273,303,304). MDS patients with RUNX1 mutations are at greater risk for the progression to AML and that AML patients with RUNX1 mutations have a worse prognosis compared with patients harboring wildtype RUNX1 (305–309). Identified mutations include missense mutation, nonsense mutations, and frame-shift mutations, and are mainly distributed in the RUNT domain, predicted to

result in reduced RUNX1 transcriptional activity (271,305–307). Gene expression analyses revealed that RUNX1 mutations in AML resulted in a distinct gene expression profile with deregulated genes involved in apoptosis, upregulated lymphoid regulator genes, and downregulated of genes required for myelopoiesis genes (307,309,310), indicating that RUNX1 abnormalities can lead to differentiation defects.

Several activating mutations of signal transduction pathways leading to cell survival and proliferation have been observed in RUNX1 mutated AML (305–307,309,310). *FLT3*-internal tandem duplication (ITD), *FLT3*-tyrosine kinase domain mutation (TKD), *MLL*-partial tandem duplication (PTD) and mutations in *NRAS*, *IDH1/2*, and *KIT* were highly associated with RUNX1 mutations in AML. Therefore, it seems that the differentiation block due to mutations in RUNX1 work together with mutations imparting growth advantage in order to promote AML development. In addition, mutations in epigenetic regulators such as *ASXL1/2* and *DNMT3A* were also frequently associated with RUNX1-deregulated AML (309,311,312).

The oncogenic potency of RUNX1-fusion proteins or mutations in RUNX1 have been shown experimentally using *in vivo* and *in vitro* systems. Mice reconstituted with BM cells transduced with retrovirus that expresses *RUNX1-MECOM*, *RUNX1-ETO* or mutated *RUNX1* all develop AML (291,313,314). *RUNX1-ETO* transgenic mice expressing the fusion gene in

progenitor cells under the *Sca-1* promoter also recapitulated the development of myeloid leukemia (290). Ectopic expression of RUNX1-ETO in $CD34^+$ human progenitor cells induced cell growth while retaining progenitor characteristics, and inhibited the differentiation (315,316), in agreement with the hypothesis that RUNX1 mutants may disturb the balance between differentiation and self-renewal.

Mutations of CBFβ, a heterodimeric partner of RUNX proteins, are also frequent in AML. Inversion of chromosome 16, inv(16)(p13q22), produces a fusion gene of *CBFβ* and with the *MYH11* (a smooth-muscle myosin-heavy-chain) gene (317). The resulting fusion protein binds to RUNX1 with higher affinity than wildtype CBFβ, inhibiting RUNX1 function and inducing AML development (318,319). The phenotypes of inv(16) knock-in mouse, which are similar to those of the Runx1-null mouse, provide evidence of dominant-negative function of the fusion protein (320).

RUNX1 is a potential tumor suppressor in certain subtypes of T-ALL

While RUNX1 deregulation has been intensively investigated in myeloid leukemia, its association with T-ALL has been less clear. Recent whole genome sequencing studies identified mutations of the *RUNX1* gene in about 15% of ETP-ALL cases (131,150,321,322). These mutations include chromosomal translocations affecting the *RUNX1* gene, heterozygous missense mutations, nonsense mutations, frame-shift mutations, and in-frame insertion mutations

(131,321,323). Similar to those identified in AML, most of the mutations besides chromosome alterations were mapped on the RUNT domain and the transactivation domain, and presumably result in loss-of-function of RUNX1 (150,321,323), indicating that normal RUNX1 activity suppress thymocyte transformation.

Tumor suppressor roles of RUNX1 were invoked in TLX1/3-positive early cortical T-ALL subtype (323). The gene expression profile revealed that TLX1 and TLX3 function to directly repress RUNX1 expression. In agreement with this, overexpression of *RUNX1* by retroviral transduction in TLX1- or TLX3-positive human T-ALL cell lines inhibited cell growth (323). However, studies of the role of RUNX1 in other subtypes of T-ALL have suggested that RUNX1 has oncogenic functions (93,237,324).

RUNX1 activation promotes T-ALL development

ChIP experiments for NOTCH1 or TAL1 performed in human T-ALL cell lines to investigate the mechanism of TAL1 and NOTCH1 regulation in T-ALL first identified the RUNX binding motif was the one of the most representative sequences in NOTCH1 or TAL1 binding sites (88). Subsequent studies found that RUNX1 actually binds 74% of NOTCH1 and 78% of TAL1 binding loci (237,324), indicating that RUNX1 regulates a subset of NOTCH1 and TAL1 regulated genes. Gene expression analysis showed that a large number of TAL1 target genes were also regulated by RUNX1, thus confirming the cooperation

between RUNX1 and TAL1 (237). RUNX1 was suggested to be a component of the TAL1 interconnected regulatory complex, which was observed in primary T-ALL patient samples as well (234,237). These results raise a possibility that RUNX1 plays oncogenic roles in T-ALL development, which I have studied in this thesis research.

Abnormal transcriptional programs in cancer cells.

As described earlier in cases of TAL1, NOTCH1, and RUNX1 in leukemogenesis, dysregulation of transcription factors and subsequent gene expression are hallmarks of cancer. Transcription factors bind to regulatory elements composed of promoters, enhancers, and silencers in a sequence-specific manner. They recruit transcription machinery, cofactors (MED1, SMC3), and chromatin regulators, such as chromatin remodeling complexes (SNI/SNF complexes), and histone modifying enzymes (SET1, MLL, and DOT1L) to DNA and regulate gene expression (326,327). A subset of transcription factors has been shown to be sufficient to induce cell type-specific gene expression programs and define cell states (328–332). In committed immature T-cells, ectopic expression of C/EBPα and PU.1 can redirect cells to macrophages and dendritic cells, respectively (332). These transcription factors, known as mater transcription factors, are highly expressed in certain cell types and typically regulate their own expression through an autoregulatory loop (237,333). Thus, dysregulation of master transcription factors in tissues can alter cell identity and

induce tumorigenesis. In addition, abnormal regulation of transcription factors involved in cell proliferation and amplification of transcriptional output, such as MYC (334,335) and other signaling pathways that cooperate with master transcription factors, can promote transformation (336,337). Besides transcription factors, aberrant cofactors, such as mutated MED12 (a mediator complex component), also contribute to cancer-associated transcription (338,339).

Among the regulatory elements, enhancers are associated with cell type-specific genes and bound by multiple transcription factors (340). Enhancers have been mapped by epigenetic marks associated with enhancer activity, including acetylated lysine residues of histone 3 and histone 4 tails (H3K27ac and H3K9ac) or di/tri-methylation of H3K4 (H3K4me2 and H3K4me3) (341). Among them, super-enhancers are large clusters of transcriptional enhancer elements regulating the expression of genes that determine cell identity (340,342). They are occupied by high levels of multiple different master transcription factors, the Mediator complex, chromatin regulators, and polymerase II to ensure significant expression of associated genes (342). Polymerase II that is bound to super-enhancers produces non-coding enhancer RNAs (eRNAs) that mediate the maintenance and activities of enhancers (343,344). In addition, enhancer loci exhibit disease-associated sequence variations (345,346). In cancer cells, it has been shown that driver oncogenes are associated with cancer type-specific super-enhancers, which are not present in healthy cell counterparts, and highly vulnerable to perturbation (340,347). Cancer cells acquire super-enhancers by

DNA translocation (348–350), focal amplification (351–353), small insertion/deletions of nucleotides (251), and overexpression of oncogenes (340).

MYC is regulated by super-enhancers in cancer cells

Recently, it has been reported that *MYC* is regulated by super-enhancers in cancer cells. In T-ALL, a super-enhancer controlled by NOTCH1 is located 1.47 Mb downstream from the *MYC* transcription start site (TSS) (N-Me) (351). The focal duplication of this region was found in T-ALL patient samples, specifically. The binding of NOTCH1, P300, and active histone marks, such as H3K27ac and H3K4me1 (monomethylation), at this locus was highly and specifically enriched in T-ALL cells indicating that this region is particularly active in T-ALL (351). In addition, this enhancer is required for the development of normal thymocytes as well as T-ALL initiation and maintenance in mice (351). Chromosome conformation capture (3C) experiments uncovered that this distal enhancer regulates *MYC* expression by a chromatin loop formation between the enhancer and promoter region of *MYC* (208,351).

In GSI-resistant persister T-ALL cells, MYC appears to be expressed by another long-range enhancer located at 1.7 Mb downstream from the *MYC* TSS in a NOTCH1-independent manner (207). BRD4, which is required for the survival of persister cells, newly bound at this enhancer region (BDME, BRD4 dependent MYC enhancer) in persister cells (208). Chromatin loop formation

between the *MYC* TSS and BDME was maintained, while the interaction of *MYC* TSS with N-Me was disrupted in persister cells (208).

Super-enhancers driving *MYC* expression have been identified in other types of cancer. In AML cells, MYC expression is regulated by BDME which is amplified in AML patient samples (352,354,355). BRG1, a component of SWI/SNF chromatin remodeling complex binds to this enhancer and regulates expression of *MYC* through controlling the interaction between the promoter and enhancer loci (352). Several transcription factors including CEBPα/β, ERG, PU.1, and LMO2, and BRD4 bind to this enhancer locus (352). Comprehensive single-nucleotide polymorphism (SNP) arrays in colorectal, breast, prostate, and ovarian cancer cells uncovered sequence variations within the upstream region of the *MYC* gene which contains a large number of enhancer elements (356–358). Individual enhancers within this region physically interact with the *MYC* promoter region in a tissue-specific way (359). The rs6983267 SNP at 335 kb upstream of the *MYC* gene in colon cancer cells results in increased TCF4 (transcription factor 4) binding and modification of active histone marks, leading to MYC upregulation (360). In addition, mice with a 538-kb deletion of the upstream region of the *Myc* gene are resistant to tumorigenesis while they do not exhibit developmental defects (361).

MYB expression is controlled by long-distance range locus.

Expression of the *MYB* gene is regulated by binding of transcription factors at its promoter regions, including MYB itself and PU.1 (362,363). In addition, a locus control-like region controlling MYB expression in mice was identified approximately 77 kb upstream from the *Myb* gene (260). Recent ChIP-seq analyses revealed that not only this locus but also other regions, including 14 kb downstream and 93 kb upstream from the *MYB* gene, are bound by several transcription factors including TAL1, GATA3, LMO2, and HEB in T-ALL cells (237). In addition, the active histone mark H3K27ac is highly enriched at these regions suggesting these regions contain enhancer elements (364). In fact, distribution analyses of H3K27ac signals in T-ALL cells indicated that MYB is associated with a super enhancer stretched around the *MYB* gene (340,364). The binding of MED1, a coactivator enriched in super-enhancer regions, is also abundant around these regions (234).

In the research presented in this thesis, I investigated roles of RUNX1 in T-ALL pathogenesis. Based on the overlapping occupancy of RUNX1 with the TAL1 complex and NOTCH1, I hypothesize that RUNX1 functions as an oncogene in T-ALL development and interrogated the effects of RUNX1 suppression in T-ALL progression. I focused on roles of RUNX1 in transcriptional regulatory elements to advance the understanding of the molecular mechanisms in T-ALL development.

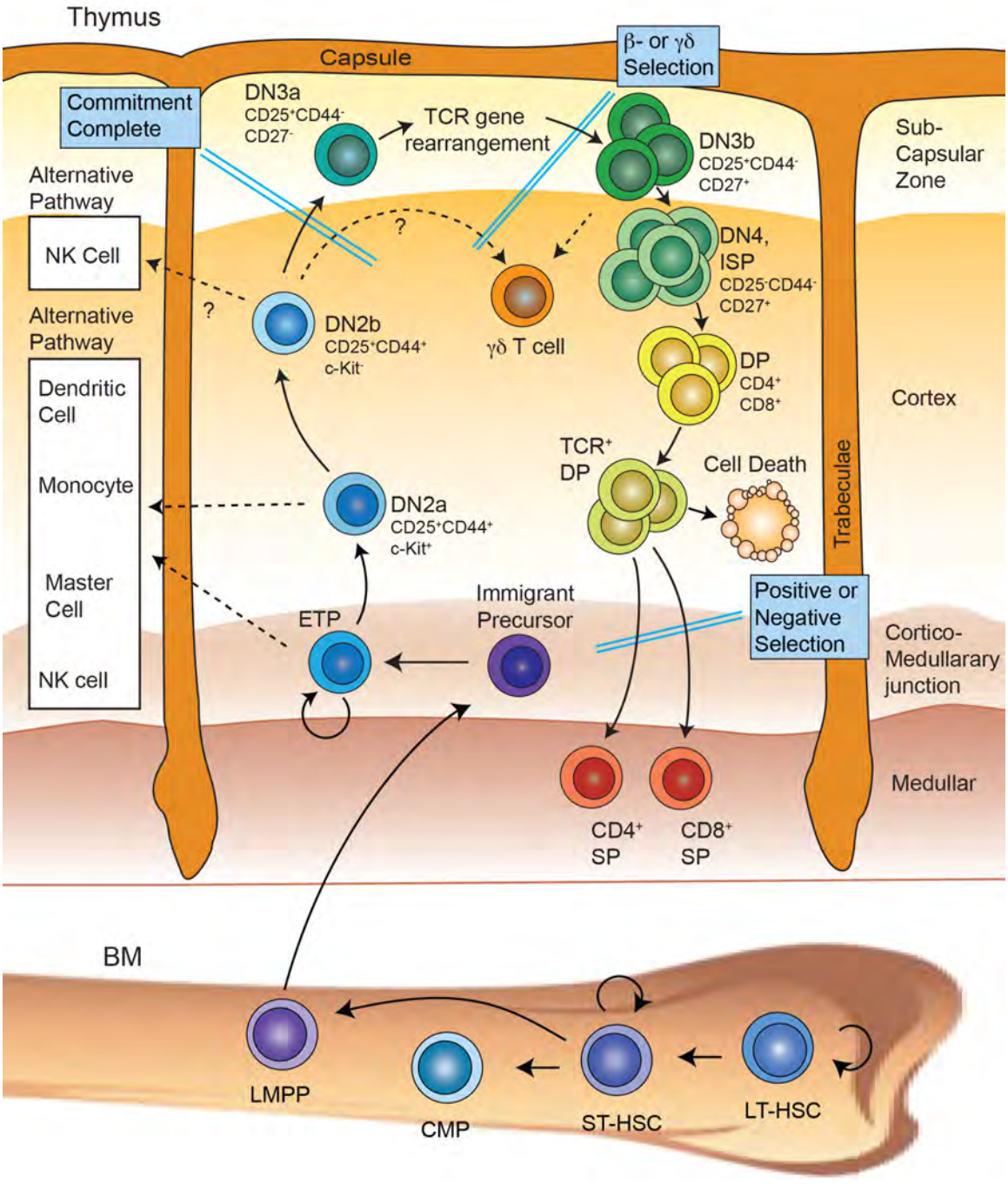

Figure 1.1. Thymocytes development. Early thymic progenitor cells (ETPs), differentiated from HSCs, are immigrated from the BM. Thymocytes travel in the thymus and differentiate while losing potentials for other lineages. Thymocytes change cell surface marker profiles during the differentiation. (Adapted from E.V.Rothenberg 2008 *Nature Review Immunology* 8:9-21)

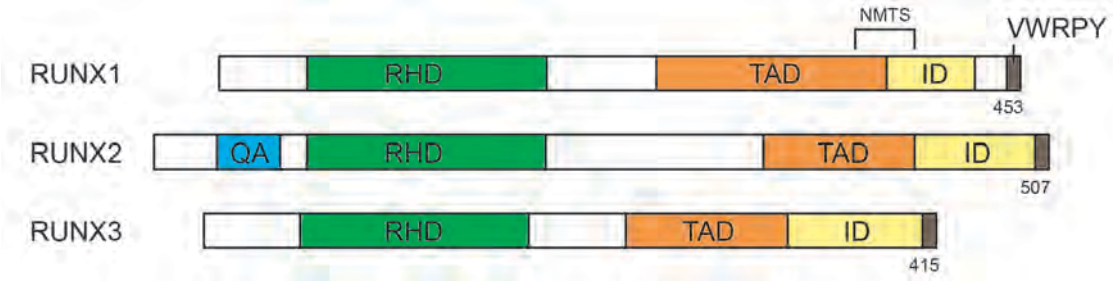

Figure 1.2. The structure of RUNX proteins. The RUNX family comprises RUNX1, 2 and 3 proteins. They share the highly-conserved RUNT-homology domain (RHD) and the C-terminal VWRPY motif. All three proteins have the transactivation domain (TAD), the inhibitory domain (ID), and a nuclear-matrix-targeting signal (NMTS). Only RUNX2 protein has the extended glutamine-alanine repeat domain (QA) at N-terminus. The numbers of amino-acid refer human RUNX proteins.

Chapter II

RUNX1 and/or RUNX3 is required for T-ALL survival

Data from the following chapter were a part of a published paper:

AHyun Choi, Anuradha Illendula, John A. Pulikkan, Justine E. Roderick, Jessica Tesell, Jun Yu, Nicole Hermance, Lihua Julie Zhu, Lucio H. Castilla, John H. Bushweller and Michelle A. Kelliher. RUNX1 is required for oncogenic *Myb* and *Myc* enhancer activity in T cell acute lymphoblastic *Blood* (2017) 12;130(15):1722-1733

The manuscript has been edited for this thesis to show the results generated by AHyun Choi.

Introduction

It has been demonstrated that suppression of RUNX1 functions to promote T-ALL pathogenesis, similar to its function in AML. Loss of function mutations in RUNX1 are enriched in the ETP-ALL subtype and are associated with poor prognosis (131,321,323). In addition, in TLX1/3-transformed T-ALL cells, disruption of the RUNX1 transcriptional network by TLX1/3 was proposed as a key mediator of T-ALL development, and overexpression of RUNX1 in these leukemic cells impairs growth (323).

In contrast, RUNX1 has also been suggested to support functions of dominant oncogenes in T-ALL. In human T-ALL cell lines and patient samples, TAL1 comprises a core transcriptional regulatory complex with RUNX1 and GATA3 (237). In addition, ChIP-seq studies for NOTCH1 and RUNX1 have revealed that RUNX1 binds to most of the same genomic loci where NOTCH1 is bound (324). These data indicate that RUNX1 contribute to TAL1- or NOTCH1-mediated leukemogenesis.

To elucidate whether RUNX1 potentiates or suppresses T cell leukemogenesis, we generated *Tal1/Lmo2/Rosa26-CreER^{T2}Runx1$^{f/f}$* mice that develop TAL1-induced T-ALL and acquire spontaneous mutations in NOTCH1 (175), and reveal a crucial, pro-survival role for RUNX1 in T-ALL. Similarly, we demonstrate that *RUNX1/3* knockdown in human T-ALL cell lines or treatment with a recently developed CBFβ/RUNX allosteric inhibitor mimics the effects of

Runx1 deletion in mouse T-ALL cells and induces apoptosis. These data provide genetic and pharmacologic evidence that RUNX1 has critical survival roles in T-ALL and support the idea that RUNX1 inhibition may have therapeutic benefit for T-ALL patients.

Results

RUNX activity is required for the growth and survival of T-ALL cells.

To examine roles of RUNX1 in T-ALL pathogenesis, we generated *Tal1/Lmo2/Rosa26(R26)-CreER^{T2}Runx1$^{f/f}$* mice and transplanted mouse leukemic cells into secondary recipients. One week after the transplantation for leukemic cells to be engrafted, mice were treated with vehicle or tamoxifen to delete *Runx1* alleles (Figure 2.1A). As results, we observed that *Runx1* deletion interfered with or prevented leukemic growth *in vivo* (Figure 2.1B). Notably, the few *Tal1/Lmo2/R26-CreER^{T2}Runx1$^{f/f}$* mice that developed disease (5568 and 7714) retained a floxed *Runx1* allele that likely escaped Cre-mediated deletion *in vivo* (Figure 2.1C). Consistently, *Runx1* deletion induced by 4-OHT treatment *in vitro* (Figure 2.2A,B) resulted in apoptosis of mouse T-ALL cells (Figure 2.2C). To rule out any potential effects of tamoxifen- or Cre-mediated toxicity on leukemogenesis, we generated *Tal1/Lmo2/R26-CreER^{T2}* mice and treated them with vehicle or tamoxifen, but observed no significant effects on disease progression or leukemic cell survival (Figure 2.3A,B). Collectively, these data

indicate that RUNX1 is required for T-ALL maintenance *in vivo* and for leukemic cell survival *in vitro*.

During mouse thymocyte development, RUNX1 is expressed in immature DN and DP thymocytes, whereas RUNX3 expression becomes distinct later in more mature CD8 single positive (SP) thymocytes (365). Consistently, we found RUNX1 expressed predominantly in mouse DP leukemic cells, with no RUNX3 protein expression detected (Figure 2.3C), thereby explaining the RUNX1 dependency observed in mouse T-ALL.

Depletion of RUNX1/3 or CBFβ *in vitro* results in apoptosis of human leukemic cells.

To determine whether human T-ALL cells were similarly RUNX1-dependent, we first examined CBFβ, RUNX1 and RUNX3 expression in human T-ALL cell lines and primary patient samples (Figure 2.4A,B). All of the human T-ALL cell lines examined expressed CBFβ and most expressed RUNX1, with low to undetectable levels of RUNX3 (Figure 2.3C). However, RUNX1 and RUNX3 were co-expressed in KOPTK1 and LOUCY cell lines and in 5 of 8 primary pediatric T-ALL samples examined (Figure 2.4A,B). We reduced RUNX1 expression in human T-ALL cell lines (Jurkat, KOPTK1, PF382 and RPMI8402) by expressing 2 independent *RUNX1*-specific shRNAs and, as reported previously (237), observed significant increases in apoptotic cells (Figure 2.5A-C). We also investigated RUNX3-dependency in KOPTK1, Jurkat, and RPMI8402

cell lines. Consistent with the expression data, *RUNX3* reduction induced significant cell death in KOPTK1 cells, but not in the Jurkat cell line (Figure 2.5D,E), indicating that when they are expressed, both RUNX1 and RUNX3 can support the survival of human T-ALL cell line. Knockdown of *CBFβ*, the binding partner of RUNX proteins, also induced apoptosis (Figure 2.5F,G), revealing pro-survival roles for the CBFβ/RUNX1 and CBFβ/RUNX3 heterodimer in TALL.

CBFβ/RUNX inhibition induces apoptosis of human T-ALL cells and patient samples.

The observation that RUNX1 and/or RUNX3 are required for the survival of mouse and human leukemic cell suggests that RUNX proteins could be potential therapeutic targets in T-ALL. The Bushweller laboratory developed a series of small molecule inhibitors designed to interfere with CBFβ binding to RUNX proteins, thereby leaving them in an auto-inhibited state (366); the inhibitor AI-10-104 is a potent derivative among them (Figure 2.6A). AI-10-104 treatment induced a dose-dependent decrease in the CBFβ/RUNX1 and CBFβ/RUNX3 heterodimers detected in human T-ALL cells without detectable effects on CBFβ, RUNX1 or RUNX3 protein levels (367). These data confirm that the AI-10-104 inhibitor interferes with the formation of the CBFβ/RUNX1 and/or CBFβ/RUNX3 heterodimers and suggest that AI-10-104 impedes the function of RUNX proteins in T-ALL cells. Consistent with the RUNX1/3 or CBFβ depletion data, treatment of human T-ALL cell lines with AI-10-104 induced apoptosis in a

dose dependent manner, whereas treatment with 10μM of the inactive analogue AI-4-88 had no effect on leukemic growth or viability (Figure 2.6B,C). Notably, LOUCY ETP-ALL cells which do not express TAL1 or mutant NOTCH1 (Table 2.1) were resistant to AI-10-104 treatment (Table 2.2: GI_{50} = 11μM).

We also examined primary pediatric T-ALL samples for their sensitivity to the CBFβ/RUNX inhibitor AI-10-104. Treatment of diagnostic and relapsed pediatric T-ALL samples with AI-10-104 *in vitro* inhibited the cell growth with an average GI_{50} of 2.4μM (Figure 2.6E) and induced apoptosis (Figure 2.6G,H), whereas treatment with the inactive compound AI-4-88 had no effect on the growth/viability of primary T-ALL samples (Figure 2.6D,H). Moreover, AI-10-104 sensitivity correlated with RUNX1/3 expression levels in 7 of 8 T-ALL patient samples selected at random (Figure 2.6F).

RUNX1 is required for hematopoietic stem and progenitor cell development and survival (56,57) raising the possibility that RUNX inhibition in leukemic patients may result in on target effects on normal hematopoietic stem and progenitor cells. We performed dose response studies on bone marrow samples from 3 independent healthy donors. Treatment of normal human hematopoietic cells with AI-10-104 resulted in an average GI_{50} of 15.4μM (Figure 2.7F), which exceeded the average GI_{50} observed for primary patient leukemic samples by 7-fold. Unfortunately, the pharmacokinetics of the current AI-10-104 inhibitor preclude its preclinical testing in vivo. Nonetheless, these data suggest a

therapeutic window may exist for optimized derivatives of AI-10-104 in T-ALL patients.

RUNX dependency extends to TAL1-negative, TLX3-transformed human T-ALL cells.

Unexpectedly, the RUNX inhibitor AI-10-104 induced cell growth arrest and apoptosis in the TAL1-negative T-ALL cell lines including TALL-1, HPB-ALL and DND-41 (Figure 2.6B, (367)). HPB-ALL and DND41 cell lines are TLX3-transformed T-ALL cells, where RUNX1 was proposed to function as a tumor suppressor (323). To validate the inhibitor results, we investigated the reliance of HPB-ALL cells on RUNX1 genetically. We transduced HPB-ALL cell lines with lentiviruses expressing shRNA against GFP control or *RUNX1* and observed that reduction of *RUNX1* expression significantly induced leukemic cell apoptosis (Figure 2.8), which supports the inhibitor data. These results indicate that RUNX1 is required for the survival of T-ALL cells in the absence of the cooperation with TAL1, and that RUNX1 might be oncogenic in TLX3-positive T-ALL cells.

Discussion

We provide genetic evidence that RUNX1/3 have crucial pro-survival roles in T-ALL *in vivo* and *in vitro* even in TAL1-negative T-ALL cells. In addition, we showed that RUNX proteins can be targeted by using a small molecule inhibitor

interfering with CBFβ binding to RUNX proteins in order to inhibit T-ALL pathogenesis.

Our data are supported by the demonstration that a recently developed CDK7 inhibitor (THZ1) exhibited selectivity for human T-ALL cells and was shown to act via suppression of the RUNX transcriptional network (364). Although CDK7 is a component of the general transcription factor IIH (TFIIH) complex, low dose THZ1 treatment of human T-ALL cells affected the transcription of a subset of genes; with RUNX1 expression most profoundly affected.

Importantly, we demonstrate that the pro-survival roles for RUNX1 revealed in our mouse TAL1/LMO2 T-ALL model translate to human T-ALL cells transformed by TAL1, TLX3 and/or NOTCH1. We hypothesize that RUNX1 supports TLX3-transformed cells through interaction with activating NOTCH1 in HPB-ALL, which will be discussed in Chapter 3. What remains unclear is whether T-ALL cells that do not express TAL1 or activated NOTCH1 also depend on the RUNX transcription factors for survival. We attempted to address this issue in LOUCY cells (TAL1- and NOTCH1-negative), which proved relatively resistant to AI-10-104 treatment (Table 2.2), suggesting that the TAL1 and/or NOTCH1 status determines the RUNX dependency. Based on the prevalence of TAL1 and NOTCH1 activation in T-ALL, we expect most T-ALLs to be sensitive to RUNX inhibition. Consistent with our findings, Jenkins et al., found mouse T-ALLs

transformed by activated NOTCH1 and all human T-ALL cell lines examined (n=15) depend on RUNX1 for their survival (Catherine Jenkins and Andrew Weng, manuscript submitted 2017).

Since RUNX1 is involved in T-cell development, we targeted RUNX1 in fully transformed leukemic cells and demonstrated that RUNX1 supports the maintenance of leukemia. However, whether RUNX1 is required for T-ALL initiation remains to be determined. A previous study that indirectly repressed RUNX1 by NOTCH1 in leukemia-initiating or stem cell population (368) implies that the role of RUNX1 in T-ALL initiation might not be the same as the role it plays in the maintenance of leukemia. In line with this, ENU treatment of chimeric *Runx1*-deficient mice (*Runx1*$^{lacZ/lacZ}$) induced T-ALL suggesting that *Runx1* depletion predisposes progenitor cells to leukemia (369). However, it is not clear how *Runx1*-deficient cells differentiate into the lymphoid lineage to give rise to leukemia. Thus, it would be worth targeting RUNX1 in developing T-cells, for example ablating *Runx1* floxed alleles using *Lck-cre*, to clearly define RUNX1 contribution to leukemia initiation.

Methods and Materials

Mice A cohort of *Tal1/Lmo2/Rosa26(R26)-CreER*^{T2}*Runx1*$^{f/f}$ mice was generated by mating *Tal1/Lmo2* mice with Rosa26-CreERT2Runx1$^{f/f}$ mice. Tal1/Lmo2/Rosa26-CreERT2Runx1$^{f/f}$ leukemic cells were transplanted into F1 (FVB/N x C57BL/6J) recipient mice and corn oil (Sigma, C-8267) or Tamoxifen

(1mg Sigma, T-5648) was intraperitoneally injected for 3 days one week after transplantation. All animal procedures performed in this study were approved by the University of Massachusetts Medical School Institutional Animal Care and Use Committee.

Primary mouse and patient T-ALL cells and cell lines. Mouse *Tal1/Lmo2/R26-CreER^{T2}Runx1$^{f/f}$* T-ALL cells were treated with ethanol or 5 or 10 nM of 4-OHT (Sigma) for 24 hours, washed with PBS, and cultured for 1 or 2 days prior to further analyses. Primary human T-ALL samples were obtained from children with T-ALL enrolled in clinical trials at the Dana-Farber Cancer Institute or collaborating Institutions, or from the University of Massachusetts Memorial Hospital. Samples were collected with informed consent and with approval of the institutional review board. Leukemic blasts were isolated from peripheral blood or bone marrow as previously described (207).

RUNX and CBFβ silencing. The lentiviral pLKO.1-puro vectors carrying shRNA targeting RUNX1 and RUNX3 were generously provided by Dr. Marjorie Brand (Ottawa Hospital Research Institute). The lentiviral pLKO.1-CBFβ vectors were purchased from the shRNA core at University of Massachusetts Medical School. Viruses were generated and human T-ALL cell lines infected as previously described (93). The level of knockdown was determined using qRT-PCR and immunoblotting 4 days after infection.

Cell viability and death assays. Human T-ALL cell lines or T-ALL patient samples were cultured for 3 days in the presence of DMSO or various concentrations of AI-10-104 or AI-4-88. Metabolic activity was assayed by MTS cell proliferation colorimetric assay (CellTitre96 AQueous One Solution Cell Proliferation Assay, Promega) or CellTiter-Glo (CellTiter-Glo Luminescent Cell Viability Assay, Promega) and measured using a Beckman Coulter DTX880 plate reader. Absorbance values were normalized to DMSO control. Human T-ALL cell lines transduced with lentiviruses or treated with AI-10-104 or AI-4-88 were stained with Annexin V-FITC and 7AAD to detect apoptotic cells and with anti-CD4 antibody, and analyzed by flow cytometry.

Genomic DNA and RNA analyses. Total RNA was extracted using Trizol and cDNA was synthesized using Superscript First-Strand Synthesis System (Invitrogen). Quantitative realtime PCR assays were performed using the AB7300 Detection System (Applied Biosystem) using POWER SYBR Green Master Mix (Applied Biosystem) and gene specific primers. Gene expression was determined using the ΔΔCT method normalized to *GAPDH* for human or *β-Actin* for mouse transcripts, unless otherwise specified. Using isolated genomic DNA, *Runx1* deletion was determined by PCR as described previously (57).

Immunoblotting. To examine protein expression in human T-ALL cells, cells were lysed in modified radioimmunoprecipitation assay (RIPA) buffer, transferred to a membrane, and probed with antibodies to RUNX1 (ab23980, Abcam),

RUNX3 (MAB3765, R&D System), TAL1 (sc-12984, Santa Cruz), MYB (05-175, Millipore), NOTCH1 (Val1744, Cell signaling), MYC (N262, Santa Cruz), or ERK1/2 (9102, Cell Signaling). Blots were imaged using ImageLab Software (Bio-Rad).

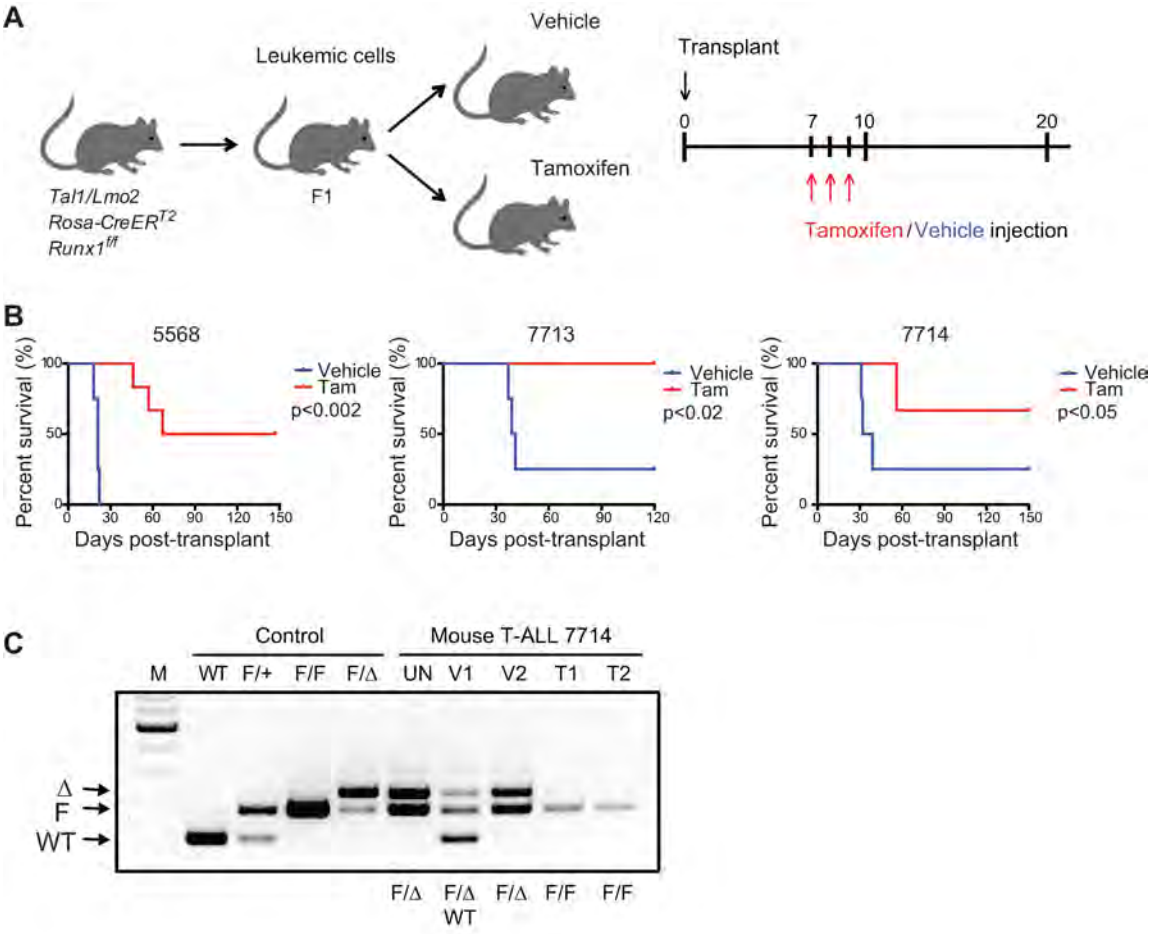

Figure 2.1. RUNX1 is required for the maintenance of leukemic growth *in vivo*. (A) Experimental strategy used to determine the effects of *Runx1* deletion on leukemia progression *in vivo*. Three independent mouse T-ALLs from *Tal1/Lmo2/R26-CreER^{T2} Runx1$^{f/f}$* mice were transplanted into mice and treated with vehicle or tamoxifen one week later for 3 days. (B) Kaplan-Meier survival curves are shown for 3 mouse T-ALLs and the difference in overall survival between vehicle and tamoxifen treated groups assessed by the log-rank test (n=4 for Vehicle, n=6 for Tam group in all 3 experiments). (C) Mice that develop disease derive from T-ALL subclones that retain the floxed *Runx1* allele. For the control samples, genomic DNA was isolated from tail biopsies of wild type, Runx1$^{f/+}$ and Runx1$^{f/f}$ mice (designated WT, F/+ and F/F). For the deleted control, DNA was isolated from mouse T-ALL cell line 1143, which was derived from a

leukemic *Tal1/Lmo2/R26-CreER^{T2}Runx1$^{f/f}$* mouse that was treated with 4-OHT in vitro for 48h (designated F/Δ). Analysis of primary mouse T-ALL 7714 reveals a *Tal1/Lmo2/Rosa26-CreER^{T2}Runx1$^{f/Δ}$* genotype likely due to leaky Cre expression in the primary tumor. DNA was isolated from untreated mouse T-ALL 7714 cells (UN) and from tumor tissue isolated from transplanted mice at the time of sacrifice. V1 and V2 refers to tumor DNA isolated from 2 independent vehicle treated mice transplanted with mouse T-ALL 7714 cells. The WT band likely reflects the presence of normal cells in the tumor specimen. T1 and T2: Tumor DNA isolated from 2 independent tamoxifen treated mice transplanted with mouse T-ALL 7714 cells. These tamoxifen-treated mice succumbed to disease and selected for leukemic clones that retained the floxed Runx1 allele. M indicates DNA ladder used to estimate fragment size.

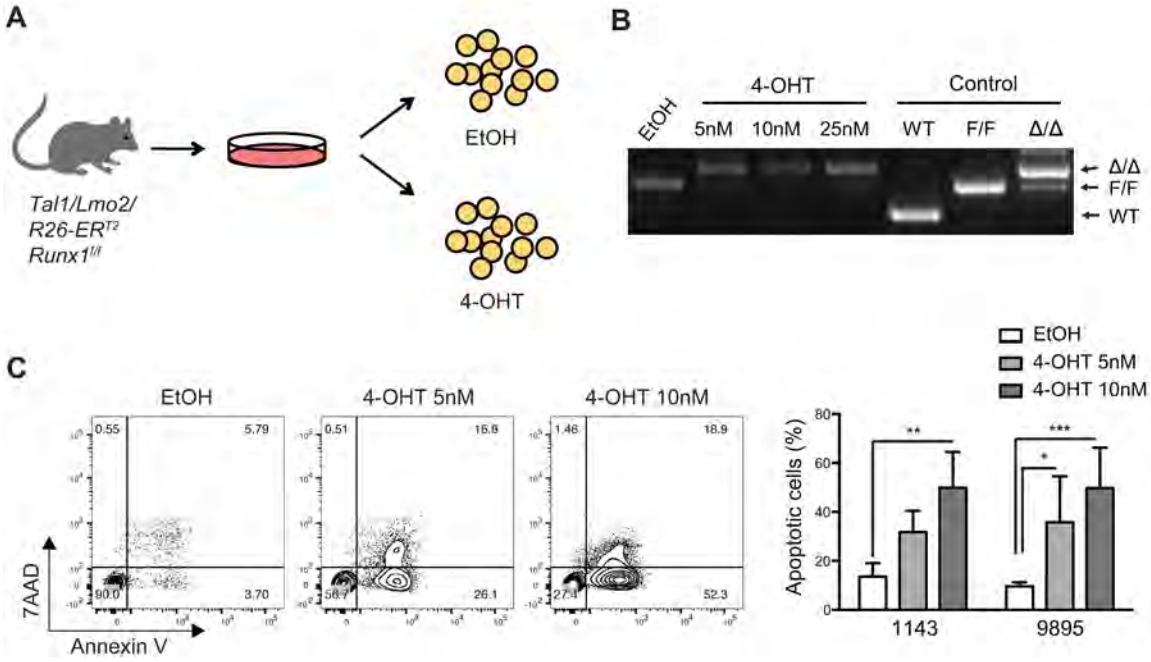

Figure 2.2. RUNX1 supports survival of mouse leukemic cells *in vitro*. (A) Experimental strategy used to determine the effects of Runx1 deletion on mouse T-ALL survival *in vitro*. (B) Genomic DNA was isolated from mouse T-ALL cells 48 hours after EtOH or 4-OHT treatment to examine *Runx1* deletion by genomic PCR. (C) Mouse T-ALLs (1143 and 9895) were treated with vehicle or 4-OHT for 72 hours, stained with Annexin V-FITC and 7-AAD, and analyzed by flow cytometry. The quantification of Annexin-V positive cells from 4 independent experiments is shown as means ± SD (right) (*p<0.05, **p<0.005, ***p<0.0005 Two-way ANOVA multiple comparisons test).

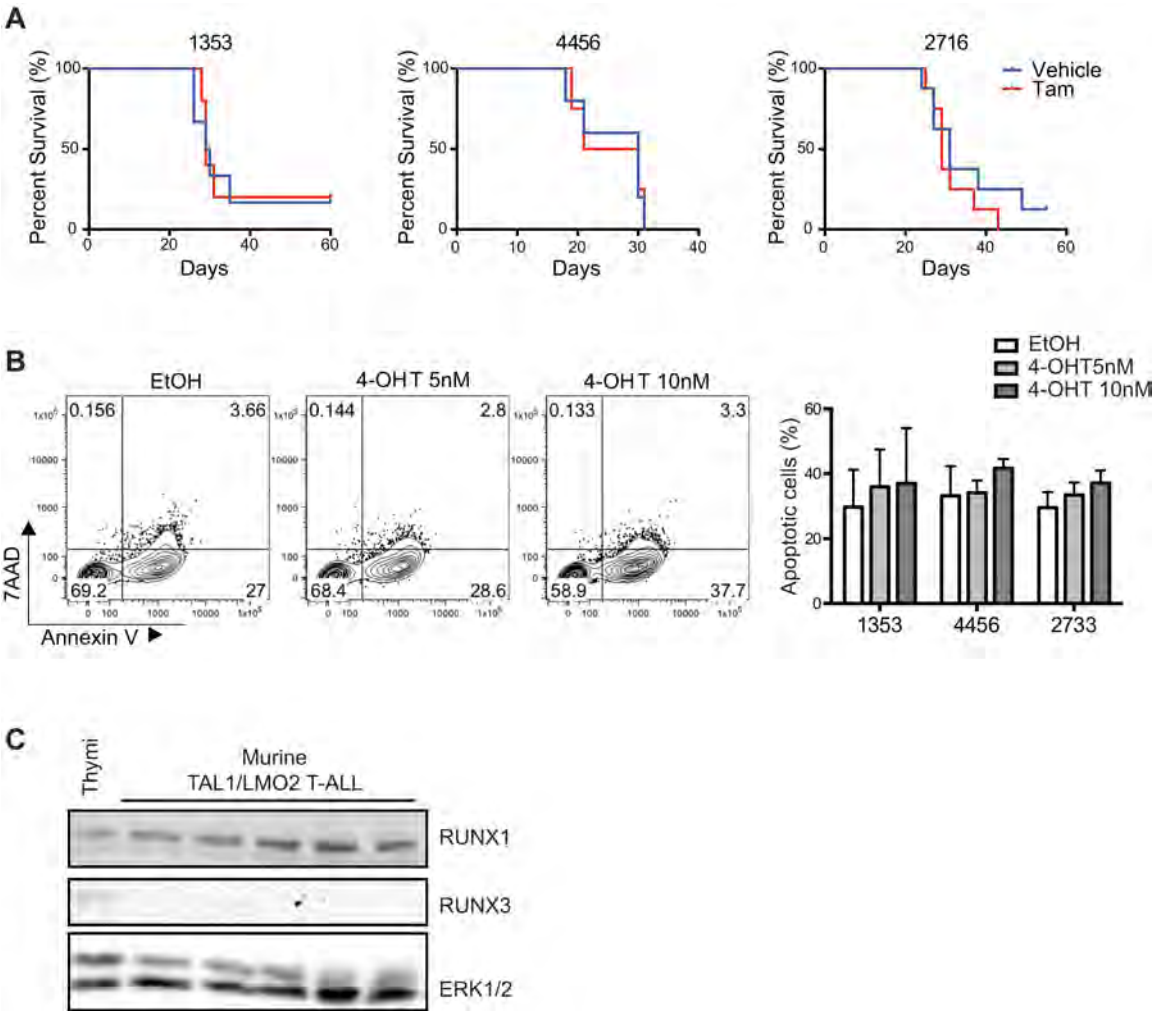

Figure 2.3. Cre activation has no significant effects on mouse T-ALL growth *in vitro* and RUNX3 protein expression in mouse leukemic cells. (A) Mouse T-ALL cells from *Tal1/Lmo2/R26-CreER*^{T2} mice were transplanted into F1 mice and one week later tamoxifen was administered for 3 days. The survival curves for 3 mouse T-ALLs (1353, 4456 and 2716) were estimated using the Kaplan-Meier method. (B) The 2 independent *Tal1/Lmo2/R26-CreER*^{T2} mouse T-ALL cells were treated with vehicle (EtOH) or 4-OHT and the apoptotic cells were determined by Annexin V-FITC and 7AAD staining followed by flow cytometry. The averages of 3 to 4 independent experiments are shown as mean ± SD. (C) RUNX1 and RUNX3 expression levels in mouse thymus and Tal1/Lmo2 mouse T-ALL cell lines were analyzed by immunoblotting. ERK1/2 was used as a loading control.

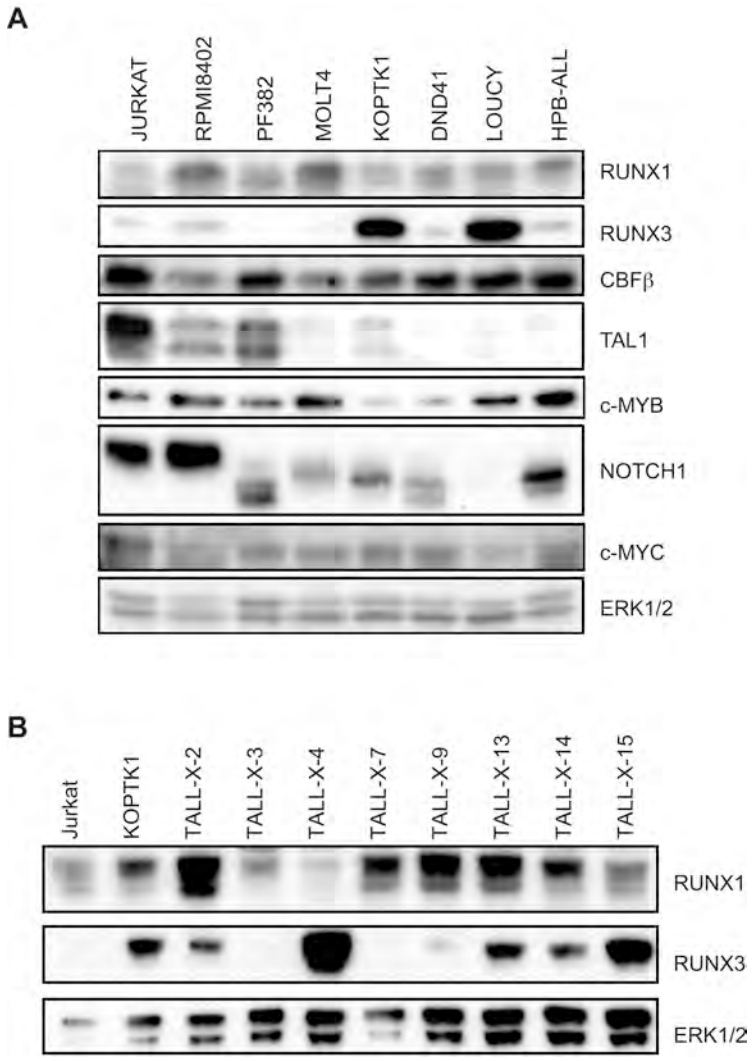

Figure 2.4. RUNX1, but not RUNX3, is ubiquitously expressed in human T-ALL cell lines and primary patients T-ALL samples. (A) Protein was isolated from human T-ALL cell lines and RUNX1, RUNX3, CBFβ, TAL1, MYB, NOTCH1, and MYC protein levels were determined by immunoblotting. ERK1/2 was used as a loading control. (B) RUNX1 and RUNX3 expression in Jurkat, KOPTK1, and 8 T-ALL patient samples were analyzed by immunoblotting. ERK1/2 was used as a loading control.

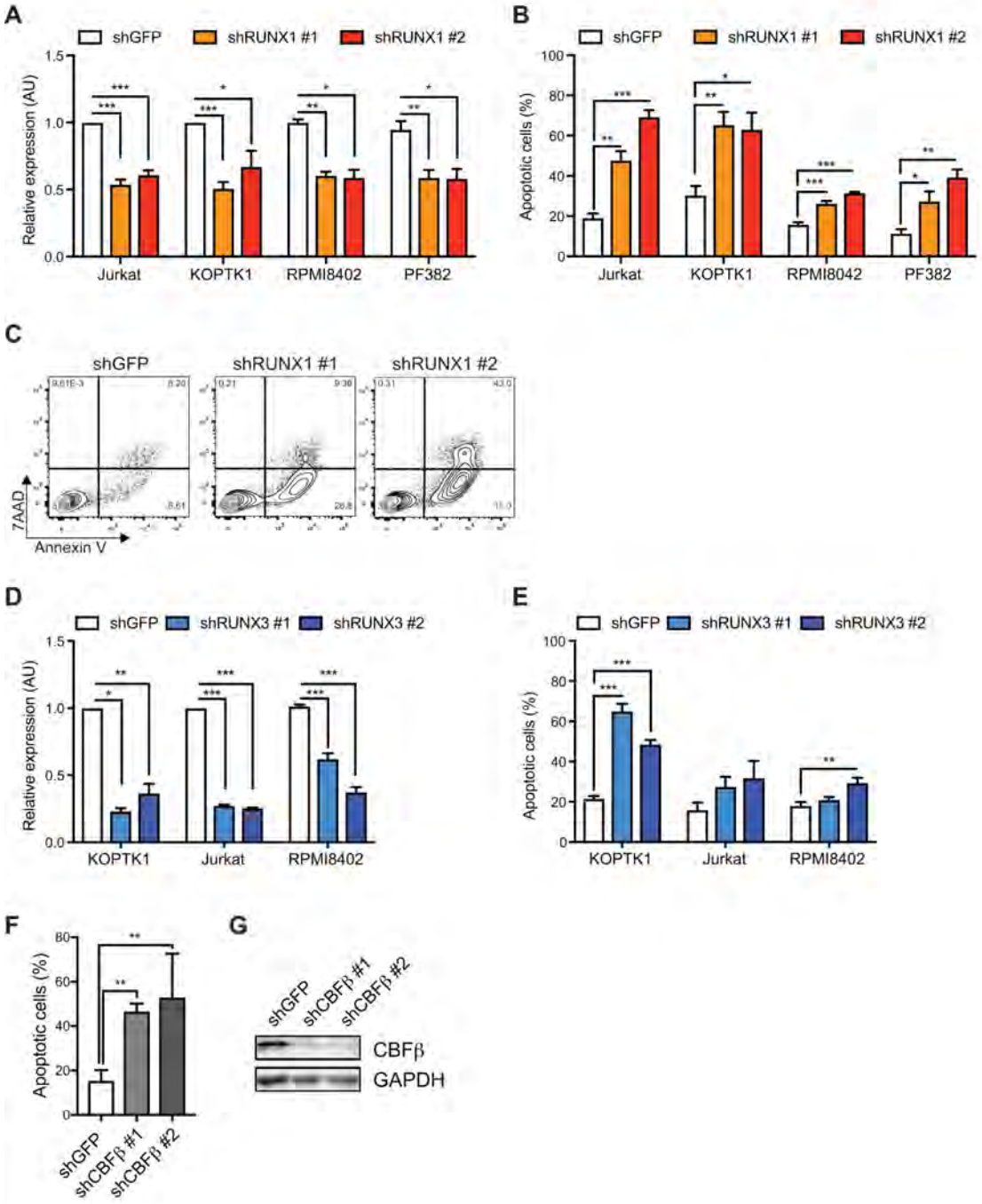
A
shGFP
shRUNX1 #1
shRUNX1 #2
Relative expression (AU)
Jurkat
KOPTK1
RPMI8402
PF382
B
Apoptotic cells (%)
C
7AAD
Annexin V
D
shRUNX3 #1
shRUNX3 #2
E
F
shCBFβ #1
shCBFβ #2
G
CBFβ
GAPDH

Figure 2.5. Knockdown of *RUNX1*, *RUNX3*, and *CBFβ* results in apoptosis. (A) Jurkat, KOPTK1, RPMI8402, and PF382 human T-ALL cell lines were infected with lentiviruses expressing control shRNA or 2 shRNAs specific for *RUNX1*. *RUNX1* mRNA and protein levels were examined by real time quantitative PCR and immunoblotting. (B) *RUNX1* knockdown results in apoptosis of leukemic cells. Control (GFP) and *RUNX1* shRNA transduced human cell lines were stained with Annexin V-FITC and 7AAD and analyzed by flow cytometry 6 days after infection. The percentage of apoptotic cells was determined by Annexin V/7AAD staining and analyzed by flow cytometry. Four independent experiments were performed, and data are shown as mean ± SD. (C) A representative cell death flow profile of the Jurkat cell line is shown. (D) *RUNX3* mRNA levels in KOPTK1, Jurkat, and RPMI8402 cells transduced with control (GFP) or RUNX3-specific shRNA were measured by qRT-PCR. *RPS9* was used for normalization. (E) Apoptotic leukemic cells upon *RUNX3* knockdown in KOPTK1, Jurkat, and RPMI8402 human T-ALL cells were determined by Annexin V-FITC/7-AAD staining followed by flow cytometry. (F) *CBFβ* knockdown also induces apoptosis. Control (GFP) or *CBFβ* shRNA transduced Jurkat cells were stained with Annexin V-FITC and 7AAD and analyzed by flow cytometry. Four independent experiments were performed, and data are shown as mean ± SD. (G) CBFβ protein levels in control and knockdown cells were analyzed by immunoblotting. (*$p<0.05$, **$p<0.005$, ***$p<0.0005$, One-way ANOVA multiple comparisons test)

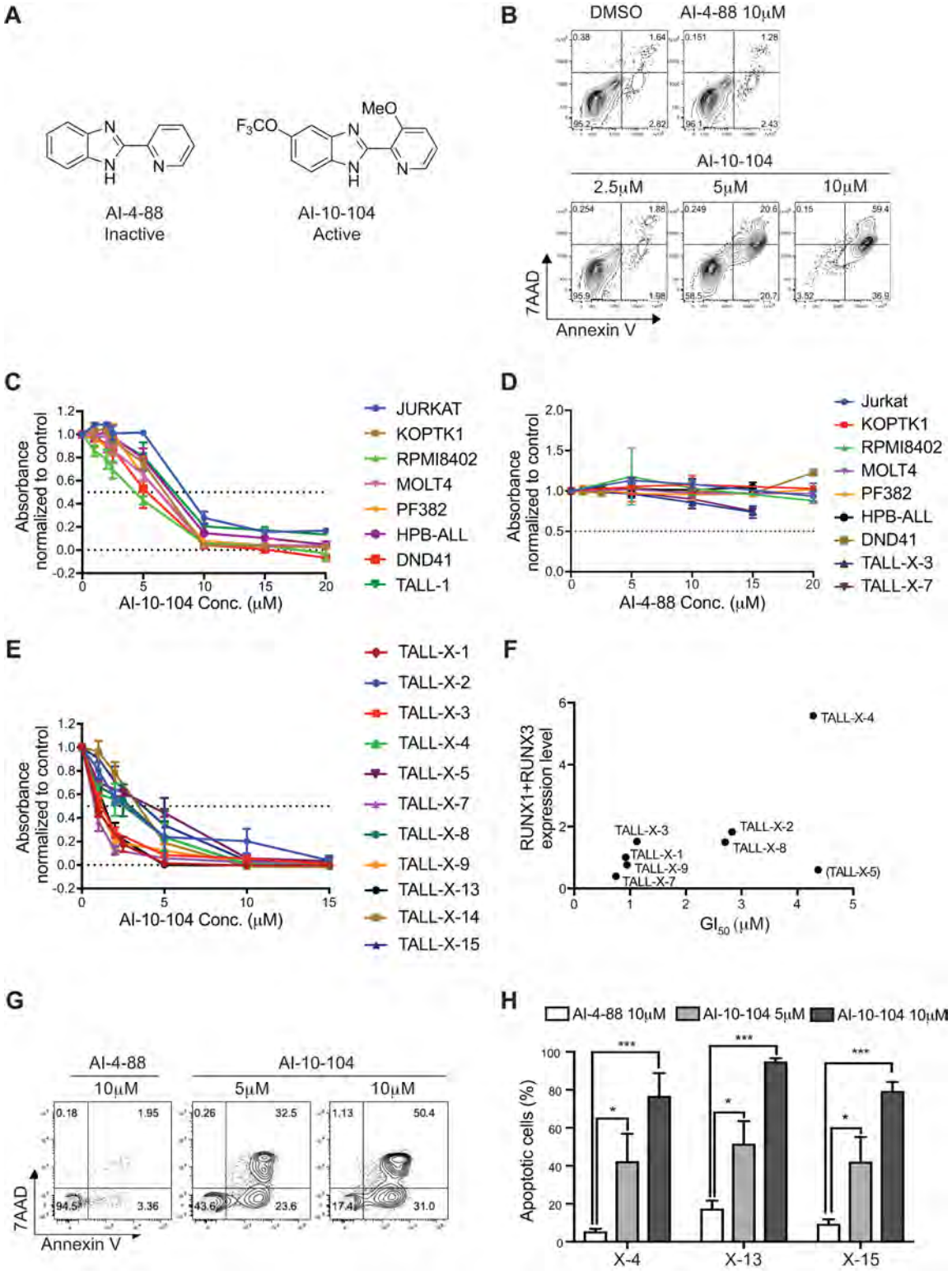
A
AI-4-88
Inactive
AI-10-104
Active
B
DMSO
AI-4-88 10μM
AI-10-104
2.5μM
5μM
10μM
7AAD
Annexin V
C
Absorbance normalized to control
AI-10-104 Conc. (μM)
JURKAT
KOPTK1
RPMI8402
MOLT4
PF382
HPB-ALL
DND41
TALL-1
D
Absorbance normalized to control
AI-4-88 Conc. (μM)
Jurkat
KOPTK1
RPMI8402
MOLT4
PF382
HPB-ALL
DND41
TALL-X-3
TALL-X-7
E
Absorbance normalized to control
AI-10-104 Conc. (μM)
TALL-X-1
TALL-X-2
TALL-X-3
TALL-X-4
TALL-X-5
TALL-X-7
TALL-X-8
TALL-X-9
TALL-X-13
TALL-X-14
TALL-X-15
F
RUNX1+RUNX3 expression level
GI50 (μM)
TALL-X-4
TALL-X-3
TALL-X-2
TALL-X-8
TALL-X-1
TALL-X-9
TALL-X-7
(TALL-X-5)
G
AI-4-88
10μM
AI-10-104
5μM
10μM
7AAD
Annexin V
H
AI-4-88 10μM
AI-10-104 5μM
AI-10-104 10μM
Apoptotic cells (%)
X-4
X-13
X-15

Figure 2.6. Treatment with a RUNX-CBFβ inhibitor impairs the growth of human T-ALL cell lines and primary pediatric T-ALL samples. (A) Structures of inactive (AI-4-88) and active (AI-10-104) inhibitors. (B) The human T-ALL cell line Jurkat was treated with vehicle, 10μM of the inactive analogue AI-4-88, or with increasing concentrations of AI-10-104 for 4 days. Cells were stained with Annexin V-FITC and 7AAD and analyzed by flow cytometry. A representative flow profile of 3 independent experiments is shown. (C) Eight human T-ALL cell lines were treated with increasing concentrations of AI-10-104 for 3 days and cell growth/metabolism was analyzed by an MTS assay. (D) Human T-ALL cell lines and T-ALL patient samples were treated with increasing concentrations of the inactive analogue AI-4-88 (1-20μM) for 3 days. Cell growth/metabolism were analyzed by an MTS assay. (E) Eleven pediatric T-ALL patient samples were treated with vehicle or increasing concentrations of AI-10-104 (1-15μM) for 3 days and cell growth/metabolism was analyzed by a CellTiterGlo assay. Absorbance values were normalized to those obtained with vehicle control. (F) Sensitivity of patient samples to AI-10-104 (GI50) correlates with RUNX1 and RUNX3 expression levels (Pearson's r=0.8781, p=0.0093, sample TALL-X-5 excluded). (G) Patient sample TALL-X-15 was treated with 10μM of AI-4-88 or with 5 or 10 μM of AI-10-104 for 6 days. Cells were stained with Annexin V-FITC and 7AAD and analyzed by flow cytometry. (H) Randomly selected patient samples (n=3) were treated with 10μM of AI-4-88 or 5, 10μM of AI-10-104 for 6 days. Apoptotic cells were determined by Annexin V-FITC and 7AAD staining followed by flow cytometry. Three independent replicates are shown as mean ± SEM (*$p<0.05$, ***$p<0.0005$, ANOVA multiple comparisons test).

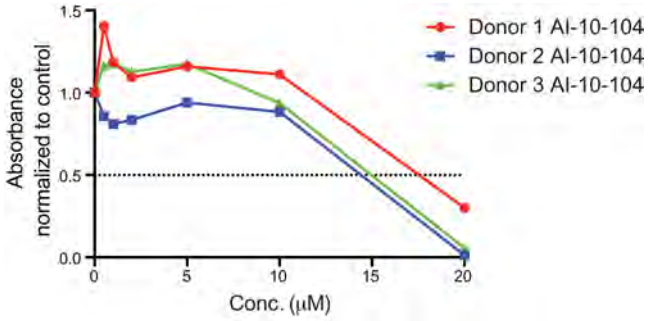

Sample ID	GI_{50} of AI-10-104 (μM)
Donor 1	16.6
Donor 2	17.04
Donor 3	12.54
Average GI_{50}	15.39

Figure 2.7. RUNX1/3-CBFβ inhibitor is not detrimental to normal human hematopoietic stem and progenitor cells at low concentration. G-CSF mobilized normal human BM cells were treated with increasing concentrations of AI-10-104 for 3 days and effects on cell growth/metabolism were determined by MTS assay. The GI_{50} of each donor cell sample was calculated using Graph Pad Prism 7 software.

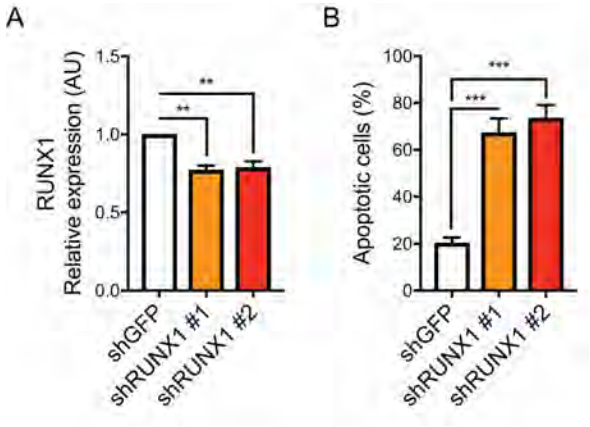

Figure 2.8. Reduction of RUNX1 expression in TLX3-transformed T-ALL cell line induces cell apoptosis. (A) The human T-ALL cell line HPB-ALL was transduced with lentiviruses expressing shRNAs against GFP or *RUNX1*. Gene expression in control or *RUNX1* knockdown cells was determined by qRT-PCR. Three independent experiments were performed, and data are shown as mean with error bars representing ± SEM. (B) Apoptotic cells were quantified by Annexin V/7AAD staining followed by flow cytometry. Data are shown as the mean of 3 independent experiments with error bars representing ±SEM (**p<0.005, ***p<0.0005).

Table 2.1. Expression and mutation status in patient samples and human T-ALL cell lines.

Patient samples

	RUNX1	TAL1 detected[+]	NICD detected[+]	NOTCH1	FBW7
TALL-X-1	WT	Yes	No	WT	WT
TALL-X-2	WT	Yes	Yes	p.P2514fs, p.F1592S	WT
TALL-X-3	WT	Yes	Yes	p.L1593fs	WT
TALL-X-4	WT	Yes	Yes	p.F1592S	WT
TALL-X-5	WT	Yes	Yes	p.L1585P	WT
TALL-X-7	WT	Yes	Yes	p.L1600P	p.R479Q
TALL-X-8	WT	Yes	Yes	p.R1598P	p.T450fs, p.R689W
TALL-X-9	WT	No	Yes	p.R1598P	WT
TALL-X-13	WT	Yes	Yes	WT	WT
TALL-X-14	WT	No	No	WT	p.R465H
TALL-X-15	WT	Yes	Yes	WT	WT

Human cell lines

	RUNX1	RUNX3	NOTCH1	FBW7
Jurkat	p.A122T	WT	WT	p.R505C
KOPTK1	N/A	N/A	p.L1600P, p.P2514fs*4	WT
RPMI8402	WT	WT	p.E1583_Q1584insPVELMPPE, p.Q1584>HRGADAAGA	p.R465H
MOLT4	WT	WT	p.L1600P, p.P2515fs	WT
PF382	WT	WT	p.L1574P, p.P2493fs*>67	WT
HPB-ALL	WT	WT	p.L1574P, p.D2443fs*39	p.R465H, p.D527G
DND41	WT	WT	p.L1593P, p.D1609V, p.V2444fs*35	WT
TALL-1	WT	WT	WT	WT
LOUCY	WT	WT	WT	WT

RUNX3 mutation status in patient samples is not available.

[+]As determined by western blot analysis.

N/A, Not available

Table 2.2. Human T-ALL cell lines and primary patient samples are sensitive to AI-10-104 treatment.

	GI_{50} ± SEM(μM)
Cell Line	
Jurkat	8.2 ± 0.4
KOTPK1	5.9 ± 0.5
PRMI8402	4.3 ± 0.4
MOLT4	5.7 ± 0.3
PF382	5.8 ± 0.3
HPB-ALL	6.6 ± 0.5
DND-41	5.2 ± 0.5
TALL-1	7.0 ± 0.5
LOUCY*	11.0 ± 1.1
Average	6.1
Patient sample	
Diagnostic	
TALL-X-1	0.9 ± 0.1
TALL-X-2	2.8 ± 0.6
TALL-X-3	1.1 ± 0.1
TALL-X-4	4.3 ± 6.2
TALL-X-5	4.4 ± 1.0
TALL-X-7	0.7 ± 0.1
TALL-X-8	2.7 ± 0.8
TALL-X-9	0.9 ± 0.1
Relapsed	
TALL-X-13	1.3 ± 0.1
TALL-X-14	3.0 ± 0.5
TALL-X-15	4.3 ± 0.8
Average	2.4

GI_{50} values of the inhibitor are shown for each cell line and patient sample analyzed 2 or 3 times.

*GI_{50} of LOUCY cell line is excluded from the average of GI_{50}.

Table 2.3. shRNA clones used in the study

shRNA clone	**Clone ID**	Target gene
shRUNX1 #1	TRCN0000013659	*RUNX1*
shRUNX1 #2	TRCN0000013660	*RUNX1*
shRUNX3 #1	TRCN0000235675	*RUNX3*
shRUNX3 #2	TRCN0000235674	*RUNX3*
shCBFβ#1	TRCN0000016644	*CBFβ*
shCBFβ#2	TRCN0000016645	*CBFβ*

Chapter III

RUNX1 supports T-ALL survival by regulating *Myb* and *Myc* enhancer activity

Data from the following chapter are a part of a published paper:

AHyun Choi, Anuradha Illendula, John A. Pulikkan, Justine E. Roderick, Jessica Tesell, Jun Yu, Nicole Hermance, Lihua Julie Zhu, Lucio H. Castilla, John H. Bushweller and Michelle A. Kelliher. RUNX1 is required for oncogenic *Myb* and *Myc* enhancer activity in T cell acute lymphoblastic *Blood* (2017) 12;130(15):1722-1733

The manuscript has been edited for this thesis to show the results generated by AHyun Choi. Data generated by others are noted.

Introduction

Transcriptional regulation is a process of interplay of transcription factors, cofactors, other chromatin regulators, and core components of basal transcriptional machinery that bind to regulatory elements such as promoters, enhancers, and silencers of genes. It has been suggested that multiple transcription factors bind cooperatively to individual enhancer loci and recruit cofactors with polymerase II to target genes for expression regulation (370–372).

RUNX1, a critical transcription factor for hematopoiesis and lymphoid lineage development, was observed to bind mostly to intergenic or intragenic regions in mouse hematopoietic stem and progenitor cells (373). In T-ALL cells, RUNX1 shares its binding sites with TAL1 and NOTCH1 (237,325). TAL1 binds to its target loci as an interconnected transcriptional regulatory complex and most of TAL1 binding sites in T-ALL cells are mapped to intergenic or intragenic regions where enhancer elements are located (93,237). ChIP-seq studies for NOTCH1 in T-ALL demonstrated that the majority of dynamic NOTCH1 binding sites that are sensitive to inhibition of NOTCH1 signaling are mainly located at distal sites rather than at promoter regions of target genes (324). Therefore, it appears that in T-ALL RUNX1 binds to enhancer regions along with TAL1 and NOTCH1 in order to regulate critical genes for T-ALL pathogenesis.

In Chapter III, we demonstrate that *Runx1* deletion in mouse T-ALL cells interferes with *Myb* and *Myc* enhancer activity resulting in decreases in gene

expression. Similarly, we observed that not only RUNX1, but also RUNX3 binds to *MYB* and *MYC* enhancer regions in the KOPTK1 human T-ALL cell line. Furthermore, we demonstrate that RUNX1 may be important for the maintenance of chromatin loop formation between promoter and enhancer elements of the MYB gene.

Results

RUNX1 supports the expression of a subset of TAL1- and NOTCH1-regulated genes

We hypothesized that *Runx1* deletion, although unlikely to influence transgenic *Tal1* mRNA levels, may suppress TAL1/LMO2-regulated genes important in mouse thymocyte survival, proliferation, and differentiation. RUNX1 regulates genes important in thymocyte development and represses CD4 expression during the DP to SP thymocyte transition (62). In addition to significant decreases in the RUNX1-regulated genes *Cxcr4* and *Bcl2*, we observed increases in *Cd4* and *Cdkn1a* mRNA expression in *Runx1*-deleted mouse T-ALLs (Figure 3.1A). Similarly, RUNX1 suppression in mouse and human T-ALL cell lines resulted in a partial derepression of the CD4 co-receptor, resulting in statistically significant increases in the mean fluorescent intensity of cell surface CD4 staining in RUNX1-deficient T-ALL cells (Figure 3.3). These data suggest that in mouse and human T-ALL cells, RUNX1 depletion may stimulate leukemic cell differentiation prior to induction of apoptosis.

Significant reductions in *Myb*, *Gata3* and *Cdk6* expression were also observed in *Runx1*-deleted mouse T-ALL cells and in the human TAL1-positive T-ALL cell line Jurkat (Figure 3.1A, 3.2). These data reveal that the TAL1-RUNX1-GATA3 autoregulatory loop is conserved in this mouse T-ALL model driven by the TAL1 oncogene. Moreover, we demonstrate that TAL1/LMO2-mediated mouse leukemic growth requires MYB *in vitro* and *in vivo* (367).

Using a RUNX1-regulated gene set and genes induced upon NOTCH1 reactivation (237,374), we performed Gene Set Enrichment Analysis (GSEA) and identified a subset of NOTCH1-regulated genes that were also affected by *RUNX1* knockdown in human T-ALL cells (Figure 3.1B; NES=1.49; FDR=0.026). We observed significant reductions in the expression of *Notch1*, *Myc*, *Il7rα*, *Igf1r,* and *Deltex1* mRNAs in the *Runx1*-deleted mouse T-ALL cell line (Figure 3.1C). This is the first report demonstrating that RUNX1 regulates NOTCH1 expression in mouse T-ALL cells. *Runx1* deletion had no effect however, on *Hes1* mRNA levels or on intracellular NOTCH1 binding to the mouse *Hes1* promoter (Figure 3.1C). Similarly, no significant change in human *HES1* expression was observed upon *RUNX1* knockdown in Jurkat cells (Figure 3.2A), indicating that a subset of NOTCH1-regulated genes is RUNX1-dependent. RUNX1 depletion in human T-ALL cell lines consistently decreased the expression of *MYC* and *IL7Rα*. These data are consistent with published chromatin immunoprecipitation sequencing (ChIP-seq) studies demonstrating that RUNX1 co-occupies a subset of

NOTCH1-regulated genes and prior demonstration that RUNX1 and NOTCH1 regulate *IL7R* expression (324).

We demonstrated that the pro-survival role of RUNX1 extends to the TAL1-negative, TLX3-transformed HPB-ALL T-ALL cell line (Figure 2.8). We hypothesized that RUNX1 supports survival of HPB-ALL cells by interaction with NOTCH1 signaling, which is aberrantly activated due to the mutations in HPB-ALL (Table 1, (167)). We validated that the expression of NOTCH1-regulated genes that were dependent on RUNX1 in TAL1-positive T-ALL cells were altered in HPB-ALL cells by RUNX1 knockdown as well; the expression of *MYC*, *IL7R* and *IGF1R* were significantly reduced (Figure 3.2). Reductions in MYB expression were also observed (Figure 3.2), suggesting that RUNX1 may regulate *MYB* expression in the absence of TAL1.

Although the features that predict a RUNX1 dependency remain unclear, several of the TAL1- and NOTCH1-regulated genes supported by RUNX1 are associated with super-enhancers in human T-ALL cells (340), suggesting that enhancer-regulated genes may be uniquely sensitive to the effects of RUNX1 depletion.

RUNX1 is required for TAL1 and NOTCH1 binding and recruitment of active histone mark to oncogene enhancers

Comparisons between the mouse and human *MYB* genes reveal the presence of conserved locus-control-like regions (LCLR) located approximately -92-kb and +15-kb from the mouse *Myb* promoter and -93-kb and +14-kb from human *MYB* promoter (Figure 3.4B, (237,260)). These sites possess several features associated with enhancer activity, including the presence of multiple transcription factors (TAL1, RUNX1, HEB, GATA3 and ETS1), as well as RNA polymerase II, Mediator, BRD4 and acetylated H3K27 (237,340,364). The mouse *Myb* (-92-kb and +15-kb) regions each harbor one canonical RUNX binding site and RUNX1 binding to these conserved regions is observed in mouse T-ALL cells (Figure 3.4B-D). To determine if *Runx1* deletion in mouse T-ALL cells affects TAL1 binding to these regions, we performed chromatin immunoprecipitation followed by real time quantitative PCR (ChIP-qPCR). We observed statistically significant reductions in TAL1 binding to the *Myb* +15-kb and -92-kb enhancer elements (Figure 3.4C,D) and decreases in *Myb* mRNA levels (Figure 3.1A) in the *Runx1*-deleted T-ALL cells. Reductions in TAL1 occupancy were accompanied by significant depletion of the active chromatin mark H3K27ac at these sites (Figure 3.4C, D).

NOTCH1 contributes to T-ALL growth via its direct regulation of MYC (179–181). NOTCH1 regulation of MYC is mediated through a distal enhancer

located 1.27 Mb 3' from the transcriptional start site (TSS) of the mouse *Myc* gene and 1.4 Mb from the TSS of the human *MYC* gene (208,351). This region was designated the NOTCH1-bound *MYC* enhancer (N-Me) and shown to be essential for NOTCH1-mediated *MYC* expression during mouse thymocyte development and for NOTCH1-mediated leukemic transformation (351). We examined intracellular NOTCH1 binding to the N-Me in the *Runx1*-deleted mouse TAL1/LMO2 T-ALL cells. Consistent with the observed reductions in *Myc* mRNA (Figure 3.1C), intracellular NOTCH1 binding at the N-Me and H3K27ac levels were significantly reduced in the *Runx1*-deficient mouse T-ALL cells (Figure 3.5C), whereas no differences in TAL1 or intracellular NOTCH1 binding to gene desert regions were observed (Figure 3.6B). We also found the Histone 3 (H3) levels increased at the enhancer regions examined (Figures 3.4D and 3.5C), suggesting that *Runx1* deletion results in increased H3 loading and a closed chromatin configuration. We used an assay for transposase accessible chromatin (ATAC) and observed decreased ATAC-qPCR enrichment at the N-Me in *Runx1*-deleted leukemic cells (Figure 3.5D). These data suggest that a RUNX1 deficiency results in transcription factor depletion and reduced chromatin accessibility at the N-Me. In addition, treatment of mutant NOTCH1 human T-ALL cells with the RUNX inhibitor resulted in statistically significant reductions in MYC mRNA levels, suggesting that AI-10-104 interferes with NOTCH1/MYC enhancer activity (Figure 3.5E).

In addition to RUNX1, we detected RUNX3 expression in a subset of human T-ALL cell lines and primary patient samples (Figure 2.4) and induced apoptosis upon *RUNX1* or *RUNX3* knockdown in KOPTK1 (Figure 2.5D,E), indicating that both RUNX1 and RUNX3 support the survival of these human T-ALL cells. Consistent with these data, we detected RUNX1 and RUNX3 binding at the N-Me and found *MYC* expression significantly reduced in the RUNX1- or RUNX3-suppressed KOPTK1 cells (Figure 3.7A,C,D). Although we detected RUNX1 and RUNX3 binding at the MYB -93-kb enhancer, neither protein was detected at the +14-kb enhancer, (Figure 3.7A). Suppression of *RUNX1* or *RUNX3* reduced *MYB* expression however, statistical significance was achieved only in the *RUNX1*-silenced cells (Figure 3.7C,D). Unlike *RUNX1*, *RUNX3* suppression in Jurkat cells did not induce apoptosis (Figure 2.5D,E) nor was RUNX3 binding detected at the *MYC* or *MYB* enhancer elements bound by RUNX1 (Figure 3.7B). These data reveal that KOPTK1 cells rely on RUNX1 and RUNX3 to maintain MYC and MYB levels, whereas in Jurkat cells, RUNX1 supports *MYC* and *MYB* expression and RUNX3 does not contribute. Our findings suggest that the relative levels of RUNX1 and RUNX3 may dictate their roles in *MYC* and *MYB* regulation and that TALL survival requires a certain threshold level of CBFβ/RUNX1 and/or RUNX3. Interestingly, we did not observe increased expression of RUNX3 upon RUNX1 knockdown and vice versa (Figure 3.8).

RUNX1 regulates chromatin structure around the *MYB* gene.

It has been demonstrated that enhancer elements located at distal sites regulate the expression of associated genes by physical interactions involving chromatin looping between the enhancer and promoter regions (370,375–377). Transcription factors and cofactors that bind to the enhancer regions have been shown to play key roles in the formation and maintenance of looping structures (378,379). To investigate whether there are chromatin loops between promoter and enhancer regions, we examined whether RUNX1 is required for the formation, we performed chromatin conformation capture (3C) analysis around the *MYB* gene in the Jurkat human T-ALL cell line with or without RUNX1 suppression by doxycycline- induced *RUNX1-shRNA* expression (Figure 3.9A). 3C analysis demonstrated that the *MYB* +14-kb or -93-kb enhancer region was placed in close proximity to the promoter region of *MYB* gene which was released by RUNX1 suppression (Figure 3.9B), consistent with reduced *MYB* expression (Figure 3.9A). These data suggest that RUNX1 regulates *MYB* expression by controlling the activity of enhancer regions and by engaging in chromatin structure formation between the enhancer and promoter elements.

Discussion

We show that a RUNX1 deficiency reduces transcription factor binding at the mouse *Myb* +15-kb and -92-kb enhancers and the NOTCH1 bound *Myc*-enhancer (N-Me). The reductions in TAL1 binding to the mouse *Myb* enhancer

regions in *Runx1*-deleted T-ALL cells are particularly noteworthy as the proximal *Lck* promoter drives *Tal1* expression and consequently, reductions in TAL1 binding at the *Myb* enhancer do not reflect RUNX1 effects on endogenous *Tal1* transcription. These data suggest that in addition to regulating TAL1 expression (237), RUNX1 supports TAL1 binding to the *Myb* enhancer. We also find that *Cdk6* expression depends on RUNX1 (Figure 3.1A), and consistent with our data, Palii et al.(93) showed that RUNX1/3 suppression in Jurkat cells reduced TAL1 binding to several genes important in thymocyte differentiation, including the *CDK6* locus. In this study however, *RUNX1/3* knockdown had no detectable effect on TAL1 expression, suggesting that RUNX1 primarily regulates TAL1 binding. These findings are relevant to T-ALL patients, as most patients activate TAL1 expression via chromosomal rearrangements that displace the TAL1 promoter and thereby subvert RUNX1-mediated effects on TAL1 transcription.

Precisely how a RUNX1 deficiency interferes with TAL1 and intracellular NOTCH1 binding to these enhancer regions, respectively is unclear. RUNX1 has been shown to interact with TAL1 and intracellular NOTCH1 in T-ALL cells (93,380), suggesting that RUNX1 may be a component of both transcriptional complexes. However, the E-box, RUNX, and NOTCH1/CSL/RBJκ consensus sites are dispersed throughout the conserved *Myb* and *Myc* enhancer regions examined, making it unlikely that TAL1/RUNX1 or intracellular NOTCH1/RUNX1 bind as single complexes.

A RUNX1 deficiency results in decreases in the active chromatin mark H3K27ac and increases in H3 loading (Figures 3.4, 3.5), raising the possibility that RUNX1 directly regulates chromatin, recruits histone modifying enzymes, and/or other chromatin regulators to these enhancer regions. RUNX1 has been shown to interact with histone acetyltransferase p300 (39) and BRG (43), the ATPase subunit of SWI/SNF chromatin remodeling complex. *BRG1* knockdown led to marked reductions in transcription factor binding and disruption of the *MYC* 1.7-Mb enhancer:promoter interaction in AML cells (352). Similarly, NOTCH1 inhibition interferes with N-Me interactions with the *MYC* promoter and suppresses *MYC* mRNA levels (208). Our data show that a RUNX1 deficiency evicts TAL1 and NOTCH1 from the *Myb* and *Myc* enhancers respectively, and that reduction of *RUNX1* expression dissociated the interaction between the +14-kb or -93-kb enhancer and the *MYB* promoter. Therefore, we speculate that RUNX1 depletion destabilizes N-Me and the promoter interaction, and that RUNX1 plays a key role in chromatin structure formation.

Attempts have been made to target enhancers in cancer therapy using BET bromodomain inhibitors or histone modifying enzymes. The obvious concern is that such treatments would have toxic side effects due to inhibition of enhancer activity in normal cells. Although the BRD4 inhibitor JQ1 has clear anti-leukemic activity via its effects on MYC (205,207,381), toxicities have been observed and RNAi-mediated inhibition of BRD4 in mice has deleterious effects on tissue homeostasis (382). These findings predict that targeting broad regulators of

enhancer activity may interfere with normal tissue repair and regeneration and may not be tolerated long term in patients.

Our genetic and pharmacologic experiments reveal that targeting RUNX1 might be an alternative strategy to disrupt oncogenic *MYB* and *MYC* enhancers in T-ALL and elicit anti-leukemia activity. With the development of more potent and stable AI-10-104 analogues, the effects of RUNX1 inhibition can be tested in preclinical mouse and human T-ALL models for efficacy and to ensure the safety of the therapeutic strategy.

Materials and Methods

RNA analyses. RNA isolation and qRT-PCR were performed as described in Chapter II.

ChIP-qPCR. Chromatin immunoprecipitation was performed as previously described (383). Mouse T-ALL cells treated with ethanol or 10nM 4-OHT were lysed and nuclei were fragmented into 150~300-bp size pieces using Bioruptor (Diagenode). Fragmented chromatin was incubated overnight at 4°C with normal IgG (sc-2027, Santa Cruz) or anti-TAL1 (C-21, Santa Cruz), anti-RUNX1 (ab23980, Abcam), anti-RUNX3 (9647, cell signaling), anti-NOTCH1 (C-20, Santa Cruz), anti-Histone 3 (ab1791, Abcam) or anti-H2K27ac (ab4729, Abcam). Chromatin antibody complexes were pulled down by incubating with magnetic

beads (Dynal) for 4 hours. Enrichment of DNA fragments was tested using qPCR with primers specific for sites of interest (Table 4).

ATAC-qPCR Assay for transposase-accessible chromatin with quantitative PCR experiment was performed as previously described (384) with minor modification to reduce mitochondria DNA contamination. Briefly, mouse T-ALL cells ($1x10^6$) treated with EtOH or 10nM of 4-OHT for 48 hours were harvested and lysed using a dounce homogenizer in 25 mM Tris pH 8.0, 2 mM $MgCl_2$ buffer. Nuclei were pelleted by centrifugation at 500 *g*, 4°C for 10 minutes and washed with cold PBS twice. Nuclei were resuspended with 50 µl of cold lysis buffer (10 mM Tris pH 7.4, 10 mM NaCl, 3 mM $MgCl_2$, 0.1% (v/v) Igepal CA-630) and tagmented as described before (384). To enrich DNA fragments of nucleosome-free and mononucleosome-occupied regions, final PCR products were selected using a negative Solid Phase Reversible Immobilization (SPRI)-size selection of 0.6x followed by a positive SPRI-size selection of 1.4x. Size-selected DNA from 3 biological replicates of each condition were amplified using qPCR with primers specific for the sites of interest (Table 5) to examine the enrichment of DNA fragments. The degree of accessibility to the N-Me region was normalized as fold of enrichment over the degree of accessibility to 2 distinct gene desert regions.

Doxycycline-inducible *RUNX1-shRNA* Jurkat clone A Jurkat clone expressing shRNA against *RUNX1* upon doxycycline treatment was a generous gift from Dr. Marjorie Brand at the Sprott Center for Stem Cell Research, Canada. Cells were

treated with 5 μg/ml of doxycycline for 48 hours in order to suppress RUNX1 expression.

3C 5x10^6 of *RUNX1-shRNA* expressing Jurkat cells were collected and crosslinked using formaldehyde. A 3C library was generated as previously described (385).

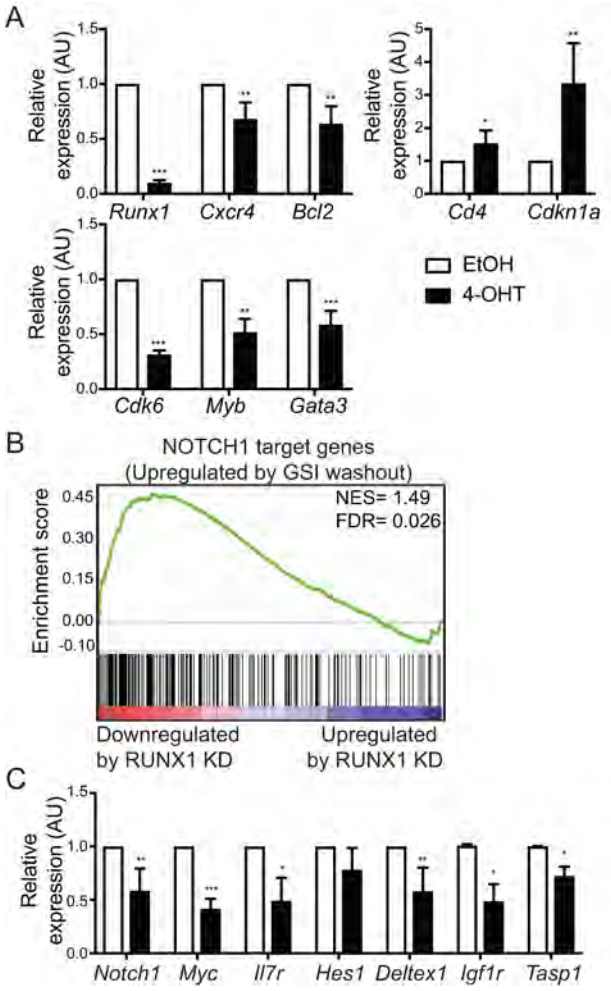

Figure 3.1. RUNX1 regulates a subset of TAL1-, and NOTCH1-regulated genes. (A) mRNA was isolated from mouse T-ALL cells 48 hours after vehicle or 4-OHT treatment and the expression of subset of a RUNX1- and TAL1- regulated genes was determined by qRT-PCR. Three to 4 independent experiments were performed, and data are shown as mean ± SEM. (B) Gene Set Enrichment Analysis (GSEA) of RUNX1-regulated genes and genes changed upon reactivation of NOTCH1 by GSI washout (325). RUNX1 target genes that were significantly downregulated by RUNX1 knockdown in Jurkat cells were used as a data set (237). (C) The expression of a subset of NOTCH1-regulated genes in *Runx1*-deleted mouse T-ALL cells was determined by qRT-PCR. Three to 4 independent experiments were performed, and data are shown as mean ± SEM (*p<0.05, **p<0.005, ***p<0.0005, Student t test). (GSEA assay [panel B] was performed by Jun Yu)

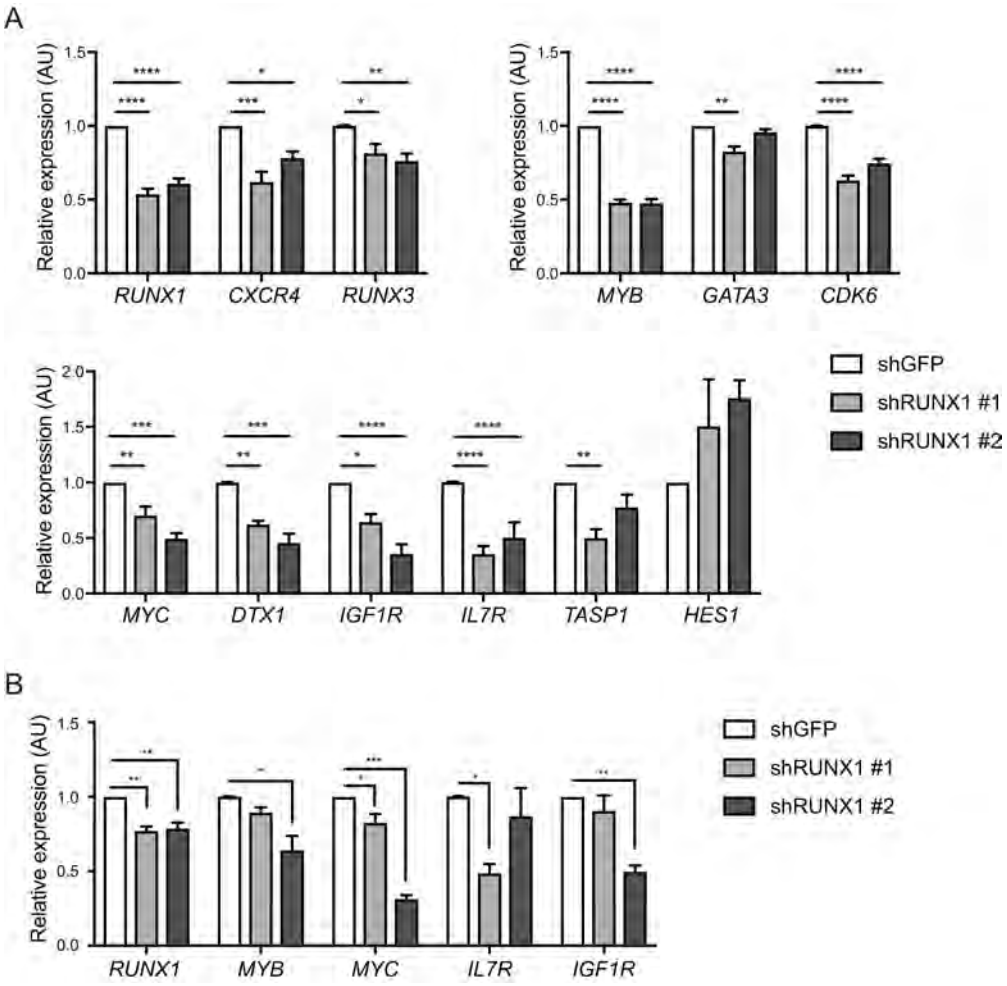

Figure 3.2. *RUNX1* knockdown in human T-ALL cell lines alters the expression of a subset of RUNX1-, TAL1-, and NOTCH1-regulated genes. (A) Jurkat cells were infected with lentiviruses expressing shRNA against *RUNX1* or GFP. RNA was isolated 4 days after infection. The expression changes of a subset of RUNX1-, TAL1-, NOTCH1-regulated gene upon *RUNX1* knockdown were determined by qRT-PCR. (B) The expression of subset of NOTCH1-regulated genes were altered by *RUNX1* reduction. *GAPDH* was used for normalization of qPCR values. Three to 4 independent experiments were performed, and data are shown as mean ± SEM (*p<0.05, **p<0.005, ***p<0.0005, ****p<0.0001, One-way ANOVA multiple comparisons test).

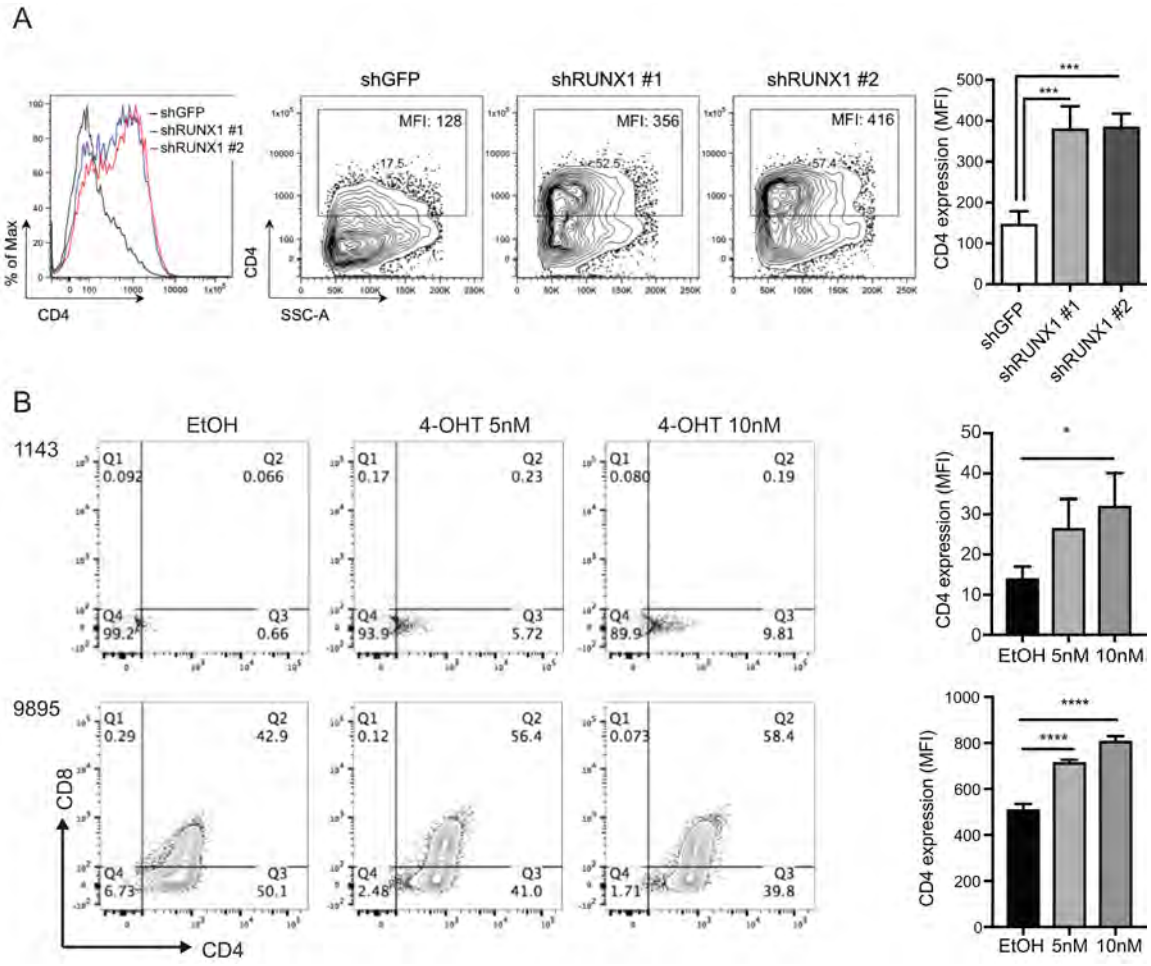

Figure 3.3. RUNX1 depletion derepresses CD4 cell surface expression on T-ALL cells. (A) CD4 cell surface expression in *RUNX1*-silenced Jurkat human T-ALL cells was determined by flow cytometry after staining with CD4 antibody. Representative flow data is shown and data from 3 independent experiments are shown as MFI ± SD (right). (B) CD4 and CD8 expression in mouse T-ALL cells were determined by flow cytometry. Mouse T-ALL cells were stained with CD4-PerCP-Cy5.5 and CD8-FITC antibodies 48 hours after EtOH or 5, 10 nM of 4-OTH treatment. One representative flow profile is shown (left). The mean of fluorescence of CD4-PerCP-Cy5.5 from 3 independent experiments is shown as MFI ± SEM (right) (*p<0.05, ***<p0.0005, **** p<0.0001, One-way ANOVA multiple comparison). Panel B data were presented for reviewers only.

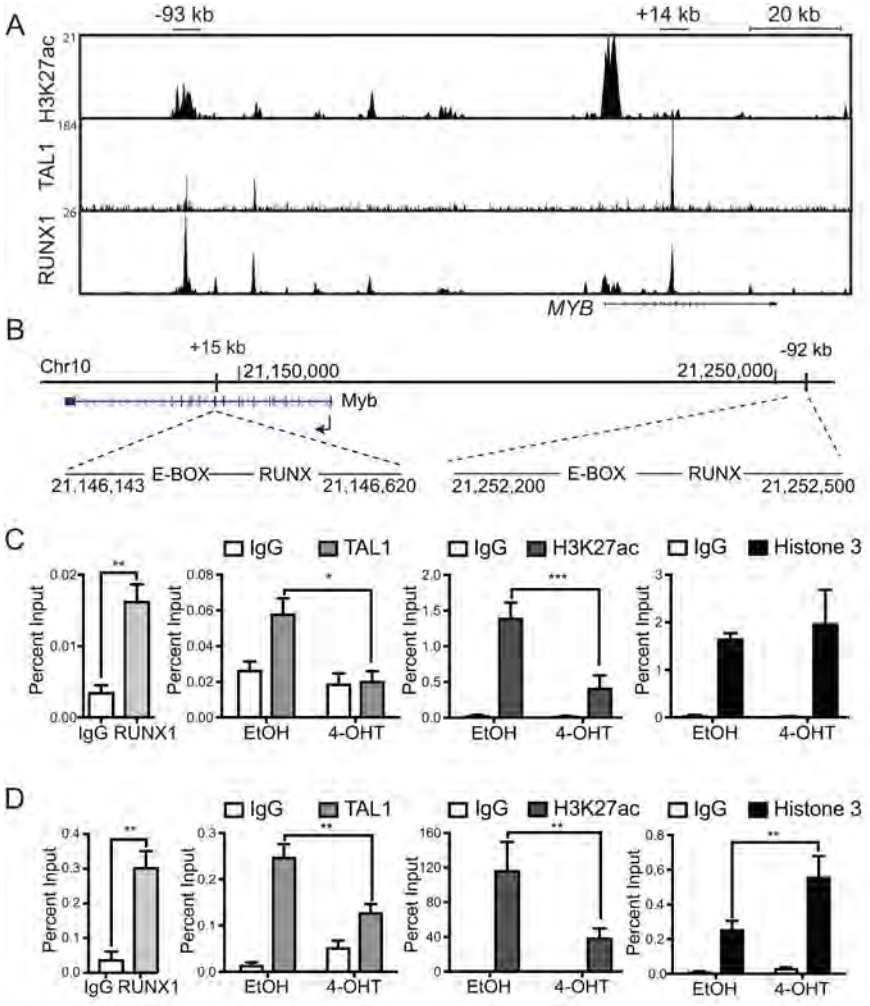

Figure 3.4. RUNX1 is required for TAL1 binding to the *Myb* enhancers and for the retention of active chromatin marks. (A) H3K27ac, TAL1, and RUNX1 enrichment at the *MYB* locus by ChIP-Seq are shown in genome browser tracks (genome.ucsc.edu/human hg19). (B) Mouse genomic region (mm10) around *Myb* locus, depicting the E-BOX (TAL1) and RUNX binding sites at positions +15 kb and -92 kb from the *Myb* TSS. (C, D) Enrichment of RUNX1, TAL1, H3K27ac, and histone 3 to +15 kb (C) and -92 kb (D) *Myb* enhancer regions determined by ChIP-qPCR in control or *Runx1*-deleted mouse T-ALL cells. Data are shown as the mean of 3 or 4 independent experiments with error bars representing ± SEM (*p<0.05, *p<0.005, p<0.0005, Two-way ANOVA multiple comparisons test).

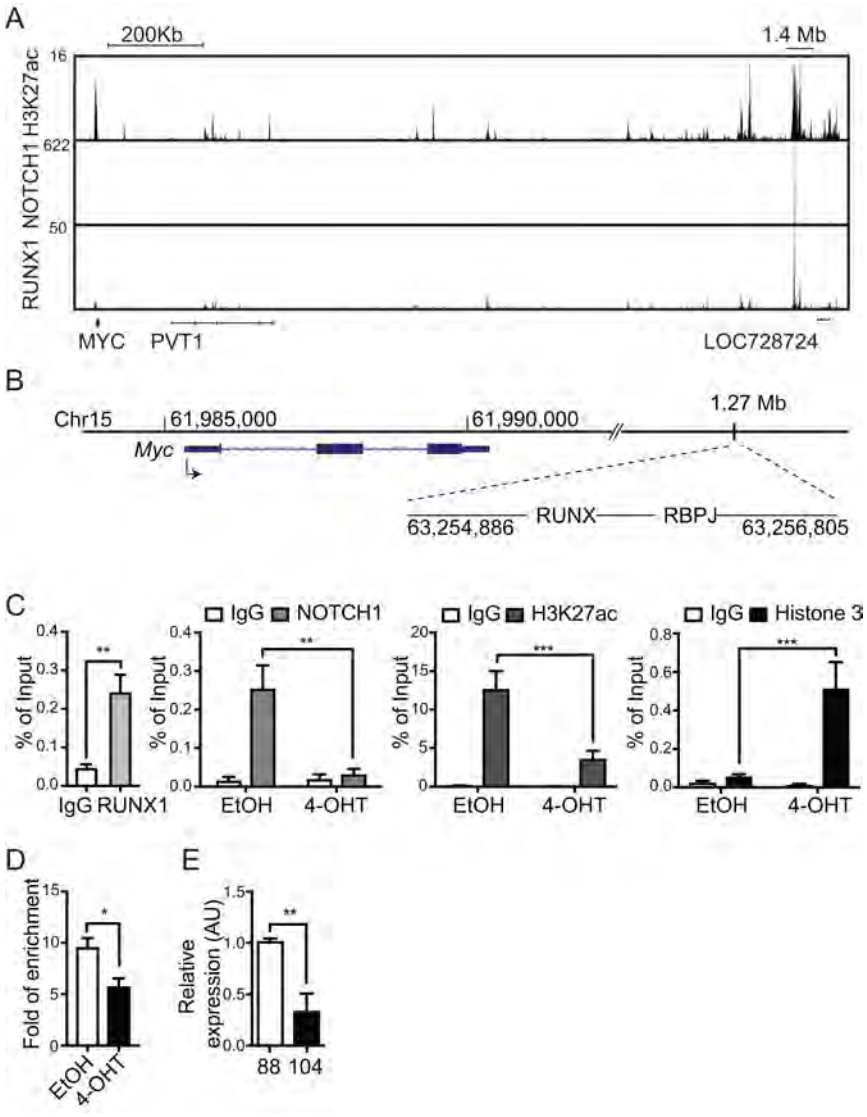

Figure 3.5. RUNX1 is required for intracellular NOTCH1 binding and for chromatin accessibility at the N-Me. (A) H3K27ac, NOTCH1, and RUNX1 enrichment at human MYC super-enhancer are shown in genome browser tracks (genome.ucsc.edu/human hg19). (B) Mouse genomic region (mm10) encompassing Myc and its enhancer loci located 1.27 Mb from the TSS. The RBPJ and RUNX binding sites are depicted. (C) Recruitment of RUNX1, intracellular NOTCH1, H3K27ac and histone 3 to mouse *Myc* enhancer was determined by ChIP-qPCR in control or Runx1-deleted mouse T-ALLs. (D) The degree of open chromatin at N-Me enhancer region in control or Runx1-deleted mouse T-ALLs was determined by ATAC-qPCR. (E) *MYC* gene expression

changes were determined in RPMI8402 cells treated with 10 μM of AI-4-88 or AI-10-104 for 12 hours. Data shown are the mean of 3 or 4 independent experiments and error bars represent ± SEM (*p<0.05, **p<0.005, ***p<0.0005, Two-way ANOVA multiple comparisons test for ChIP-qPCR, Student *t* test for ATAC-qPCR and qRT-PCR).

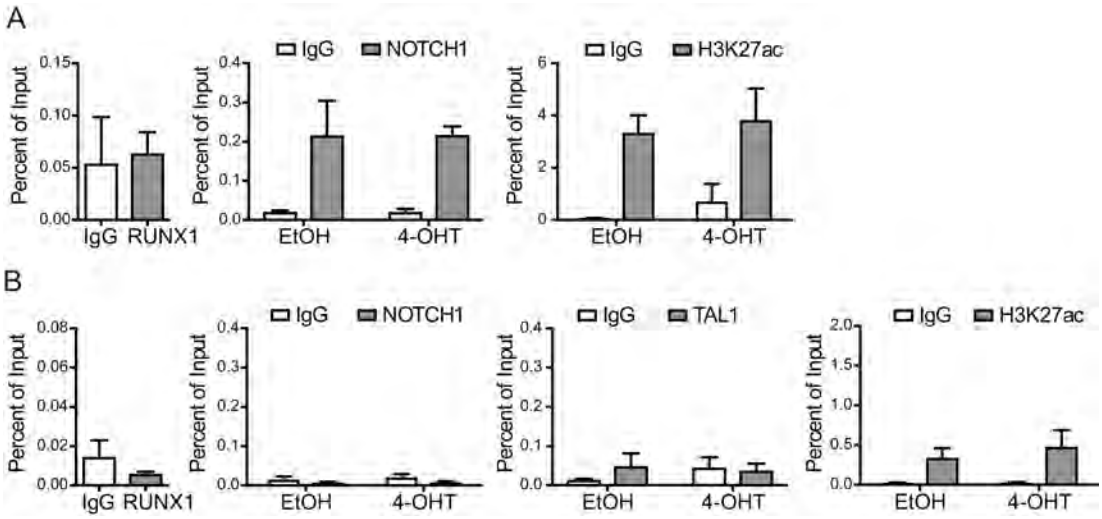

Figure 3.6. *Runx1* depletion has no effect on intracellular NOTCH1 binding to the Hes1 promoter or to gene desert regions. (A) *Runx1* deletion did not change the recruitment of intracellular NOTCH1 or H3K27ac to the mouse Hes1 promoter. (B) *Runx1* deletion has no effect on TAL1, NOTCH1, or H3K27ac binding to gene desert region. Two to 4 independent experiments were performed and data are shown as mean ± SEM.

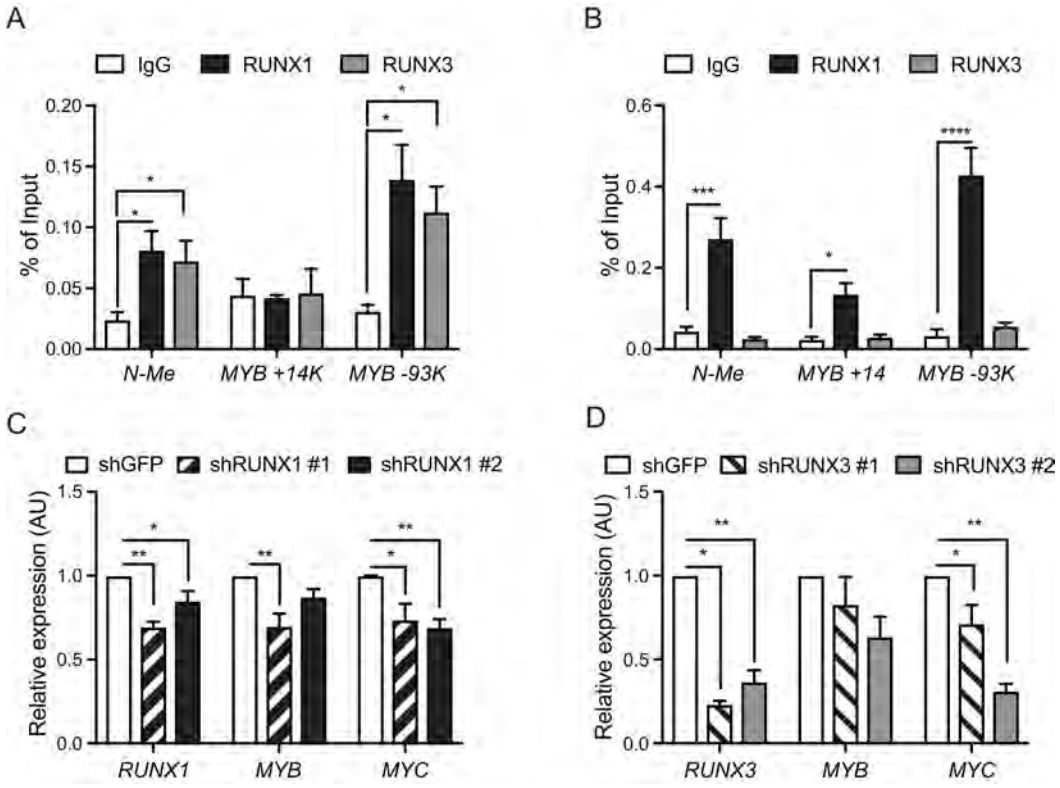

Figure 3.7. RUNX1/3 binding to the oncogenic enhancers reflects their regulation of gene expression. (A, B) RUNX1 and RUNX3 binding to *N-Me*, *MYB+14* kb, and *MYB-93* kb enhancer loci was determined by ChIP-qPCR in (A) KOPTK1 or (B) Jurkat cell lines. Data are shown as the mean of 4 independent experiments with error bars representing ± SEM (*p<0.05, Multiple t test). (C, D) The expression of *MYB* and *MYC* in (C) *RUNX1-* or (D) *RUNX3*-silenced KOPTK1 cells were determined by qRT-PCR. Data are shown as mean of 3 or 4 independent experiments with error bars representing ± SEM (*p<0.05, **p<0.005, ***p<0.0005, One-way ANOVA multiple comparisons test).

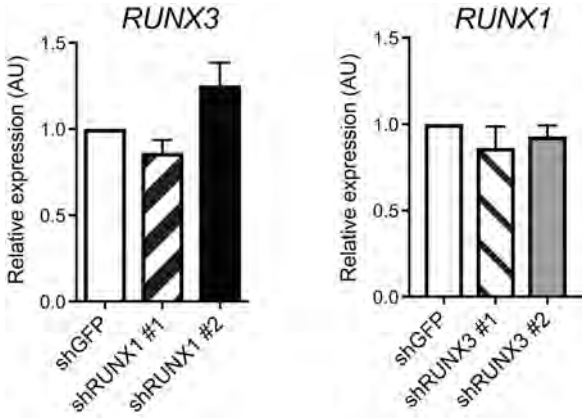

Figure 3.8. The reduced expression of *RUNX1* or *RUNX3* does not lead to increased expression of the other. The mRNA expression level of *RUNX3* and *RUNX1* upon knockdown of *RUNX1* and *RUNX3,* respectively, was tested by qRT-PCR. Three to 4 biological replicates were collated.

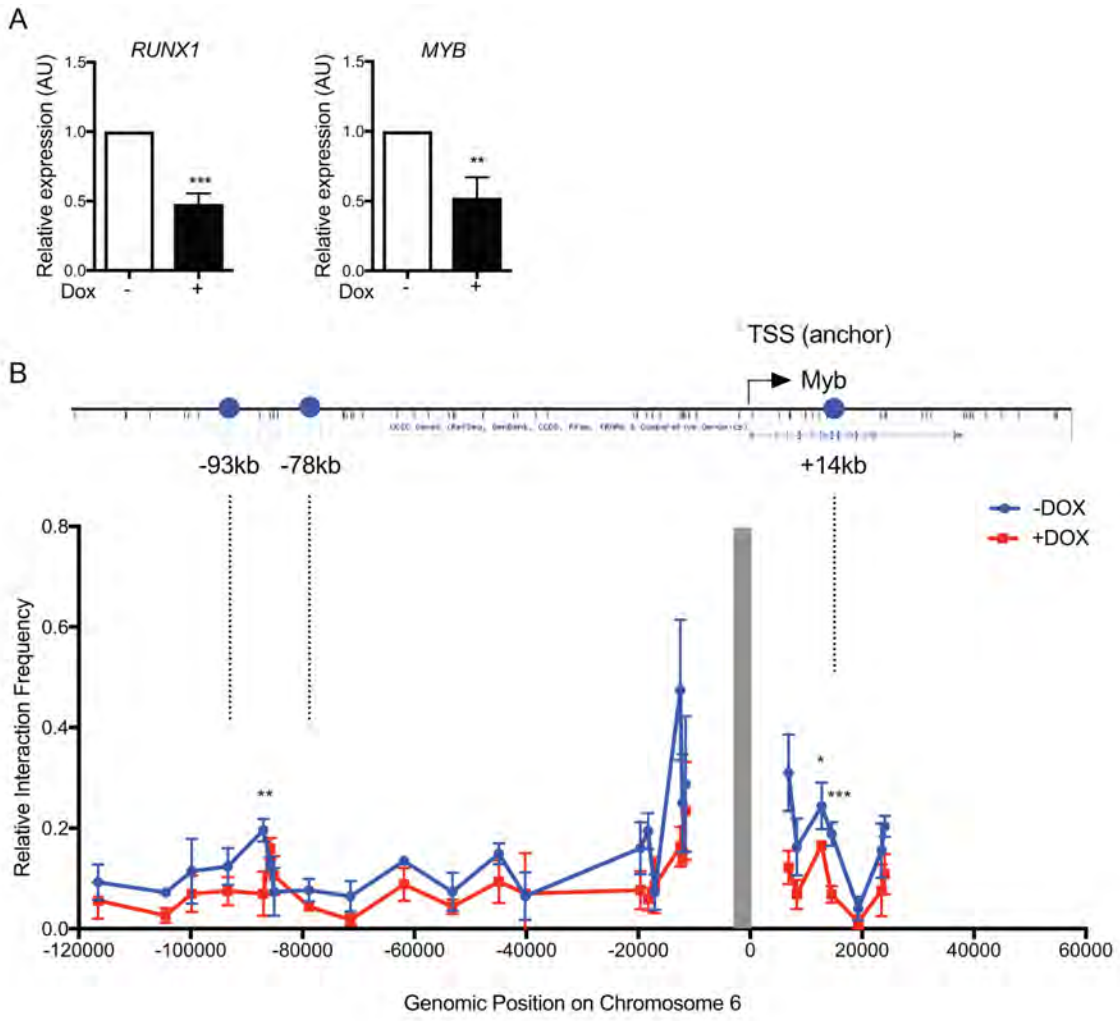

Figure 3.9. RUNX1 reduction interferes with the formation of loop between the MYB promoter and -94-kb and +14-kb enhancers. (A) The expression of *RUNX1* and *MYB* in Jurkat cells expressing inducible shRNA against *RUNX1* was determined by qRT-PCR after 48 hours of doxycycline treatment. (B) The Interaction between the *MYB* promoter region and downstream or upstream regions of the *MYB* TSS in Jurkat cells was analyzed by a 3C assay. Jurkat cells were treated with doxycycline for 48 hours to reduce *RUNX1* expression. Data are shown as mean of 3 technical replicates with error bars representing ± SD (*p<0.05, **p<0.005, **p<0.0005). This result is unpublished data.

Chapter IV

Discussion

This thesis research has focused on investigating the roles of RUNX1 in T-ALL leukemogenesis. In contrast to the tumor suppressing functions of RUNX1 in AML, I have demonstrated that RUNX1 is required for the survival and proliferation of human and mouse T-ALL cells. RUNX1 depletion reduces the expression of genes that are essential for T-ALL survival. Especially, RUNX1 supports *Myb* and *Myc* expression by regulating transcription factor binding and acetylation of H3K27 at the *Myb* and *Myc* enhancers. In addition, RUNX1 appears to change the chromatin structure around the *MYB* gene. Furthermore, I provided evidence that RUNX1 can be a therapeutic target in T-ALL by using a recently developed RUNX1/CBFβ inhibitor.

RUNX1 contributions to T-ALL cell leukemogenesis.

Previously, RUNX1 was proposed to be a tumor suppressor in T-ALL based on the findings of recurrent mutations in the *RUNX1* gene in the early T-cell precursor acute lymphoblastic leukemia (ETP-ALL) subtype (131,321,323). The identified mutations have been shown to, or are predicted to, result in loss of function of RUNX1 (305,323), suggesting that disturbing RUNX1 role would lead to T-ALL leukemogenesis. In addition, *Runx1* deficient mice treated with N-ethyl-nitrosourea (ENU) predisposed to T-ALL development (369). However, I have demonstrated that RUNX1 depletion resulted in apoptosis in T-ALL cells, arguing a pro-survival function of RUNX1. In contrast to previous studies, all human T-ALL cell lines and patient samples examined in this research are typical T-ALLs.

In addition, except the Jurkat cell line, they harbor wildtype RUNX1 (Table 1.1). Consistently, it has been reported that RUNX1 mutations are very rare in non-ETP-ALL patients (131), indicating that RUNX1 has distinct functions depending on T-ALL subtypes. The immunophenotype and gene expression profile of ETP-ALL cells suggests that ETP-ALL arises from ETP cells; they are recent immigrants from BM to thymus expressing one or more of myeloid or stem-cells markers, such as CD117, CD34, CD13, and CD13, but not lymphoid markers, such as CD8 and CDa1, and have both lymphoid and myeloid development potential (130,386). Thus, in ETP cells, loss-of-function RUNX1 mutations likely promotes leukemogenesis, similarly to how it does in myeloid lineage cells. On the other hand, during cortical T-ALL development, normal RUNX1 regulation seems to be sustained until the emergence of more mature DN3 thymocytes, the presumed target cell clones of cortical T-ALL (175,205). Deregulated TAL1 or NOTCH1 may prevent RUNX1 downregulation that normally occurs during DP to SP thymocyte differentiation (63). RUNX1 overexpression resulted in resistance to TCR-mediated apoptosis (387) while reduction of RUNX1 activity in DP cells sensitizes cells to apoptosis induced by TCR signaling (388). These studies indicate that RUNX1 plays a pro-survival role in the DN4 or DP late stage thymocyte developments. Consistently, the expression levels of *RUNX1* in TAL1-positive T-ALL patient samples is higher than in other T-ALL subtypes (237).

It was reported that Jurkat cells harbor a *RUNX1* mutation within the RUNT domain, which could affect the DNA binding capability of RUNX1 (323).

However, ChIP-seq studies of RUNX1 in Jurkat cells displayed a significant level of DNA binding affinity (237,389). In addition, reduction of RUNX1 expression in this cell line induced apoptosis and altered the expression of known RUNX1 target genes such as *CD4* and *CXCR4.* Therefore, the RUNX1 mutation in Jurkat cells does not seem to result in loss of function of RUNX1.

Analyses of signal distribution of acetylated histone 3 lysine 27 (H3K27ac), which locates at active enhancer regions, have identified super-enhancers enriched with high- and broad-signals of H3K27ac, and their associated genes in Jurkat and PRMI8402 T-ALL cells lines (340,364). These studies reveal that the *RUNX1* gene is expressed by a super-enhancer that contains the hematopoietic cell-specific enhancer at 23kb downstream from RUNX1 TSS in T-ALL cell lines (340,364,390). This is also supported by the finding that in T-ALL, expression of RUNX1 is exceptionally sensitive to a low dose of THZ1 (50nM), an inhibitor of CDK7 (an essential cofactor of transcriptional machinery), given that super-enhancers are highly sensitive to disruption (347,364). These studies indicate that RUNX1 is a master transcription factor determining the identity of T-ALL cells. Consistently, I have demonstrated that RUNX1 depletion using *RUNX1-shRNA* and AI-10-104 inhibitor resulted in cell death of multiple T-ALL cell lines and patient samples.

RUNX1 regulates the activity of super-enhancers and chromatin structure in T-ALL.

I have demonstrated that *Runx1* deletion in murine T-ALL cells results in reduced modification of active histone mark, H3K27ac, to the *Myb* and *Myc* enhancer loci, which have been identified as super-enhancers (351,364). Consistently, the expression of *MYB* and *MYC* are downregulated following RUNX1 depletion in both human and mouse T-ALL cells, suggesting that RUNX1 is involved in the activation of super-enhancer elements. It has been shown that RUNX1 can recruit histone acetyltransferases such as CBP/P300 and monocytic leukemia zinc finger protein (MOZ) to the DNA where it binds (39,391) and becomes capable of regulating histone acetylation. In addition to control of the recruitment of histone acetyltransferase to DNA, open chromatin regions in *Runx1* deleted mouse T-ALL cells defined by ATAC-seq experiment suggest that RUNX1 may regulate expression of histone modification enzymes (Appendix II). The accessibility of promoter regions of genes involved in histone modification including *Setd2* (Histone-lysine N-methyltransferase SETD2), *Kmt5a* (lysine methyltransferase 5A), *Kat14* (lysine acetyltransferase 14), and *Dot1l* (DOT1 like histone lysine methyltransferase), is increased upon *Runx1* deletion in mouse T-ALL cells. However, the gene expression profile using a microarray assay in *RUNX1*-silenced human T-ALL cells did not reveal expression changes of these genes (237). This discrepancy might be caused by human versus mouse species difference or by lack of sensitivity of the array assay. Therefore, it needs to be

tested whether RUNX1 depletion in mouse T-ALL cells alters the expression levels of these enzymes leading to changes in histone modifications using an RNA-seq experiment. Collectively, RUNX1 appears to be responsible for marking regulatory regions for the activation or repression and the recruitment of transcriptional machinery, regulating the expression of target genes.

Interestingly, I observed that RUNX1 depletion inhibited binding of transcription factors, TAL1 and NOTCH1 to the *Myb* and *Myc* super-enhancer loci, respectively, leading to disruption of TAL1-MYB and NOTCH1-MYC oncogenic pathways in mouse T-ALL cells. Given that RUNX1 shares a significant portion of its binding sites with members of the transcriptional complex in T-ALL (234,237,324) and NOTCH1, it is possible that RUNX1 regulates TAL1 and NOTCH1 binding to other loci besides the MYB and MYC enhancers. Consistently, I observed that RUNX1 reduction resulted in downregulation of a subset of TAL1- and NOTCH1-target genes. Interestingly, these genes are also associated with super-enhancers that are bound by RUNX1 (324,364). Thus, RUNX1 inhibition will lead to disruption of TAL1 and NOTCH1 regulation by preventing them from binding to super-enhancers that drive expression of genes critical for defining the identity of T-ALL cells.

How RUNX1 controls TAL1 and NOTCH1 binding to enhancer regions is not clear either. Although TAL1 and NOTCH1 have been shown to interact with RUNX1 in T-ALL (93,380), it is unlikely that they bind to their binding sites as

single complexes based on the distances between their consensus binding motifs in the *MYB* and *MYC* enhancer regions. Instead, it seems that they indirectly cooperate for their binding to target regions. It is possible that RUNX1 acts as a 'pioneer factor' (372,392) that induces chromatin remodeling where it binds and repositions the nucleosome to expose binding motifs for other transcription factors, allowing their binding. RUNX1 has been shown to interact with the BRG1 SWI/SNF chromatin remodeling complex in T-ALL (43), although whether BRG1 recruitment to DNA is a cause or result of RUNX1 binding remains to be tested. Open promoter regions revealed by ATAC-seq in *Runx1* deleted mouse T-ALL cells are enriched with genes involved in chromosome organization such as *Smarcb1* (SWI/SNF-related matrix-associated actin-dependent regulator of chromatin subfamily B member 1), *Wdhd1* (WD repeat and HMG-box DNA binding protein 1), and *Phf19* (PHD finger protein 19) (Appendix II). These data indicate that RUNX1 might regulate chromatin structure changes by controlling the expression of chromatin modifiers. In addition, MOZ, a coactivator interacting with RUNX1, has a motif that is responsible for nuclear localization and coactivation and is homologous to the H15 domain found in linker histones such as histone 1, and histone 5 (391). The H15 domain of histone 5 has been implicated in binding to the nucleosome (393), therefore, RUNX1 might bind to the compacted chromatin and induce chromatin structure changes through interaction with the MOZ coactivator. During the definitive hematopoiesis, it was shown that induced RUNX1 bound to distal

regulatory regions having low or absent active histone mark, H3K9ac, and subsequently increased the level of active histone mark. Furthermore, ChIP-seq for TAL1 demonstrated the increased number of TAL1 binding peaks next to the RUNX1 binding sites, indicating that RUNX1 binding to DNA provides new binding sites for TAL1 (394). To examine RUNX1 roles as a pioneer factor in T-ALL, binding of RUNX1 to silent chromatin, which does not contain histone modification, after RUNX1 induction in RUNX1-deficient cells can be tested using ChIP-seq for RUNX1. To prevent cell death caused by the RUNX1 deficiency, BCL-2 can be ectopically expressed. Change of histone modifications around RUNX1 bound regions will also demonstrate RUNX1 function as a pioneer factor. It can be validated by recruitment of other transcription factors, such as TAL1 and NOTCH1, to the RUNX1 bound regions after the RUNX1 induction.

On the other hand, RUNX1 can remain bound at its binding sites and prevent nucleosome repositioning, thus serving as a placeholder to let other transcription factors bind to adjacent sites. Consistently, I observed increased H3 loading to the *Myc* enhancer region and global changes in the nucleosome position upon *Runx1* deletion, indicating that RUNX1 may regulate nucleosome relocalization/positioning. Genome-wide changes of TAL1 or NOTCH1 binding after *Runx1* deletion can be examined to verify the RUNX1 role as a placeholder in T-ALL cells.

Whether TAL1 or NOTCH1 is required inversely for RUNX1 binding to these enhancer loci remains to be tested. In T-ALL cells overexpressing *TAL1* by somatic mutations in *TAL1* enhancer region, MYB binding appears to be critical for the binding of other transcription factors to the enhancer; the somatic mutations found in this newly generated super-enhancer region introduce only de novo MYB binding sites to the DNA resulting in binding of MYB and TAL1 complex members, which does not occur in the wildtype allele that contains E-Box, RUNX, ETS, and GATA3 but not MYB binding motifs (234). This study indicates that a specific transcription factor can determine binding of other transcription factors. In KOPTK1 cells, which express a minimal level of TAL1, I detected RUNX1 and RUNX3 binding to the -93-kb *MYB* enhancer locus. This result suggests that TAL1 may not be the determinant factor of RUNX1 binding to DNA. In addition, transgenic mice expressing *Lmo2* and a DNA-binding mutant of *Tal1* develop T-ALL indicating that TAL1 direct binding to DNA is not required for its regulation (87). Using CRISPR/CAS9-mediated genome editing to delete the binding sites of individual transcription factors in the enhancer region, we can examine the hierarchy of transcription factors binding to these regions.

Formation of looping structures connecting regulatory element regions has been proposed as a method of communication between long-range regulatory elements (351,395–397). 3C and 3C-based technologies have demonstrated that enhancers are placed in close physical proximity to the gene promoter regions to drive gene expression (181,352,377) and that RUNX1 mediates these

interactions (398–400). RUNX1 has been known to repress CD4 expression by binding to the silencer of the *CD4* gene (62). 3C experiments have further shown that RUNX1 can induce the formation of chromatin loops between the enhancer and the silencer of the *CD4* gene in DN thymocytes and a CD8ISP thymoma cell line. Consistent with this, RUNX1 silencing resulted in interaction between the enhancer and the promoter of CD4 gene, which induced the CD4 expression (398). RUNX1 regulation of the expression of CD34 in HSCs is also associated with chromatin loop formation connecting the enhancer and the promoter of the *CD34* gene (399). In line with this, I demonstrated that RUNX1 suppression reduces the interaction frequency of the promoter with the enhancer regions of *MYB* gene and downregulates *MYB*, supporting a role for RUNX1 in local chromatin structure arrangement for transcriptional regulation. However, due to a difficulty to acquire sufficient suppression of RUNX1 in this inducible shRNA expressing system, inhibited DNA loop formation in RUNX1 depleted cells was not prominent. To confirm RUNX1 regulation of DNA looping, interaction frequency between the promoter and enhancer region can be examined in the RUNX1 binding site deleted cells using CRISPR/CAS9 system.

It has been demonstrated that although the topologically associating domains (TADs), self-interacting domains, are conserved across different cell types, chromatin architectures within TAD are established in cell type-specific ways (401–403). Cell type-specific transcription factors and cofactors, such as mediator and cohesin, have been suggested to mediate the interaction between

regulatory regions within TAD (379,404). In *Med1* (a component of mediator complex) or *Smc1* (a component of cohesion complex) depleted embryonic stem cells (ESCs), the interactions of *Nanog* locus with other chromatin regions were disrupted which leading to decreased expression of *Nanog* and differentiation of ESCs (404). The binding sites of ESCs-specific transcription factors, including SOX2, KLF4, and ESRRB, are enriched at the interacting loci of *Nanog* suggesting roles of these transcription factors in the interaction of *Naong* locus with other regions (404). Therefore, it would be interesting to evaluate a role of RUNX1 in local chromatin organization around its other target genes besides *MYB* and throughout the genome in T-ALL cells in comparison to normal thymocytes. Genome-wide chromatin interaction in T-ALL cells in the presence or absence of RUNX1 can be tested by Hi-C (a genome-wide and unbiased method that combines 3C with deep sequencing) whether RUNX1 depletion rearranges chromatin interaction of T-ALL cells to a similar way of normal thymocytes.

RUNX3 shares oncogenic roles of RUNX1 in T-ALL.

RUNX1 and RUNX3 are expressed differently during mouse thymocyte development in that RUNX1 is highly expressed in immature thymocytes while RUNX3 is expressed in mature $CD8^+$ thymocytes (62,63). Consistently, I detected RUNX1 but not RUNX3 protein expression in our mouse T-ALL cells which resemble DP thymocytes. However, I also detected RUNX3 expression in

several human T-ALL cell lines and primary patient samples. Although there is a report that RUNX3 is significantly downregulated in CD4ISP ($CD4^+CD8^-CD3^-$) and DP ($CD4^+CD8^+CD3^-$) human immature thymocytes (405), the expression pattern of RUNX1 and RUNX3 may be different in human T-cell development. For example, RUNX3 and RUNX1 may be expressed in immature human thymocytes. In addition, target cells of transformation could be more heterogeneous in human T-ALL compared to mouse T-ALL.

In contrast with the large number of studies of RUNX1 in leukemogenesis, not much is known about RUNX3 in leukemia development. In other types of cancer, including colon and pancreatic cancer, RUNX3 has been suggested to function as either tumor suppressor or oncogene depending on tissue type (55,406–409). In this thesis, I have demonstrated that when co-expressed RUNX3 supports the survival of T-ALL cells similarly to RUNX1, indicating that RUNX1 and RUNX3 are functionally redundant. In addition, sensitivity to the RUNX inhibitor AI-10-104 correlates with the combined RUNX1 and RUNX3 expression levels in patient samples (Figure 2.6F). I showed that RUNX3 regulates *MYB* and *MYC* expression by binding to the *MYB* and *MYC* enhancer regions in KOPTK1 cells where RUNX1 binds, in accordance with the idea that they share DNA binding sites due to the highly-conserved RUNT domain. This is also in line with the finding that both RUNX1 and RUNX3 bind to the *Cd8* enhancer and *FOXP3* (forkhead box P3) promoter regions in CD8SP cells and in naïve $CD4^+$ T-cells, respectively (63,410). However, RUNX 1/3 do not appear to

functionally compensate for one another; depletion of RUNX1 or RUNX3 induces apoptosis. It is possible that a certain amount of time is required to see the compensatory effects. It has been shown that *RUNX1* downregulation in AML results in alteration of RUNX1 target gene expression at early time points, that were not evident at later time points, with the increased expression of *RUNX2* and *RUNX3* (411). The kinetics of RUNX1 and RUNX3 functions in T-ALL can be examined using inducible expression of *shRNAs* against *RUNX1* and *RUNX3*. The target gene expression also can be tested in both RUNX1 and RUNX3 depleted cells to confirm functional redundancy of RUNX1 and RUNX3. Its possible that the total amount of RUNX proteins might be critical for their function and T-ALL survival. The presence of RUNX binding motifs in regulatory regions of RUNX1 and RUNX3 indicate that RUNX1 and RUNX3 are likely to regulate each other, as seen in AML cells (411). However, I do not detect significant changes in *RUNX1* expression upon *RUNX3* knockdown, or vice versa, in KOPTK1 cells. In T-cells, a distinct regulatory mechanism seems to govern the expression of RUNX1 and RUNX3. In $CD4^+$ native T-cells, both RUNX1 and RUNX3 regulate *FOXP3* expression by binding to the promoter of the *FOXP3* gene. (410). During regulatory T (Treg)-cells development from human $CD4^+$ naïve T-cells, RUNX3 expression was preferentially upregulated whereas RUNX1 expression was not changed. In addition, silencing of individual *RUNX1* and *RUNX3* using siRNA did not induce the alteration of each other's expression (410), suggesting that RUNX1 and RUNX3 do not regulate each other's

expression in T-cells. During hematopoietic development, RUNX1 expression is regulated by a hematopoietic-specific enhancer located at 23kb downstream from the TSS (390) which is bound by TAL1, GATA2, and PU.1. This enhancer also mediates RUNX1 expression in T-ALL cells (237). However, upstream regulators of RUNX3 expression in T-ALL cells as well as in T-cells remain to be identified. Motif analysis in the regulatory regions of RUNX3 can uncover regulators of RUNX3 expression.

RUNX proteins as therapeutic targets.

The results of genetic depletion of RUNX/CBFβ complexes and treatment with the AI-10-104 inhibitor suggest that targeting RUNX proteins could be an effective treatment for T-ALL. The AI-10-104 compound was designed to interfere with CBFβ binding to RUNX proteins, leading to inhibition of the transcriptional activities of the RUNX/CBFβ complexes. Consistent with this, AI-14-91, an analog of AI-10-104, was shown to reduce the binding of RUNX1 at its target sites and interfere with RUNX1-regulated genes in an *in vitro* hematopoietic progenitor cell differentiation system (366). AI-14-91 may also impede the role of RUNX1 in chromatin structure formation, which could be tested in future experiments.

Due to the toxicity of AI-10-104 in mice (sedative effects), it was not possible to test its anti-leukemic activity *in vivo*. Instead, the analog compounds AI-14-91 and AI-12-126 are well-tolerated in mice (366). I tested the potency of

AI-12-126 in *NOD-Scid IL2rγ*$^{-/-}$ (NSG) mice transplanted with a primary T-ALL patient sample and in FVB/N mice transplanted with *Tal1/Lmo2* mouse T-ALL cells, but did not observe any inhibition of T-ALL growth *in vivo* (Appendix I). The relatively low activity of AI-12-126 compound (366) might not be able to target RUNX proteins *in vivo*. Therefore, testing the efficacy of AI-14-91 in T-ALLs *in vitro* and *in vivo*, which exhibits similar activity to AI-10-104 in fluorescence resonance energy transfer (FRET) assay (366), will be valuable to evaluate the benefit of targeting RUNX proteins in T-ALL inhibition.

In my experiments, treatment of human T-ALL cell lines with AI-10-104 reduced *MYC* expression, consistent with the notion that the inhibitor interferes with RUNX1 binding to the *MYC* enhancer locus. However, I did not detect significant reductions in MYB expression upon inhibitor treatment, in contrast to what was observed with genetic depletion of RUNX1. In addition, AI-10-104 treatment downregulated NOTCH1 target genes including *IL7R* and *DTX1,* whereas genes that are regulated by TAL1 complex did not respond to AI-10-104 treatment (data not shown). Based on these data, I hypothesize that CBFβ is not necessary for RUNX1 to form the TAL1 transcriptional complex, while it binds as a heterodimer with RUNX1 to DNA regions that are also bound by NOTCH1. Other transcription factors that comprise the TAL1 autoregulatory complex can enhance the DNA binding capability of RUNX1, as a substitute for CBFβ function. It has been suggested that ETS1 can form a complex with RUNX1 and increase RUNX1 DNA binding affinity without CBFβ (412,413). ETS1 has been shown to

be a component of the TAL1 transcription complex in multiple hematopoietic cell types (373,414). In addition, the ETS binding motif was one of the top enriched sequences near TAL1 binding sites in T-ALL (93,237), indicating that a RUNX1 ETS1 may be a component of the TAL1 complex and regulate TAL1 regulated genes in leukemic cells. Thus, AI-10-104, which inhibits RUNX1 activity by preventing CBFβ binding may not affect RUNX1 regulation of TAL1 target genes, like *MYB*. To clearly elucidate the contribution of CBFβ to the formation of the TAL1 complex and regulation of TAL1 complex-target genes, genetic analysis of CBFβ in T-ALL will be necessary. Binding of CBFβ at regulatory loci of the TAL1 complex-target genes can be examined. In addition, expression of the TAL1 complex-target genes can be tested in CBFβ depleted T-ALL cells using shRNA or CRISPR/CAS9 system. Nevertheless, based on the prevalence of NOTCH1 activation in T-ALL, interfering with NOTCH1 pathway by inhibiting CBFβ binding to RUNX1 could be a viable T-ALL therapy.

Recently, the dosage-dependent function of RUNX proteins has been proposed that profound suppression of RUNX proteins result in cell cycle arrest and death in AML (415). Partial reduction of RUNX activity by expressing a loss-of-function mutant of RUNX1 resulted in the expansion of myeloid progenitor cells and AML development, consistent with the tumor-suppressive role of RUNX1. On the other hand, RUNX depletion inhibited the growth of cord blood cells transduced with RUNX1-ETO or MLL-AF9 fusion genes indicating the pro-

survival function of RUNX1. Moreover, double deletion of RUNX1 and CBFβ, which further suppresses total RUNX activity, led to substantial reduction of cell growth (415). Similarly, the pro-survival role of wildtype RUNX1 has been demonstrated in AML expressing CBFβ-SMMHC and in B-ALL expressing MLL fusion proteins. Decrease of wildtype RUNX1 in the Kasumi-1 cell line that harbors a t(8;21) translocation, creating *RUNX1-ETO* fusion gene, or in the inv(16) ME-1 cell line expressing CBFβ-SMMHC fusion protein resulted in leukemic cell apoptosis (416). In addition, RUNX1 was shown to support the growth of MLL-AF4 leukemic cells as a direct target of the MLL-AF4 fusion protein and a component of MLL-AF4 complex (417). It is supported by the observation that RUNX1 mutations have not been identified in primary patient AML cells transformed by fusion genes (305,306,310) and that high expression levels of RUNX1 is associated with poor prognosis in MLL-rearranged leukemia (417). Therefore, targeting wildtype RUNX1 may be beneficial in treating other types of leukemia besides T-ALL.

It should be noted that RUNX1 inhibition as an anti-leukemia strategy has risks as recurrent mutations of RUNX1 are associated with familial platelet disorder (FPD) which predisposes to AML. FPD patients harbor mutations that result in dominant-negative or loss-of-function in RUNX1 activity (418,419). Furthermore, the acquisition of additional somatic loss of function mutations in the wildtype *RUNX1* allele is frequently associated with AML development (278,420,421). Induced pluripotent stem cells (iPSCs) from FPD/AML patients

harboring RUNX1 mutations exhibit megakaryopoiesis defects, supporting that RUNX1 suppression can result in platelet disorder (422–424). Therefore, long-term inhibition of RUNX1 in T-ALL may increase the incidence of thrombocytopenia or AML development. Recently, de novo RUNX1 mutations were also reported in patients with thrombocytopenia (421,425). Thus, the intensity and duration of RUNX1 targeted therapy will need careful consideration to minimize adverse effects.

Future directions

I have investigated the role of RUNX1 in T-ALL leukemogenesis, especially focused on how RUNX1 controls oncogenic enhancer activity. Since I demonstrated that RUNX1 is involved in chromatin looping formation around the *MYB* gene, it would be interesting to explore the chromatin looping structures around the *MYC* gene using a 5C (Chromosome conformation capture carbon copy) assay. The distance between the promoter and enhancer (N-Me) of MYC is around 1.4 Mb, which is not suitable for 3C experiment. While 3C assay can examine interactions of a selected fragment with others within several hundred kb, 5C assay can investigate interactions between all digested fragments within a given region, which can be up to megabases (426). Getting the adequate suppression of *RUNX1* expression in the doxycycline-inducible *shRNA-RUNX1* cell line was difficult when I performed the 3C experiment for MYB region. To overcome this difficulty, we could use *Tal1/Lmo2/R26-CreER^{T2}Runx1$^{f/f}$* mouse T-

ALL model system, where the *Runx1* deletion is easily achieved by 4-OHT treatment. Furthermore, since mouse T-ALL cell lines proliferate faster than human T-ALL cell lines, we should be able to find a time point that would be long enough to detect chromatin structure change without having significant effects on cell death. It was shown that the interaction between the promoter and *MYC* enhancer locus (N-Me) was not altered by short-term (6 hours) NOTCH1 inhibition with γ-secretase inhibitor (GSI) treatment, while it was disrupted in persister cells treated with GSI for a longer time (208). These results indicate that cells need a certain amount of time to undergo chromatin structure changes.

Interestingly, the interaction between the promoter region and a super-enhancer locus at 1.7 Mb downstream from the TSS of MYC, that is highly bound by BRD4 (bromodomain-containing protein 4), (BRD4 Dependent Myc Enhancer, BDME), was maintained in GSI-resistant persister cells although the NOTCH1 expression was undetectable (207,208). In those cells, binding of BRD4, which is required for the survival of persister cells, was sustained or even increased at BDME while diminished at N-Me, suggesting that a chromatin modification protein BRD4, not NOTCH1 is responsible for the loop formation (208). In AML cells, reduced BRG1 altered the interaction of BDME with MYC promoter without changes in binding of transcription factors (352). Thus, it is possible that RUNX1 does not determine the interaction between the *MYC* promoter and enhancer loci. In GSI-resistant persister cells, on the other hand, RUNX1 is one of the top-ranked genes bound by BRD4 (207), suggesting upregulation and a role of

RUNX1 in GSI-resistant cells. Since RUNX1 binds to BDME, it is possible that RUNX1 regulates BRD4 binding to BDME as it does for TAL1 and NOTCH1 binding to MYB and MYC enhancer, and contributes to the interaction between MYC promoter and BDME regions, which can be tested by ChIP and 5C experiments (207). The results of these experiments raise the possibility that RUNX1 regulates chromatin structure associated with epigenetic alterations in GSI-resistant cells. By using a Hi-C (high-resolution chromosome conformation capture) technique, we can examine the genome-wide chromatin conformation changes in naïve and GSI-resistant leukemic cells and test the role of RUNX1 in these epigenetic changes by deleting RUNX1 in inducible CRISPR/CAS9 system. To examine a case that chromatin modification proteins but not RUNX1 mediate the chromatin structure changes, occupancy of chromatin modifiers at the interacting loci can be tested in the absence of RUNX1. Based on my preliminary ATAC-seq data (Appendix II), RUNX1 may control DNA accessibility to promoter regions of genes involved in chromatin organization and histone modification, suggesting that RUNX1 indirectly regulates chromatin conformation.

I have studied the function of RUNX1 in T-ALL leukemogenesis in the context of TAL1 and NOTCH1 activation based on their shared target genes. Even though it appears that RUNX1 shares approximately 70% of target loci with TAL1 and NOTCH1, ChIP-seq and gene expression profile data revealed a subset of genes that are regulated by RUNX1 only (237,325). One of the intriguing pathways enriched with RUNX1-only-regulated genes is mTOR

signaling. The PI3K-AKT-mTOR pathway is upregulated in 70-85% of pediatric patients with T-ALL (209). In addition, activation of mTOR signaling has been implicated in the survival and proliferation of T-ALL LICs (427,428). *RICTOR*, a specific component of the mTORC2 complex is identified as a direct target gene of RUNX1. The mTORC2 complex was proposed to activate AKT through phosphorylation (429). Deletion of *Rictor* delayed NOTCH1-induced T-ALL development *in vivo*, suggesting a role for mTORC2 in T-ALL (430). Notably, NOTCH1 has been known to mediate mTOR signaling through the transcriptional repression of *PTEN* by HES1 (154) whereas expression of HES1 is not changed by RUNX1 depletion. Therefore, in future studies, it would be interesting to investigate whether RUNX1 inhibition ablates mTOR signaling in T-ALL development.

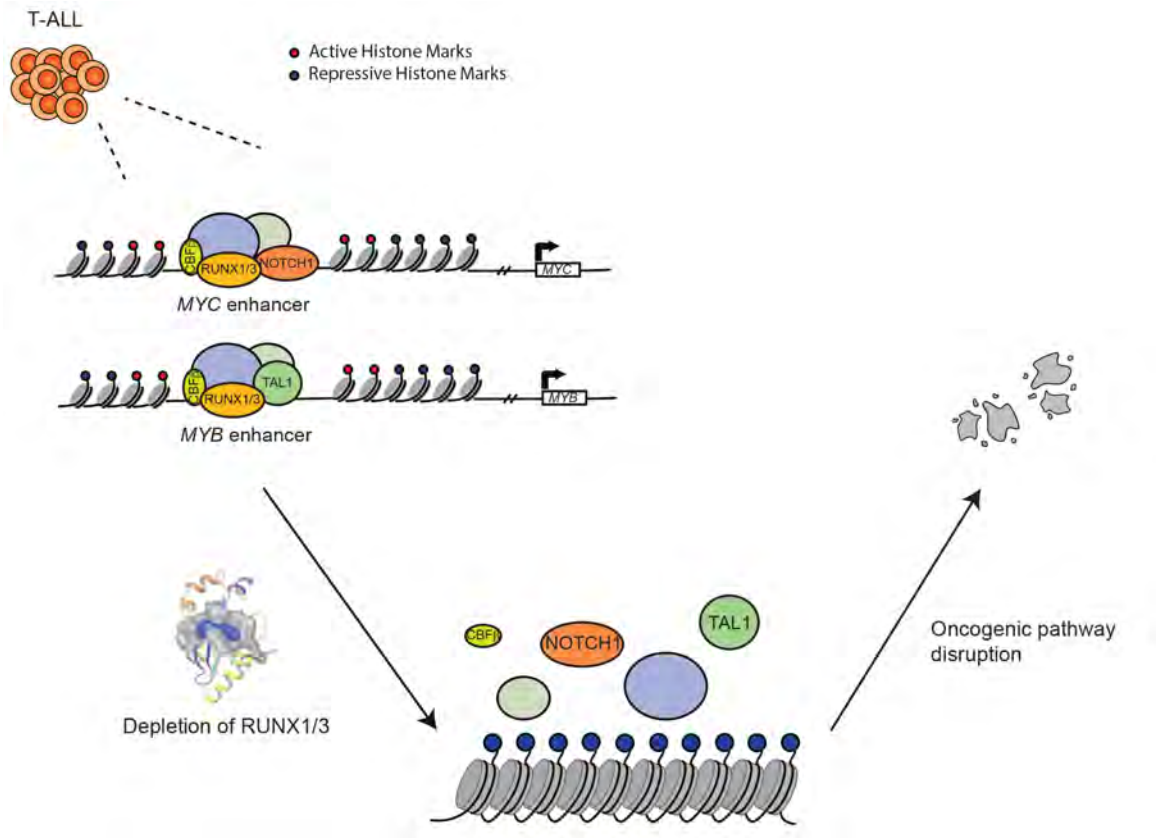

Figure 4.1. Proposed Model. This thesis research demonstrates that RUNX1 functions as an oncogene in T-ALL cells by regulating the transcriptional activity of TAL1 or NOTCH1. RUNX1 regulates the expression of MYB and MYC, which are critical oncogenes of T-ALL, by controlling TAL1 and NOTCH1 binding and acetylation of histone 3 lysine 27 at the MYB and MYC enhancer regions. Inhibition of RUNX1/3 activity interferes with NOTCH1 and TAL1 binding to the enhancer loci and leads to closed chromosome configuration resulting in disruption of the oncogenic pathway and death of leukemic cells.

Appendix

Appendix I

Evaluation of the efficacy of RUNX/CBFβ inhibitor AI-12-126 on T-ALL progression *in vivo.*

I have demonstrated that the RUNX/CBFβ inhibitor AI-10-104 induces growth inhibition and apoptosis in human and mouse T-ALL leukemic cells *in vitro* (Chapter II). These data suggest that targeting RUNX proteins can be a therapeutic option for patients with T-ALL. However, due to observed toxicity in mice, I was not able to test the efficacy of AI-10-104 inhibitor *in vivo*. An analog molecule, AI-12-126, was subsequently developed by Dr. Bushweller's laboratory, which is well-tolerated in mice (366). Thus, I attempted to validate the therapeutic effects of RUNX proteins inhibition *in vivo* using the AI-12-126 inhibitor.

The efficacy of AI-12-126 was determined in mice transplanted with a primary human T-ALL sample or *Tal1/Lmo2* mouse T-ALL cells. *NOD-scid Il2rγ*$^{-/-}$ (NSG) mice were transplanted with the TALL-X-7 primary human T-ALL sample ($1x10^6$), which expresses TAL1, RUNX1, and mutated NOTCH1. When $CD45^+$ human T-ALL blasts reached approximately 10% engraftment in the mouse peripheral blood, vehicle (Captisol) or AI-12-126 was administered at 100 mg/kg to mice by intraperitoneal (IP) injection daily for 2 weeks (Figure A.I.1A). *Tal1/Lmo2* mouse T-ALL cells ($1x10^5$) were transplanted to syngeneic mice and vehicle or the same dose of AI-12-126 were administered for 3 weeks starting at the time of transplant (Figure A.I.2B). For the survival assay, mice were

monitored and euthanized when they became moribund. To assess the leukemic burden *in vivo,* mice were sacrificed after 2 (for NSG mice) or 3 weeks (for FVB/N syngeneic mice) of treatment. The spleen weights and total BM cellularity of AI-12-126 treated mice were similar to those of vehicle treated mice (Figure A.I.1B and 2B). In addition, AI-12-126 treatment did not prolong the survival of mice transplanted with leukemic cells (Figure A.I.2C), indicating that AI-12-126 did not inhibit leukemic cell growth *in vivo*.

Pharmacokinetic analyses revealed that the half-life of AI-12-126 in the mouse peripheral blood was approximately 179 minutes a following IP injection, which seems to be reasonable (366). However, a FRET assay (366) and cell growth assay (Figure A.I.3) suggested that AI-12-126 has lower activity compared to AI-10-104 compound. These data suggest that AI-12-126 might not effectively target RUNX/CBFβ proteins *in vivo*, which should be examined using RUNX1/3-target gene expression profiling in leukemic cells of AI-12-126 treated mice. In addition, the development of other compounds that target RUNX proteins more efficiently without *in vivo* toxicity is required in order to evaluate RUNX1 as a therapeutic target for T-ALL.

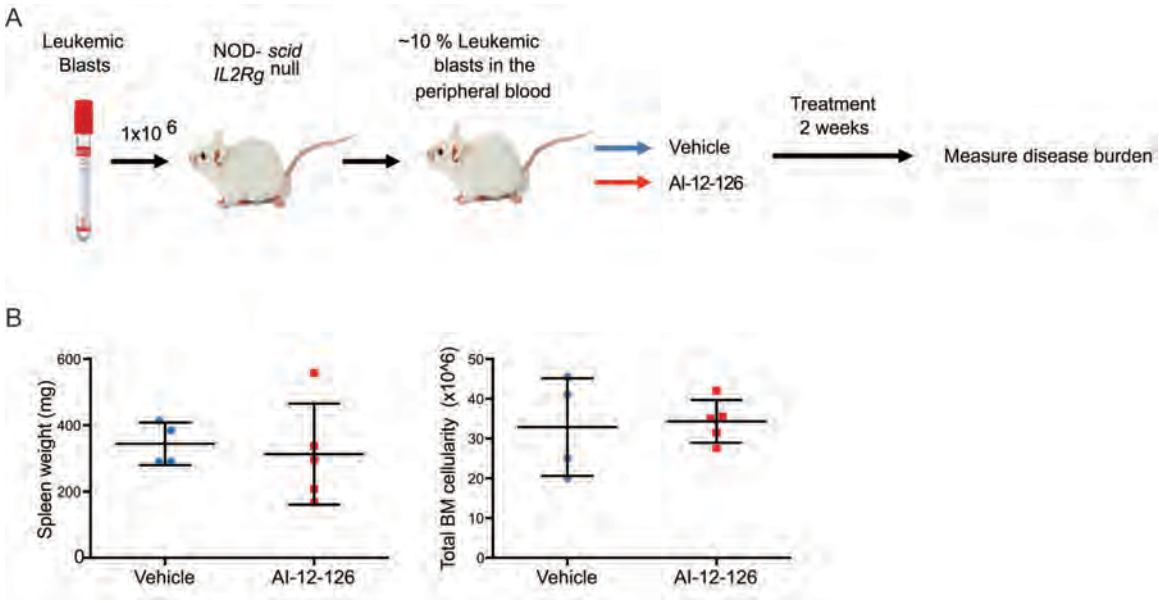

Figure A.I.1. AI-12-126 treatment does not suppress leukemia progression in mice transplanted with primary patient T-ALL sample. (A) Experimental scheme to determine the efficacy of AI-12-126 compound on leukemia progression *in vivo*. NSG mice were intravenously injected with $1x10^6$ primary human T-ALL blasts (TALL-X-7) and bled weekly to determine the percentage of circulating human $CD45^+$ cells in the mouse peripheral blood. When human leukemic blasts reached approximately 10% engraftment in the peripheral blood, vehicle (Captisol, n=4) or AI-12-126 (100 mg/kg, n=5) were administered daily to mice by intraperitoneal injection for 2 weeks. (B) The *in vivo* response of the primary human T-ALL sample to AI-12-126 treatment was assessed by spleen weight and total BM cellularity.

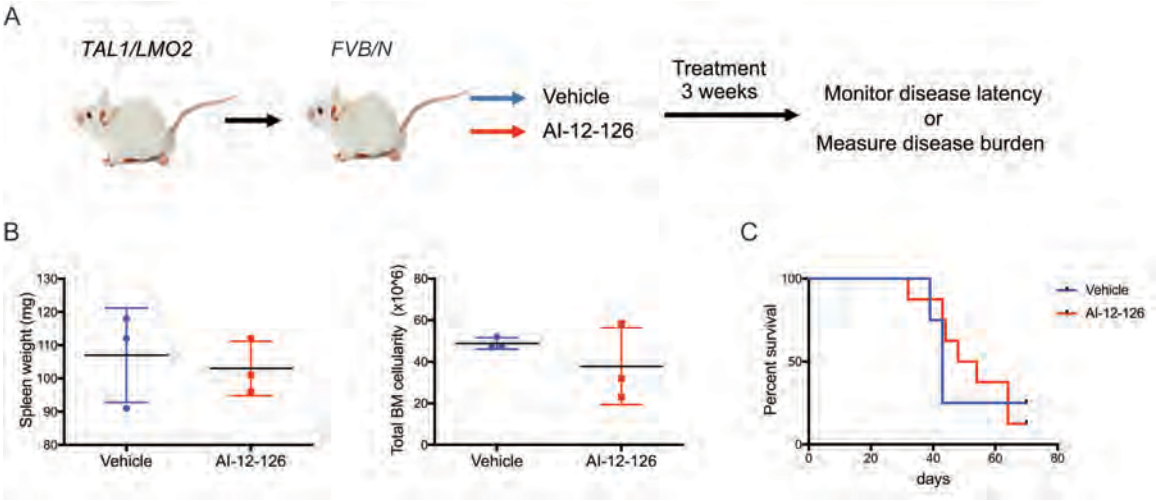

Figure A.I.2. Treatment of AI-12-126 does not inhibit leukemic growth *in vivo.* (A) Experimental strategy to determine the efficacy of AI-12-126 on leukemic cell growth *in vivo. Tal1/Lmo2* mouse T-ALL cells ($1x10^5$) were transplanted into syngeneic recipients and vehicle or AI-12-126 was administered at 100 mg/kg daily for 3 weeks. Administration of vehicle or AI-12-126 started at the time of transplant. (B) To examine leukemic burden, mice were sacrificed following 3 weeks of treatment and spleen weight and total BM cellularity were determined (C). For the survival assay, mice were monitored for disease and sacrificed when moribund. Kaplan-Meier survival curve is shown.

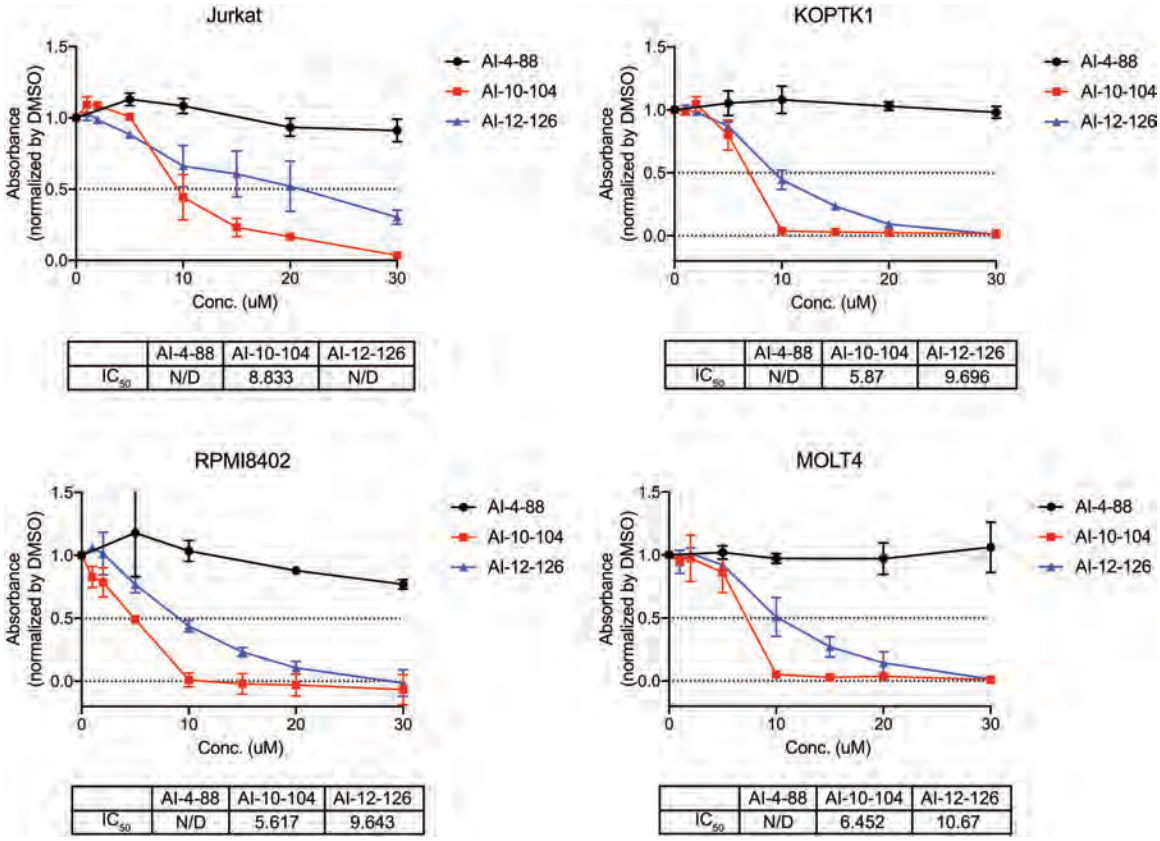

	AI-4-88	AI-10-104	AI-12-126
IC_{50}	N/D	8.833	N/D

	AI-4-88	AI-10-104	AI-12-126
IC_{50}	N/D	5.87	9.696

	AI-4-88	AI-10-104	AI-12-126
IC_{50}	N/D	5.617	9.643

	AI-4-88	AI-10-104	AI-12-126
IC_{50}	N/D	6.452	10.67

Figure A.I.3 AI-12-126 treatment inhibits the growth of human T-ALL cell lines. Jurkat, KOPTK1, PRMI8402, and MOLT4 human T-ALL cell lines were treated with AI-4-88, AI-10-104, or AI-12-126 for 3 days and the growth of leukemic cells were determined using an MTS cell viability assay reagent. IC_{50} was calculated using Prism7 software.

Appendix II

RUNX1 regulates DNA accessibility in mouse T-ALL cells

RUNX1, as a transcription factor, binds to DNA to activate or repress its target genes and is also suggested to play a role in chromatin structure formation (43,394). RUNX1 interacts with BRG1, a component of the SWI/SNF chromatin remodeling complex (43). During definitive hematopoiesis, RUNX1 has been shown to unfold chromatin and increase DNaseI accessibility around the *Pu.1* gene leading to expression of *Pu.1* (431). I have demonstrated that *Runx1* deletion in mouse T-ALL cells increases histone 3 recruitment to the *Myb* and *Myc* enhancers (Figure 3.4, 3.5). Therefore, I investigated genome-wide changes in chromatin accessibility upon *Runx1* deletion in mouse T-ALL cells using an ATAC-seq experiment (Assay for Transposase-Accessible Chromatin using Sequencing).

To delete *Runx1*, I treated *Tal1/Lmo2/Rosa26-CreER^{T2}Runx1$^{f/f}$* mouse T-ALL cells with 4-OHT for 24 hours and collected cells after an additional 24 hours. I isolated nuclei to reduce mitochondrial DNA contamination, which accounts for 40% of the total DNA quantity in mouse T-ALL cells, and generated the ATAC-seq library as described (384) (Chapter III methods and materials). Fragments from the library were sequenced using paired-end reads on the Illumina HiSeq 2000 instrument and the resulting sequence reads (approximately 200 million reads) were aligned to the mouse genome (mm10) using the Bowtie2

algorithm with help of Dr. Jun Yu and Dr. Julie Zhu at the University of Massachusetts Medical School. To identify nucleosome free-DNA regions, we focused on ATAC-seq signals aligned with reads smaller than 100 base pairs (432).

ATAC-seq analysis revealed that *Runx1* deletion induces genome-wide changes in chromatin accessibility (Figure A.II.1). A large number of regions became accessible (open chromatin regions) upon *Runx1* deletion. In the presence of RUNX1, 8081 loci were accessible while 11776 loci became accessible upon RUNX1 deletion. Since chromatin accessibility corresponds to transcriptional activity (433,434), we annotated genes associated with open or closed chromatin upon *Runx1* deletion to identify RUNX1-regulated genes. Since we do not have information about genome-wide enhancer loci in mouse T-ALL cells, we examined the ATAC-seq signals around promoter regions (5 kb up and downstream from the TSS, false discovery rate (FDR) <0.05, absolute log2-fold-change<2). Consistent with the result that *Runx1* deletion induced cell death, the accessibility to promoters of several pro-apoptosis genes such as *Bad*, *Bag6*, *Bcl7a*, and *Bcl2l11* were increased upon *Runx1* deletion. ATAC-seq signals at the promoter of *Cdkn1a*, which was upregulated upon *Runx1* deletion (Chapter III, Figure 3.1A) and negatively regulates cell cycle progression (435), was also increased in *Runx1* deleted cells. In addition, the promoter of *Cdkn2c*, which has been suggested as a tumor suppressor as a member of the INK4 family (436), was open upon *Runx1* deletion. These results support the idea that *Runx1*

deletion represses the growth of T-ALL cells by regulating involved gene expression. Examination of expression change of these genes should be followed to confirm RUNX1 regulation of these genes.

Interestingly, 2082 gene promoters became accessible whereas only 120 promoter regions were closed upon *Runx1* deletion, which precluded functional annotation analyses. Thus, we performed pathway and gene ontology (GO) enrichment analyses with open promoter regions upon *Runx1*-deletion. These analyses revealed that genes involved in RNA biogenesis, including RNA transport, ribonucleoprotein complex biogenesis, and splicing, were associated with open chromatin structures in *Runx1*-deleted T-ALL cells. In addition, promoter loci of genes that mediate histone modification and regulation of chromosome organization were accessible in *Runx1* deleted cells, suggesting that RUNX1 may repress the expression of genes involved in RNA biogenesis and chromatin remodeling. Genes belonging to each group are listed in Table A.II.1.

RUNX proteins are known to regulate ribosome biogenesis, which involves cell growth, cell cycle, and differentiation (437–439). The total amount of ribosome protein mRNAs and rRNAs in *Runx1*-deficient hematopoietic stem cells (HSCs) is reduced compared to wild-type HSCs, which is not evident in *Runx1*-deleted multipotent progenitor cells (MPPs) (437). RUNX1 and RUNX2 were shown to localize at nucleolar organizing regions in mitotic chromosomes where

rRNA genes reside. RUNX2 depletion, on the other hand, enhanced the synthesis of *rRNAs* in the SAOS-2 human osteosarcoma cell line (439). Therefore, RUNX1 appears to regulate *rRNA* expression and ribosome biogenesis in a cell-type dependent manner. The increased accessibility to promoter regions in *Runx1*-deleted cells suggests that RUNX1 represses ribosome biogenesis in T-ALL, which needs to be validated by expression change of the rRNA genes upon *Runx1* deletion. To examine the RUNX1 regulation of rRNA genes, which would change the total transcript amount, normalization of the gene expression should be performed based on the amount of external RNA controls (spike-in controls) added in proportion to the cell number. The enriched RUNX1 binding at *rRNA* genes can be tested using ChIP-seq to confirm direct RUNX1 regulation of those genes. However, the decreased cell growth in RUNX1 depleted cells (Chapter II) indicates that ribosome biogenesis would be decreased in *Runx1* deleted cells, which contradicts the ATAC-seq data.

Promoters of genes encoding histone modification enzymes, including histone methyltransferases (*Kmt2a* [histone-lysine N-methyltransferase 2A], *Setd1a* [histone-lysine N-methyltransferase SET domain 1A], *Ehmt2* [euchromatic histone-lysine N-methyltransferase 2]), and histone demethyltransferase (*Jmjd6* [arginine demethylase jumonji domain containing 6], *Kdm6b* [lysine demethylase 6B]), and histone acetyltransferase (EP300, *Kat14* [lysine acetyltransferase 14], and *Msl1* [male specific lethal 1 homolog]) became

accessible upon *Runx1* deletion, suggesting that RUNX1 may repress the expression of these genes. RUNX1 has been demonstrated to bind and cooperate with histone modification or remodeling cofactors such as EP300 and BGR1 (39,43). Therefore, it would be interesting to investigate whether RUNX1 regulates chromatin conformation by controlling the expression of these genes. Histone modification changes resulting from gene expression alteration can be evaluated using ChIP-seq for methylated or acetylated histones. Since both histone methyltransferase and demethyltransferase were suggested to be activated, the net change in methylation is unclear.

More number of loci were accessible in *Runx1*-deleted cells than in *Runx1*-wildtype cell (11776 versus 8081 loci), suggesting that *Runx1* deletion results in open chromatin structure overall. It is an unexpected result because that an accessible chromatin structure is associated with active gene expression and that a similar number of genes were upregulated or downregulated in a RUNX1-depleted Jurkat human T-ALL cell line (237). Furthermore, in contrast to the gene expression profiles that were downregulated by *Runx1* deletion (Chapter III, Figure 3.1), increased accessibility at promoters of *Gata3*, *Cdk6,* and *Igf1r* upon *Runx1* deletion was identified by ATAC-seq, suggesting active transcription of these genes. In addition, the accessibility to the *Myb* and *Myc* enhancer regions was increased in *Runx1*-deleted cells (Figure A.II.2), which is not consistent with increased histone 3 recruitment to these enhancers (Chapter III. Figure 3.5, 3.5). These inconsistencies suggest that the experiment may not

have been performed optimally. During the additional nuclei isolation process for reducing mitochondrial DNA contamination, nuclei could be damaged or fewer number of nuclei were collected, which would result in increased accessibility of transposase to DNA. On the other hand, cells used for library generation might have already initiated apoptosis and lost chromatin integrity. Even though I did not detect a significant amount of dead cells at the time of cell collection and also performed live-cell purification using ficoll-plaque gradient centrifugation, it is possible that cells undergoing apoptosis were still retained in the population. In these cases, DNA could be over-tagmented by transposase, resulting in non-specific ATAC-seq signals. Thus, careful validation of the ATAC-seq results by examination of gene expression alteration or polymerase II recruitment is required. Furthermore, since ChIP-seq for RUNX1 showed that more than 60% of RUNX1 binding loci are located at enhancer regions in human T-ALL cells (324), evaluation of chromatin accessibility changes at the enhancer loci upon *Runx1* deletion may be more informative. To map enhancer regions in the mouse T-ALL genome, ChIP-seq experiments for H3K27ac or H3K4me1, which marks active enhancer regions (440,441), should be performed.

A study of DNase I hypersensitivity combined with an expression profile showed that, even though there is a trend, a correlation between the degree of DNAase I hypersensitivity and the expression level is not strong (Pearson's R=0.09) (433). Therefore, in addition to ATAC-seq, RNA-seq and ChIP-seq for

histone marks of *Runx1* deleted mouse T-ALL cells will be required to reveal correlations between gene expression and chromatin accessibility.

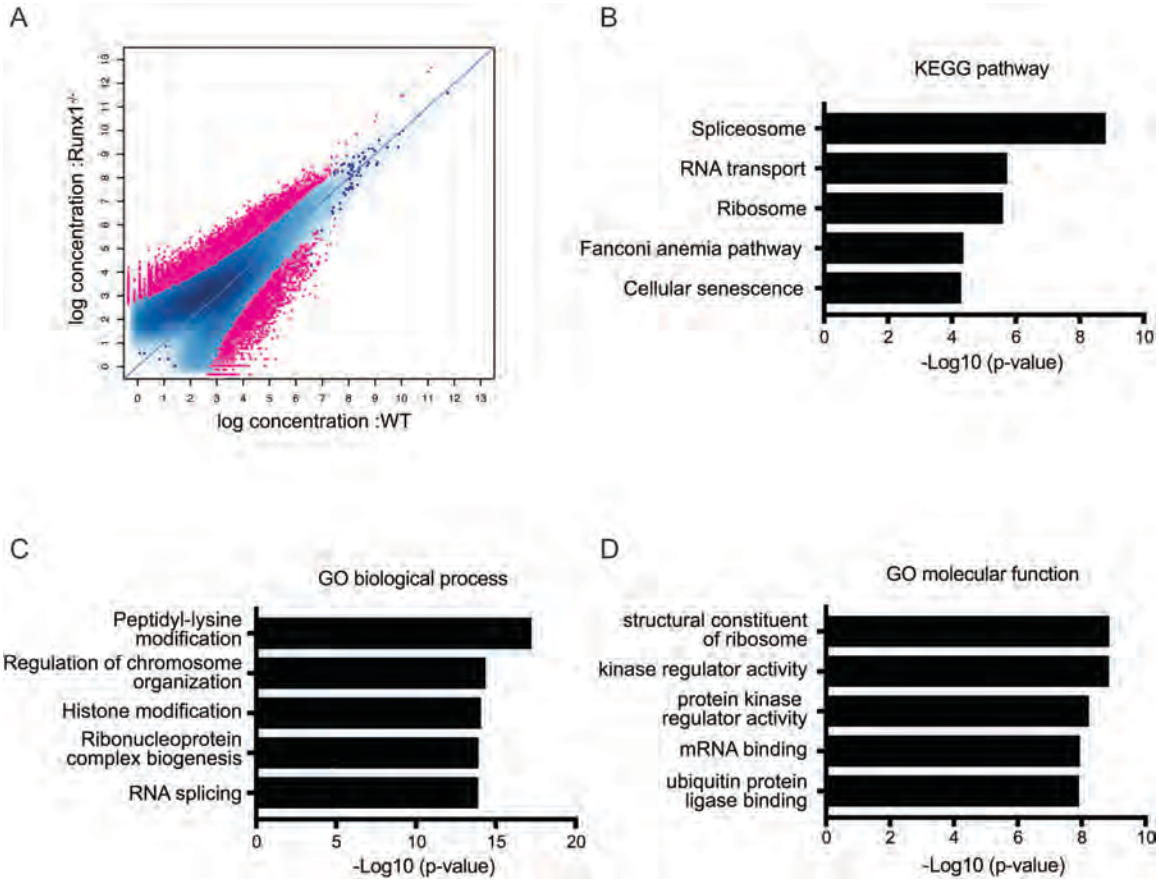

Figure A.II.1. Signals of ATAC-seq in *Runx1* deleted mouse T-ALL cells and over-represented pathways. (A) Scatter plot of ATAC-seq in *Runx1* deleted mouse T-ALL cells compared to untreated cells. (B-D) KEGG pathway, GO biological process, and GO molecular function analyses with promoter regions which are open upon *Runx1* deletion (Cutoff: FDR<0.05, |log2FC|>2 for promoter regions).

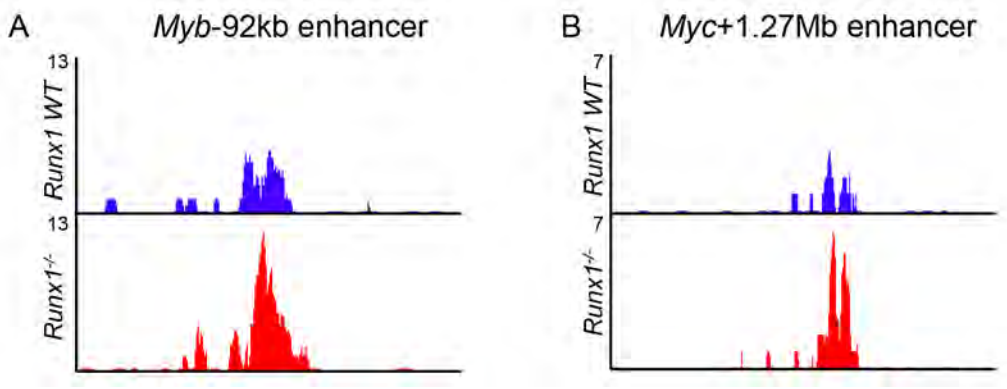

Figure A.II.2. The accessibility to the *Myb* and *Myc* enhancer regions is increased in *Runx1*-deleted cells. (A,B) Genome browser tracks show ATAC-seq signals around *Myb* -92 kb (A) and *Myc* +1.27 Mb (B) regions. The signals are increased in *Runx1*-deleted cells compared to *Runx1*-wildtype cells.

Table A.II.1. Gene lists of functional annotation analyses.

KEGG Pathway

ID	Description	qvalue	pvalue	Count	geneID
mmu03040	Spliceosome	3.51E-07	1.66E-09	34	Dhx8/Acin1/Ccdc12/Srsf2/Ddx42/Ddx5/Srsf10/Srsf1/Sf3a2/Bcas2/Syf2/Hnrnpk/Hnrnpa3/U2af1/Dhx16/Ddx39b/U2surp/Puf60/Tra2a/Cdc40/Ppil1/Ncbp2/Pcbp1/Ddx46/Snu13/Hspa2/Eif4a3/Thoc3/Sf3b2/Hnrnpu/Snrpb/Snrpd1/Aqr/Lsm2
mmu03013	RNA transport	0.000194	2.01E-06	33	Acin1/Fxr2/Ube2i/Nup50/Kpnb1/Snupn/Eif4a1/Casc3/Eif4g1/Eif2b4/Nup133/Ddx39b/Eif4b/Eif3c/Eif4a2/Nxf1/Eif2b1/Eif3a/Nupl1/Ncbp2/Eif2b3/Upf3a/Nup188/Eif4a3/Thoc3/Eif2s3x/Fxr1/Eif3i/Eif3d/Cyfip2/Ranbp2/Nup85/Eif3b
mmu03010	Ribosome	0.000194	2.75E-06	34	Rpl27/Rps27l/Rpl3/Mrpl30/Rpl23/Rpl13/Rps18/Rps12/Rpl18/Rps15/Rpl19/Rps15a/Rps10/Uba52/Rps28/Rps26/Rpl38/Rps17/Mrpl12/Rpl8/Rpl10/Rps25/Rpl26/Mrpl10/Rpl5/Rpl7a/Mrpl16/Rpl4/Mrpl23/Mrps5/Mrps6/Mrpl27/Rpl32/Mrpl3
mmu03460	Fanconi anemia pathway	0.002032	4.69E-05	14	Rpa2/Brca1/Cenps/Rmi1/Rev1/Hes1/Rmi2/Rad51/Top3a/Mlh1/Faap100/Rad51c/Rev3l/Eme1
mmu04218	Cellular senescence	0.002032	5.51E-05	32	Zfp36l1/Rras/Rad9b/Tsc1/Itpr2/Pten/Pik3r2/Smad3/Ppp1cc/Cdkn1a/Rad50/Zfp36l2/Rbl1/Mapk3/Sirt1/Foxo3/Cdk2/Akt2/Nras/Map2k1/E2f2/Sqstm1/Rela/Vdac1/Nfatc1/Vdac3/H2-T24/Hipk1/Lin9/Tgfb3/H2-Q2/Tgfb1

GO Biological Process

ID	Description	qvalue	pvalue	Count	geneID
GO:0018205	peptidyl-lysine modification	2.66E-14	6.35E-18	71	Arnt/Ube2i/Kmt5a/Jmjd6/Mettl8/Ep300/Gnl3/Brca1/Kmt2a/Hmg20a/Gata3/Suz12/Senp8/Kat6a/Msl1/Setd1a/Ehmt2/Rtf1/Wdr5/Jade2/Dhps/Setd4/Lipt2/Plod1/Setdb1/Ctnnb1/Supt6/Brd8/Pias1/Mapk3/Taf12/Vps33b/Sirt1/Kat14/Taf5l/Kmt2d/Kat5/Taf9/Ash1l/Tcf3/Rbbp5/Bag6/Smarcb1/Ctbp1/Setd2/Sirt5/Rela/Ldb1/Hint2/Pwp1/Mbd3/Phf20/Jarid2/Sae1/Phf1/Ndufab1/Hist1h1c/Sirt3/Dot1l/Brd4/Eef1akmt2/Pias3/Zfp335/Flcn/Atat1/Wdr82/Mllt6/Tg
GO:0033044	regulation of chromosome organization	1.02E-11	4.88E-15	65	Hnrnpa2b1/Tinf2/Cdc6/Cdt1/Ep300/Gnl3/Brca1/Kmt2a/Gata3/Ten1/Cdca5/Klhl22/Rnf40/Zfp207/Cct3/Setd1a/Ehmt2/Wdhd1/Rtf1/Mad1l1/H3f3a/Bub1/Smg6/Sart3/Rad50/Setdb1/Ctnnb1/Supt6/Mapk3/Ing2/Rmi2/Ctc1/Sirt1/Fen1/Ubr5/Srebf1/Aurkb/BC004004/Bcl6/Cdc45/Apc/Map2k7/Smg5/Smarcb1/Ctbp1/Tlk2/Hnrnpu/Axin2/Cct4/Slk/Sfpq/Recql4/Jarid2/
GO:0016570	histone modification	1.18E-11	9.5E-15	78	Jmjd6/Mettl8/Ep300/Brca1/Kmt2a/Usp3/Kdm6b/Uimc1/Gata3/Pagr1a/Suz12/Rnf40/Kat6a/Msl1/Setd1a/Ehmt2/Trim37/Rtf1/Wdr5/Jade2/Kmt2c/Sart3/Setdb1/Ctnnb1/Supt6/Brd8/Elk4/Mapk3/Ing2/Taf12/Sirt1/Ring1/Kat14/Taf5l/Ubr5/Srebf1/Kmt2d/Aurkb/Kat5/BC004004/Taf9/Bap1/Cdk2/Bcl6/Leo1/Pkn1/Ash1l/Tcf3/Jmjd1c/Rbbp5/Smarcb1/Ctbp1/Setd2/Satb1/Epop/Ldb1/Prkca/Atxn7l3/Pwp1/Mbd3/Slk/Sfpq/Phf20/Jarid2/Phf1/Hist1h1c/Dot1l/Br
GO:0022613	ribonucleoprotein complex biogenesis	1.18E-11	1.36E-14	74	Rpl27/Rps27l/Tsc1/Gnl3/Rpl3/Srsf10/Srsf1/Nol8/Pten/Nop2/Ftsj3/Rpusd2/Exosc4/Sf3a2/Utp6/Rps18/Rps15/Ago2/Setd4/Rps10/Sart3/Nop58/Utp18/Rps28/Ddx39b/Rpl38/Rps17/Hsp90aa1/Rpl10/Rps25/Rpl26/Mrpl10/Sirt1/Rpl5/Urb2/Lsg1/Sfswap/Taf9/Eif4b/Eif3a/Nop56/Wdr46/Nsun5/Snu13/Eif6/Rpl7a/Scaf11/Gnl1/Snrpb/Atxn2l/Snrpd1/Nufip1/Exosc8/Usp4/Ago1/Eif3d/Dhx30/Wdr37/Tfb2m/Exosc3/Ddx17/Luc7l3/Ybey/Tsr3/Rrp1b/Dhx9/Aam
GO:0008380	RNA splicing	1.18E-11	1.41E-14	69	Dhx8/Hnrnpa2b1/Scaf1/Acin1/Jmjd6/Polr2a/Sugp2/Srsf2/Ddx5/Cdk12/Srsf10/Tia1/Srsf1/Srek1/Clk4/Sf3a2/Tsen54/Bcas2/Syf2/Thrap3/Malat1/Hnrnpk/Hnrnpa3/U2af1/Casc3/Dhx16/Sart3/Tfip11/Supt6/Ddx39b/Rps26/Clk3/Nsrp1/Cactin/Tra2a/Cdc40/Puf60/Sfswap/Ppil1/Akt2/Ncbp2/Spen/Ptbp3/Ddx46/Snu13/Eif4a3/Thoc3/Hnrnpu/Raver1/Scaf11/Snrpb/Snrpd1/Sfpq/Ddx19b/Dbr1/Lsm1/Usp4/Aqr/Fastk/Rbm15b/Ddx17/Luc7l3/Rrp1b/Dhx9/Rsrc

GO Molecular Function

ID	Description	qvalue	pvalue	Count	geneID
GO:0003735	structural constituent of ribosome	5.31E-07	1.42E-09	35	Rpl27/Rps27l/Rpl3/Mrpl43/Mrpl30/Rpl23/Rpl13/Rps18/Rps12/Rpl18/Rps15/Rpl19/Rps15a/Rps10/Ndufa7/Rps28/Rps26/Rpl38/Rps17/Mrpl12/Rpl8/Rpl10/Rps25/Rpl26/Mrpl10/Rpl5/Dap3/Mrpl16/Rpl4/Mrpl23/Mrps6/Mrps5/Mrpl27/Rpl32/Mrpl3
GO:0019207	kinase regulator activity	5.31E-07	1.46E-09	40	Hexim1/Pik3r5/Hexim2/Rara/Tsacc/Socs7/Socs4/Pik3r2/Cd24a/Epo/Cdkn1a/Sh3bp5l/Iqgap1/Rptor/Lamtor3/Prkrip1/Rtn4rl1/Cdkn2c/Cks1b/Socs1/Cdc37/Socs3/Ccny/Ccnl1/Apc/Trib2/Wnk1/Nck1/Parp16/Itprip/Trib1/Socs6/Pak2/Taok1/Cdk5r1/Nyx/Rac2/Tgfb1/Smc
GO:0019887	protein kinase regulator activity	1.49E-06	6.16E-09	36	Hexim1/Hexim2/Tsacc/Socs7/Socs4/Cd24a/Epo/Cdkn1a/Sh3bp5l/Iqgap1/Rptor/Prkrip1/Rtn4rl1/Cdkn2c/Cks1b/Socs1/Cdc37/Socs3/Ccny/Ccnl1/Apc/Trib2/Wnk1/Nck1/Parp16/Itprip/Trib1/Socs6/Pak2/Taok1/Cdk5r1/Nyx/Rac2/Tgfb1/Smcr8/Map2k1
GO:0003729	mRNA binding	1.83E-06	1.18E-08	41	Hnrnpa2b1/Zfp36l1/Fxr2/Rara/Gnl3/Ddx5/Rnf40/Srsf1/Dcp1b/Hnrnpk/Ago2/Hnrnpa3/Eif4g1/Rps26/Zfp36l2/Igf2bp3/Hsp90aa1/Rpl26/Nsrp1/Rpl5/Jrk/Nxf1/Larp1/Eif3a/Ncbp2/Upf3a/Eif4a3/Cpsf1/Secisbp2l/Hnrnpu/Pcbp1/Fxr1/Lsm1/Carhsp1/Eif3d/Luc7l3/Dhx9/Calr/S
GO:0031625	ubiquitin protein ligase binding	1.83E-06	1.26E-08	52	Rpa2/Polr2a/Nlk/Brca1/Fzd5/Anapc2/Rnf40/Spop/Rpl23/Trim37/Faf2/Ube2r2/Ambra1/Smad3/Smad6/Ywhae/Casc3/Faf1/Ubxn1/Cdkn1a/Pias1/Gabarap/Triobp/Rpl5/Atp6v0c/Ube2z/Arrb2/Smad5/Dnajb2/Ube2k/Bag6/Apc/Smg5/Trib2/Hspa9/Tuba1b/Rela/Erlin2/Traf4/Axin2/Bag4/Dnaja1/Trib1/Ube2g2/Rffl/Ube2o/Sqstm1/Calr/Ube2n/Cul5/Map1lc3b/Tsg1

Appendix III

Repression of mTORC1 activity sensitizes T-ALL cells to ABT-263 treatment

Data from the following section were submitted as a manuscript not yet in print:

Anahita Dastur[#], **AHyun Choi[#]**, Carlotta Costa, Xunqin Yin, August Williams, Justine Roderick, Joseph McClanaghan, Neha U. Patel, Jessica Boisvert, Ultan McDermott, Mathew J. Garnett, Jorge Alemenara, Steven Grant, Kathryn Rizzo, Jeffrey A. Engelman, Michelle Kelliher, Anthony C. Faber, and Cyril H. Benes. NOTCH1 represses MCL-1 levels in T-ALL, making them susceptible to ABT-263. (2018) *Cancer Research,* Under review.
# Denotes co-first author

The manuscript has been edited for this thesis to show the results performed by AHyun Choi.

Activating mutations of NOTCH1 have been identified in more than 50% of T-ALL patient cases (151). Accordingly, therapies targeting NOTCH1 have been evaluated in clinical trials, but they have not been successful; patients treated with GSI suffered from continued disease progression and on-target toxicities in other tissues, such as the gastrointestinal tract (229). In an effort to identify alternative therapeutic strategies for T-ALL, Benes and colleagues previously performed a high-throughput drug screen across hundreds of human cancer cell lines (442). This screen uncovered that both GSI-sensitive and resistant T-ALL cell lines were highly sensitive to the BH3-mimetic ABT-263 (Navitoclax) compound, an inhibitor of anti-apoptotic proteins BCL-2, BCL-xL, and BCL-w (442,443). Apoptosis process is regulated by interactions among BCL-2 family

proteins that either promote or inhibit apoptosis. Anti-apoptotic proteins, such as BCL-2, BCL-xL, BCL-w, and MCL-1, bind and sequester pro-apoptotic proteins, including BAK, BAX, BIM, and BAD, to prevent cells from death, following mitochondrial outer membrane permeabilization (MOMP) (444). ABT-263 inhibits BCL-2, BC-xL and BCL-w by binding to them that results in release and activation of pro-apoptotic proteins (443,444).

In this study, treatment of human T-ALL cell lines with ABT-263 resulted in growth inhibition and apoptosis of leukemic cells. Consistent with previous studies, we found that low expression levels of MCL-1 determines the high-sensitivity of T-ALL cell lines to ABT-263 (442,445). MCL-1 is not bound by ABT-263 and MCL-1 sequesters free BIM released from BCL-2/BIM or BCL-xL/BIM complexes upon ABT-263 treatment (446). In addition, among the human T-ALL cell lines, GSI-sensitive T-ALL lines, such as KOPTK1, DND-41, and ALL-SIL (which express relatively lower levels of MCL-1 compared to GSI-resistant lines), were more sensitive to ABT-263 treatment. It has been known that mTORC1 controls the translation of MCL-1 in a cap-dependent manner (447–449) and, in agreement with this, mTORC1 inhibition by treatment of an mTORC1/2 inhibitor, AZD8055, decreased MCL-1 protein levels. Furthermore, combination treatment of AZD8055 and ABT-263 significantly induced apoptosis of T-ALL cell lines and primary patient samples *in vitro* (data not shown).

In order to validate the therapeutic effects of the combination treatment, we administrated ABT-263 and AZD8055 to *NOD-scid Il2rγ*$^{-/-}$ (NSG) mice

transplanted with primary human T-ALL blasts. A GSI-sensitive (TALL-X-7) and a GSI-resistant (TALL-X-2) primary patient sample were engrafted into mice and administered when 55-65 % of leukemic blasts were detected in the blood (Figure A.III.1). When both ABT-263 and AZD805 compounds were administered to mice transplanted with GSI-resistant patient sample, mice survived significantly longer than those treated with either ABT-263 or AZD8055 alone (Figure A.III.2A). In addition, the combination treatment of ABT-263 and AZD8055 more effectively inhibited the growth of human leukemic cells in mice (Figure A.III.3). However, in mice transplanted with the GSI-sensitive primary patient sample, the efficacy of combination treatment was similar to that of ABT-263 treatment alone (Figure A.III.2B and 4). These data are consistent with *in vitro* results that combination treatment is more effective in GSI-resistant T-ALL cells (data not shown).

These results suggest that ABT-263 could be an effective therapeutic compound for patients with T-ALL. In addition, treatment with mTOR inhibitor AZD8055 augmented the efficacy of ABT-263 in GSI-resistant T-ALL cells. Given that activation of the mTOR pathway is prevalent in T-ALL (154,209,210), the combination of ABT-263 and AZD8055 could be a promising therapy for T-ALL patients. Interestingly, we did not detect a difference in expression levels of MCL-1 across GSI-sensitive and resistant primary patient samples, which is not consistent with T-ALL cell lines (Data not shown, Figure A.III.5). This indicates that something other than the level of MCL-1 expression can influence the

sensitivity of ABT-263. We also observed that growth of one of primary relapse T-ALL samples (TALL-X-15) was not inhibited by ABT-263 treatment at all (data now shown). Therefore, further studies designed to understand the underlying mechanism of ABT-263 efficacy are required.

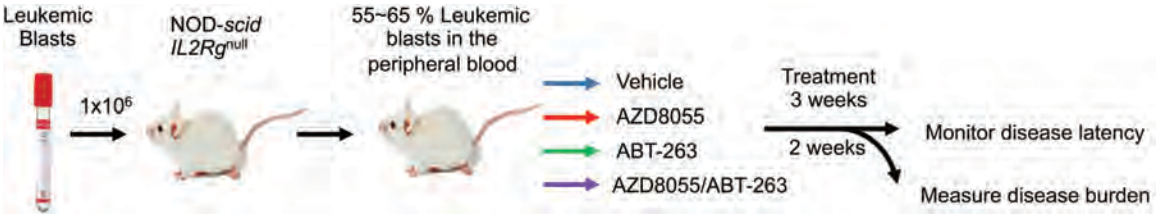

Figure A.III.1. Experimental strategy of used to determine the efficacy of combination treatment of AZD8055 and ATB-263 on leukemia progression *in vivo*. NSG mice were intravenously injected with 1 x 10^6 primary human T-ALL blasts and bled weekly to determine the percentage of circulating human $CD45^+$ cells in the peripheral blood. Once the leukemic burden reached 55% (TALL-X-7) or 65% (TALL-X-2) human leukemic blasts in the peripheral blood, mice were randomized to one of four treatment groups. Vehicle, AZD8055 (16mg/Kg, diluted in Captisol), ABT-263 (80mg/Kg, diluted in 60% Phosal 50 PG, 30% PEG 400 and 10% EtOH) or both AZD8055 and ABT-263 were administered to mice by oral gavage for 2 or 3 weeks using a 6-day on, 1-day off regimen. For the survival assay, mice were administrated with compounds for 3 weeks, monitored daily, and sacrificed when moribund. To assess leukemic burden, animals were sacrificed following 2-weeks of treatment and the percentage of human $CD45^+$ leukemic cells in mouse spleen, bone marrow, and peripheral blood were determined by flow cytometry. All mouse procedures used in this study were approved by the University of Massachusetts Medical School Institutional Animal Care and Use Committee.

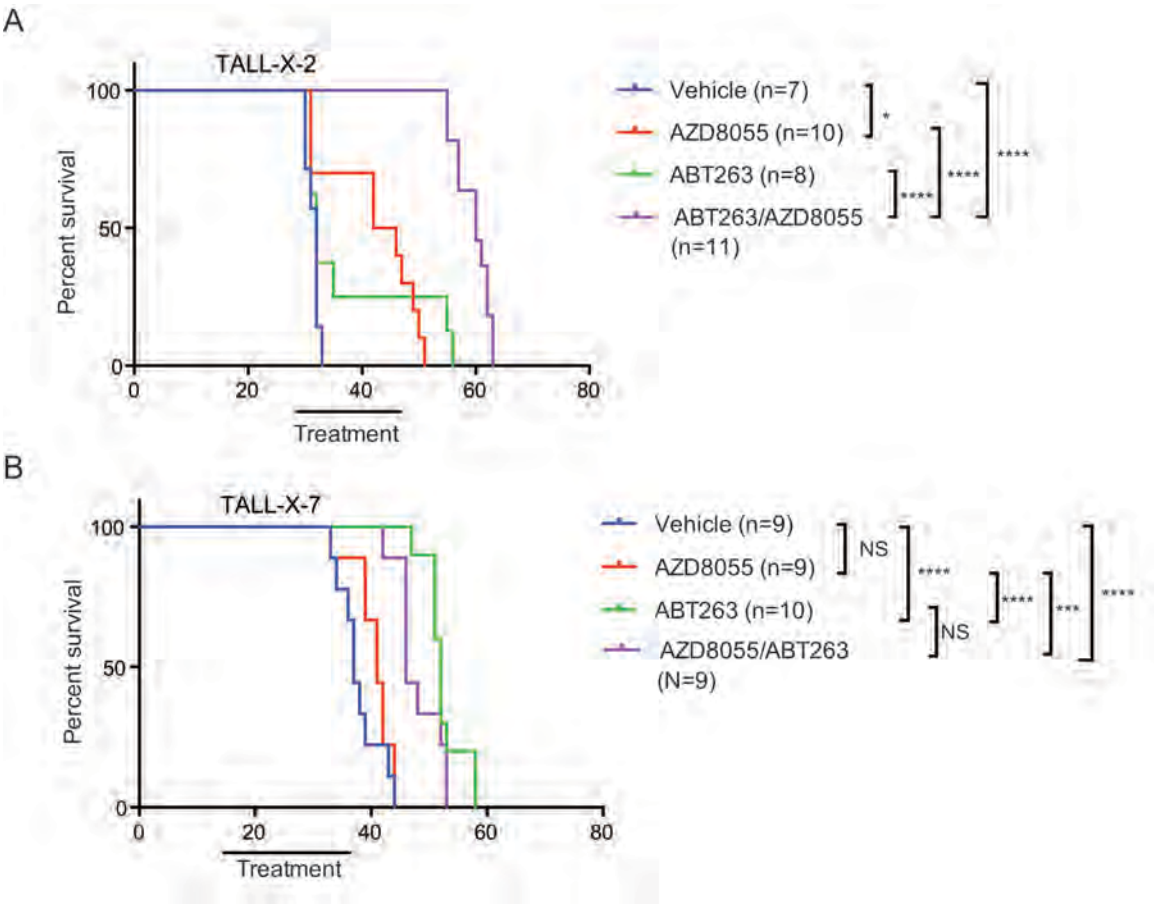

Figure A.III.2. Treatment of AZD8055 and ABT-263 prolong survival of mice transplanted with primary T-ALL patient samples. Kaplan-Meier survival curves are shown for TALL-X-2 (B) and TALL-X-7 (C) samples. The difference in overall survival between the treatment groups was assessed by log-rank test using GraphPad Prism software, V7.0 (*p<0.05, *** p<0.001, **** *p*<0.0001).

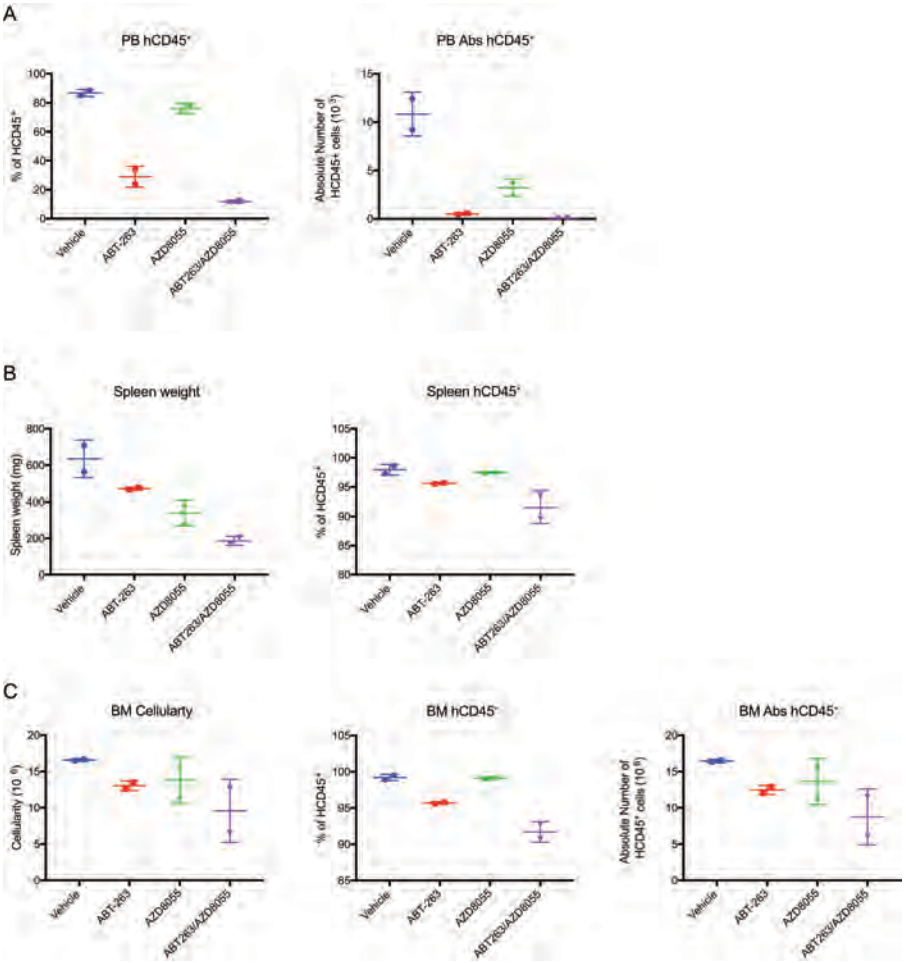

Figure A.III.3. Combination treatment of AZD8055 and ABT-263 inhibits leukemic burden *in vivo*. *In vivo* response of the TALL-X-2 primary T-ALL sample to ABT-263, AZD8055, or combination of ABT-263 and AZD8055 treatment was determined by counting total number or percentage of human $CD45^+$ leukemic blast in mouse peripheral blood (A), spleen (B), and bone marrow (C). Mice were sacrificed at 2-weeks post-treatment.

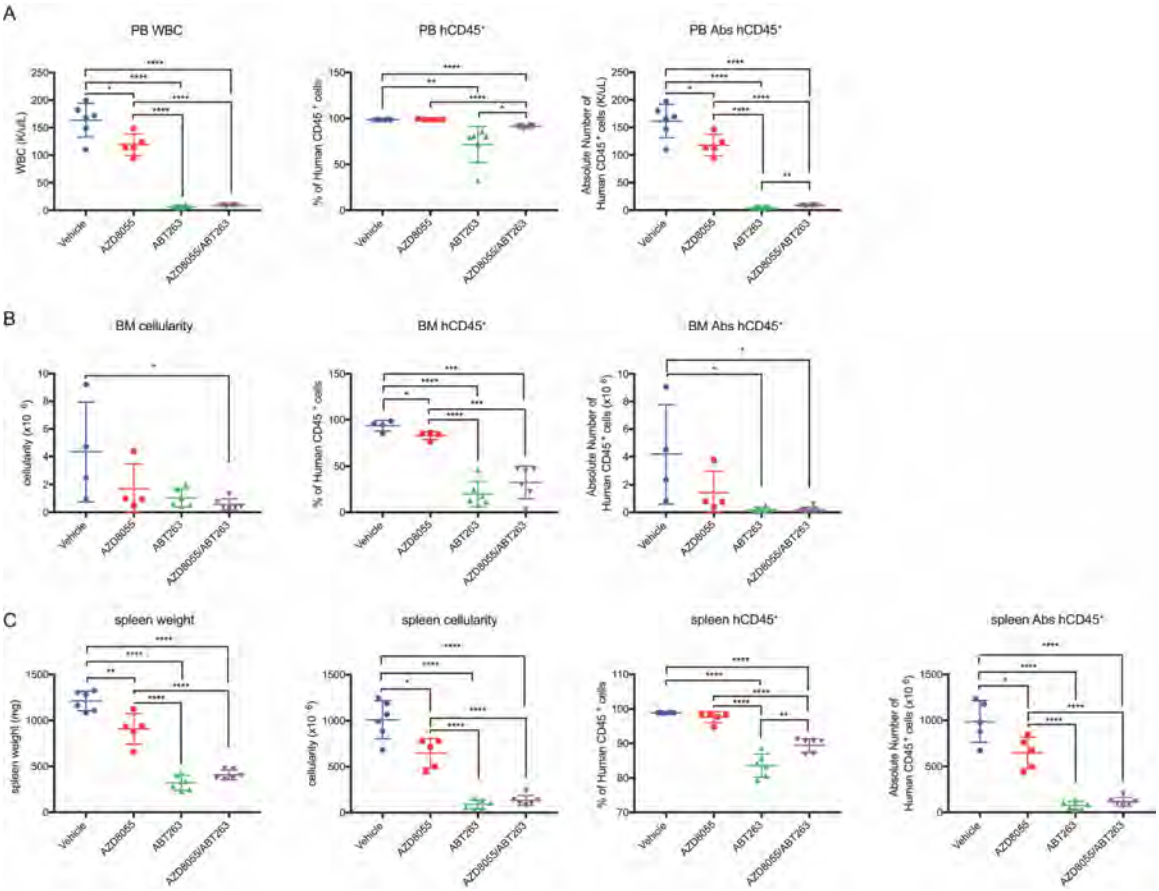

Figure A.III.4. The *in vivo* growth of TALL-X-7 primary T-ALL patient sample is suppressed by treatment with ABT-263. The total number and percentage of human CD45^{+} leukemic blasts in mouse peripheral blood, bone marrow, and spleen were counted to determine the *in vivo* response of TALL-X-7 primary T-ALL patient sample to 2-week administration of ABT-263, AZD8055, and combination of ABT-263 and AZD8055.

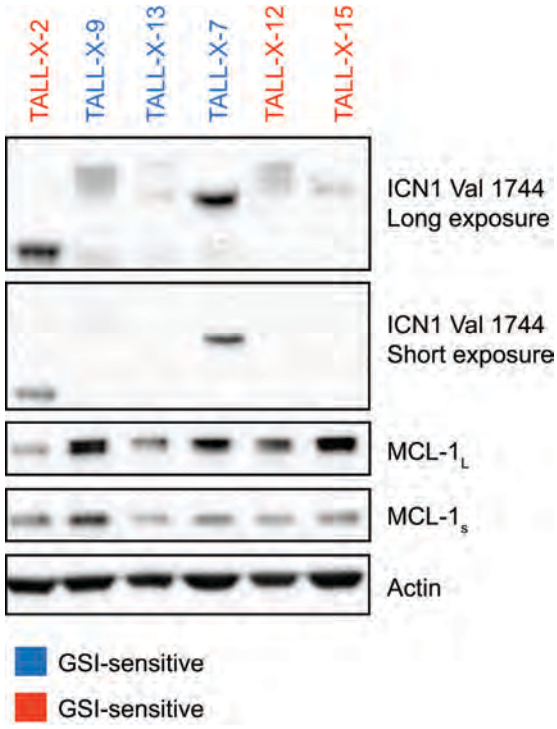

Figure A.III.5. The expression of intracellular NOTCH1 and MCL-1 in primary T-ALL patient samples. Protein lysates from primary T-ALL patient samples were separated on an SDS-PAGE gel and intracellular NOTCH1 and MCL-1 protein levels were determined by immunoblotting. β-Actin was used as a loading control.

Appendix IV

Attempts to identify a compound that selectively kills ETP-ALL cells

Early T-cell precursor acute lymphoblastic leukemia (ETP-ALL) is a subtype of T-ALL that accounts for approximately 15% of pediatric and 10-30% of adult patients with T-ALL (130,450–453). It is distinguished from typical T-ALL subtypes by a distinct immunophenotype of $CD1a^{-}$, $CD8^{-}$, and $CD5^{weak}$ with aberrant expression of hematopoietic stem or myeloid cell markers including CD13, CD33, CD34, and CD117 (130). Genomic analyses have demonstrated that ETP-ALL is associated with increased genomic instability and harbors diverse mutations (131,130). Activating mutations of cytokine receptors and RAS signaling, such as FLT3, IGFR1, JAK1/3, KRAS, and NRAS, and inactivating mutations in hematopoietic development pathways and histone-modification has been frequently identified in ETP-ALL samples (131). Patients with ETP-ALL have an especially high-risk of treatment failure and relapse; the overall incidence of induction failure and relapse is over 50% in ETP-ALL patients (130,453,454). Therefore, there is an urgent need for development of alternative targeted therapies for this chemotherapy-refractory subtype of T-ALL.

To identify pharmacologically effective compounds to inhibit ETP-ALL survival, we performed small molecule screening using the Loucy cell line as a human ETP-ALL model. In collaboration with Dr. Sangram Parelkar and Dr. Paul Thompson at Small Molecule Screening Facility, University of Medical School

Massachusetts. The primary screen identified 42 compounds cytotoxic to Loucy cells. We selected 19 compounds that target pathways disrupted in cancer, including protein kinase C (PKC) and the NF-kB pathway, and tested their efficacy in Loucy cells in comparison to the Jurkat cell line, a typical T-ALL cell line (Table A IV.1). Six out of 19 compounds inhibited the proliferation of Loucy cells at low concentrations but were not deleterious to Jurkat cells (Figure A IV.1). These compounds included inhibitors of PKC, protein phosphatase 2A (PP2A), CDC25A phosphatase, or Vitamin A acid analog (Table A IV.2).

PKC is a family of serine/threonine protein kinases that functions in cell proliferation, survival, and differentiation through mediation of signal transduction (455–457). PKC has been implicated in the tumorigenesis of several types of cancer including prostate, breast, lung cancer, and chronic lymphocytic leukemia (455,456,458–460). PP2A is also known to mediate PKC signaling (461). Thus, we further validated the screening results by treating Loucy and Jurkat cells with various concentration of Rottlerin (an PKCδ and θ inhibitor) and Cantharidin (an PP2A inhibitor). We also tested the efficacy of Retinoic acid p-hydroxyanilide (a Vitamin A acid analog) in the suppression of ETP-ALL cell growth since all-trans retinoic acid (ATRA) therapy has improved the outcome of acute promyelocytic leukemia (APL) (462). We observed that only Rottlerin inhibited the growth of Loucy cells selectively at a low concentration (Figure A.IV.2A). It also effectively repressed survival of primary ETP-ALL patient samples, though primary typical

T-ALL patient cells were equivalently sensitive to Rottlerin treatment (Figure A.IV.3B).

Targeting PKC signaling in ETP-ALL is especially intriguing based on the fact that several PKC isozymes are involved in RAS-mediated tumorigenesis (458,463–466). To date, 10 isozymes of PKC have been identified, which are sub-grouped into conventional (α, βI, βII, and γ), novel (δ, ε, η, and θ), and atypical (ζ, λ/ι) groups based on their structural similarity and co-factor requirements (455,456). PKCδ and ι have been shown to be required for K-RAS mediated lung cancer (458,463,464). PKCε isozyme activates RAF, a downstream kinase of RAS pathway (465,466). Thus, inhibiting certain PKC isozymes might suppress the activated RAS pathway in ETP-ALL.

However, targeting the PKC pathway to inhibit tumor progression does not appear to be straightforward. First, certain tissues express several PKC isozymes; some of these are functionally redundant and others interact to promote or antagonize each other's activity (455,467,468). T-lymphocytes are known to express 8 PKC isozymes: α, β, δ, ε, η, θ, ζ, and ι, and PKCα and PKCβ regulate IL-2 expression cooperatively (467,469). In addition, some PKC isozymes such as PKCα and δ have been shown to function as tumor suppressors, depending on cellular context (456). A study with K-RAS-dependent lung cancer showed that PKCα suppresses tumor initiation and progression through p38 MAPK/TGFβ signaling (470). Several studies implicate PKCδ as a

pro-apoptotic and anti-proliferative kinase (471,472). Common mutations found in PKC isozymes resulting in reduced or abolished PKC activity also support tumor suppressing roles of PKC (473). Lastly, PKC-mediated K-RAS phosphorylation at Serine-181 reduced K-RAS activity, suggesting that inhibiting PKC might enhance K-RAS mediated transformation (474). Thus, further understanding about the roles of each PKC isozyme in various tissues is needed. In addition, developing molecules targeting specific PKC isozymes that function in ETP-ALL will be required.

Table A IV.1. The list of compounds selected for the secondary screening.

LOPAC ID	Name	Description
1839	rac-2-Ethoxy-3-octadecanamido-1-propylphosphocholine	Protein kinase C (PKC) inhibitor
1982	Retinoic acid p-hydroxyanilide	Vitamin A acid analog with antiproliferative activity in cultured human breast cancer cells
1908	rac-2-Ethoxy-3-hexadecanamido-1-propylphosphocholine	Protein kinase C (PKC) inhibitor
1598	Chelerythrine chloride	PKC inhibitor; affects translocation of PKC from cytosol to plasma membrane
1787	ET-18-OCH3	Phosphoinositide-specific Phospholipase C (PI-PLC) inhibitor
1648	CGP-74514A hydrochloride	Cdk1 inhibitor
1605	Cantharidin	Protein phosphatase 2A inhibitor
1675	Cantharidic Acid	Protein phosphatase 1 (PP1) and 2A (PP2A) inhibitor
2098	PM-20	Novel Cdc25A phosphatase inhibitor.
1674	Calcimycin	Ca2+ ionophore used to potentiate responses to NMDA, but not quisqualate glutamate receptors
2570	Terfenadine	Non-sedating H1 histamine receptor antagonist
1540	Bay 11-7085	Inhibits cytokine induced IkB (Inhibitor of NFkB) phosphorylation
2409	Rottlerin	PKC and CaM kinase III inhibitor
2473	DL-Stearoylcarnitine chloride	Protein kinase C (PKC) inhibitor
1392	5-azacytidine	DNA methyltransferase inhibitor
2281	TPCA-1	Potent and selective inhibitor of human IkB kinase-2 (IKK-2) used to study inflammation in animal models.
2302	Parthenolide	Inhibits serotonin release from platelets; inhibits production of leukotriene B4 and thromboxane B2
2111	Mevastatin	Antibiotic; inhibits post-translational prenylation of proteins such as Ras and geranylgeranylation of Rho
1862	Picropodophyllotoxin	Insulin-like growth factor-I (IGF-I) receptor kinase inhibitor.

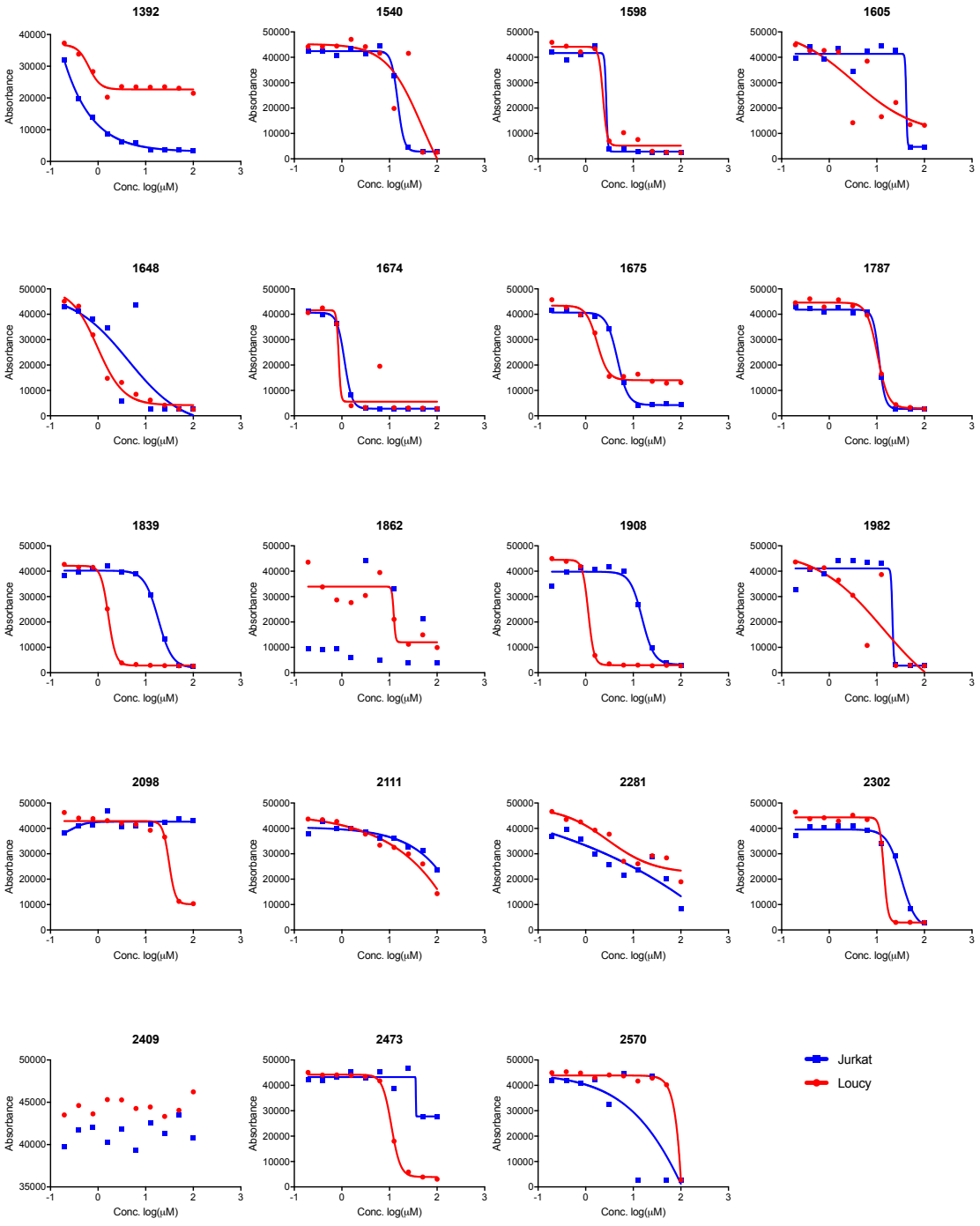
1392
1540
1598
1605
1648
1674
1675
1787
1839
1862
1908
1982
2098
2111
2281
2302
2409
2473
2570
Absorbance
Conc. log(μM)
Jurkat
Loucy

Figure A.IV.1. Secondary screening identifies compounds that are selectively effective against the Loucy ETP-ALL cell line. Loucy and Jurkat cells were treated with compounds selected from primary screening for 3 days and the viability was measured using Celltiter-Blue cell viability assay reagent (Promega). Dr. Parelkar at the Small Molecule Screening Facility conducted experiments and I analyzed data using Prism7 Software.

Table A.IV.2. The list of 6 compounds identified in the secondary screening

LOPAC ID	Name	Cas No.	Description	IC_{50} (μM)	
				LOUCY	Jurkat
1839	rac-2-Ethoxy-3-octadecanamido-1-propylphosphocholine	163702-18-9	PKC inhibitor	1.641	18.41
1982	Retinoic acid p-hydroxyanilide	65646-68-6	Vitamin A acid analog	13.58	~ 21.28
1908	rac-2-Ethoxy-3-hexadecanamido-1-propylphosphocholine	112989-01-2	PKC inhibitor	1.138	15.32
1605	Cantharidin	56-25-7	PP2A inhibitor	3.268	~ 41.54
2098	PM-20	863886-38-8	Cdc25 phosphatase inhibitor	N/D	N/D
2473	DL-Stearoylcarnitine chloride	18822-91-8	PKC inhibitor	10.98	35.93

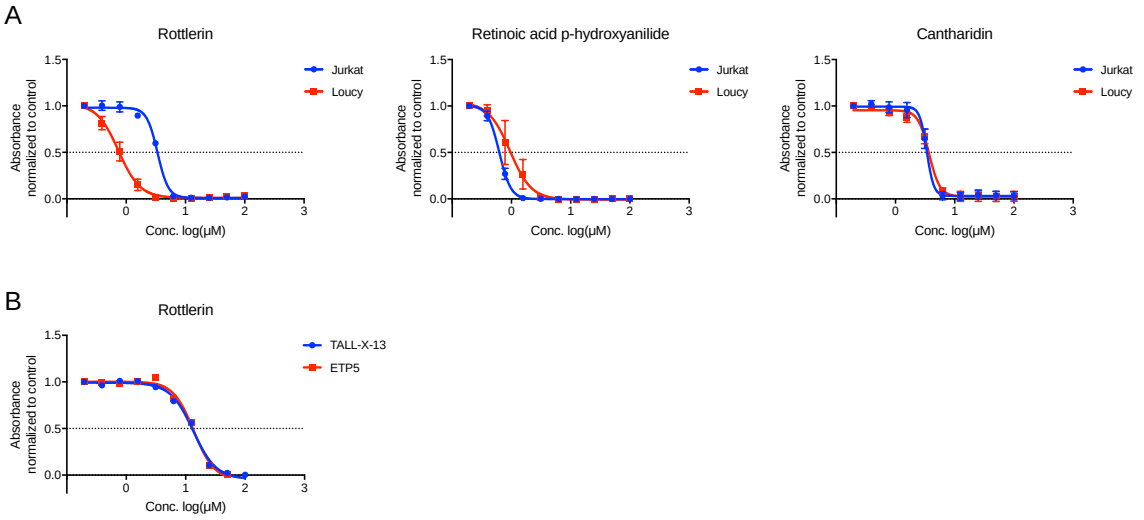

Figure A.IV.2. The sensitivity of compounds in ETP-ALL cell lines and primary patient samples. (A) Loucy and Jurkat cells were treated with a PKCδ inhibitor Rottlerin (Santa Cruz Biotechnology), a Vitamin A acid analog Retinoic acid p-hydroxyanilide (Santa Cruz Biotechnology), and a PP2A inhibitor Cantharidin (Cayman) for 3 days. Jurkat and Loucy cells were plated with 10^4 and $5x10^4$ cells per well, respectively, in 96-well plates before treatment with the compounds. Cell viability was measured using Celltiter-Blue cell viability assay reagent, following the manufacturer's instructions. Data presented are from 4 biological replicates. (B) Primary typical T-ALL and ETP-ALL patient samples plated in 96-well plates at 10^5 cells per well density were treated with Rottlerin for 3 days. Data are shown as mean of 2 to 4 biological replicates. Cell viability was determined using CelltiterGlo cell vitality assay reagent.

Appendix V

Identification of tumor suppressor(s) in chromosome 6q deleted region that cooperate with TAL1 to cause T-ALL

Among the cytogenetic abnormalities identified in T-ALL, broad deletions of chromosome 6q have been observed in 10-30% of T-ALL and are associated with poor early treatment response (475–478). Downregulation of genes in these regions such *CASP8AP2* (478), *GRIK2* (479), and *EPHA7* (480) have been observed in T-ALL and are proposed to be tumor suppressors. However, tumor suppressor(s) function has yet to be demonstrated.

Recently, Mullighan's group at St. Jude Children's Research Hospital performed an integrated analysis that combined sequence mutations, DNA copy-number alteration, and structural variant/rearrangement analysis of 264 pediatric T-ALL patient samples. They demonstrated that broad deletions with variant sizes on chromosome 6q14-q23 were present in 19.3% of cases, which were enriched in cases with *TAL1*, *TLX1*, *LMO2*, and *NKX2-1* deregulation (150). The deleted regions were further refined using a computational approach called GRIN (genomic random interval model) into a 79.5 Mb to 97.1 Mb segment on chromosome 6, which was again highly associated with subgroups of *LMO1/2* rearrangement (30%), *TAL1* (29%), *TLX3* (23%). Furthermore, using RNA-seq

and copy number loss data, 38 genes were identified as the most commonly affected genes in the deleted region of 6q14.1 to q16.1 (150).

Given that loss of gene(s) in this region appears to collaborate with LMO1/2 or TAL1 in T-ALL pathogenesis, we plan to test the transforming function of the candidate genes in our *Tal1 or Tal1/Lmo2* T-ALL mouse model. Using the USCS genome browser, I identified mouse chromosome 4qA3-qA5 and mouse chromosome 9qE3-qE3.1 as the orthologous regions to human chromosome 6q14.1-16.1 (Figure A.V.1). Thirty-two of 38 candidate genes identified in human T-ALL samples are conserved in the mouse genome. To identify genes involved in T-ALL development, shRNA library will be constructed consisting of multiple shRNAs to each of the conserved genes. Lentiviral stocks will be prepared and used to infect *Tal1* or *Tal1/Lmo2* T-ALL cells. Following puromycin selection, the growth of virus-infected cells will be examined *in vitro* or in transplanted syngeneic mice. DNA from Cells that outcompete control-shRNA infected cells for growth will be collected and sequenced to identified silenced genes.

We expect that suppression of the putative tumor suppressors will stimulate leukemic growth/survival in vivo and accelerate leukemogenesis *in vivo.* Since most of the deleted regions are broad containing more than one gene, multiple genes in the deleted regions appear to collaborate simultaneously in T-ALL pathogenesis.

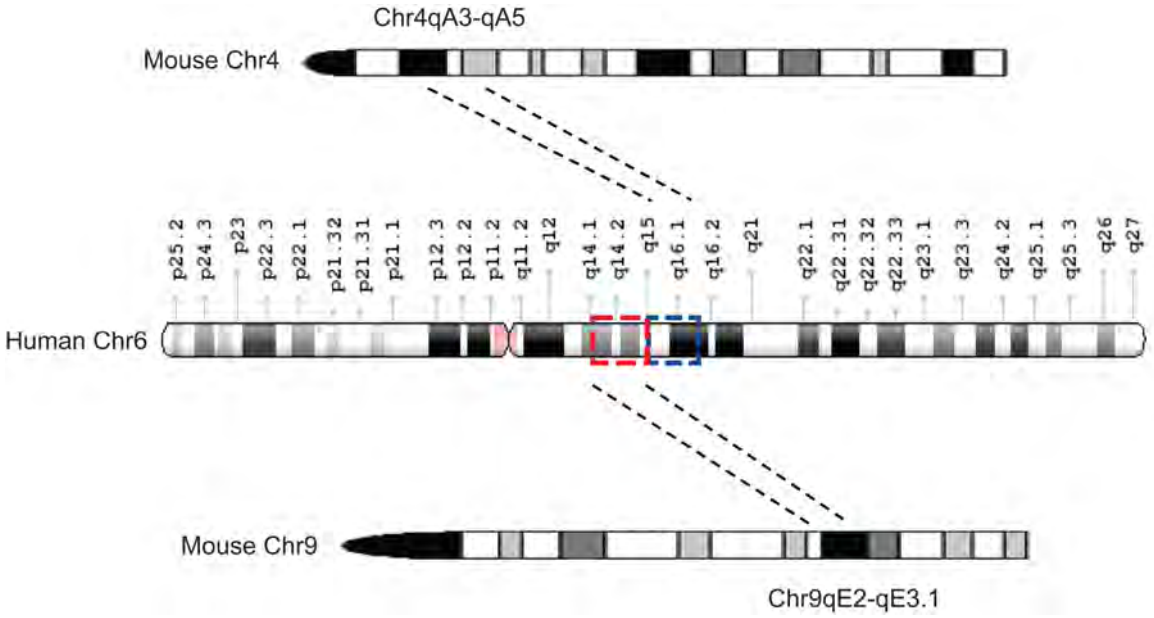

Figure A.V.1. The orthologous mouse genomic loci of human chromosome 6q deleted regions. The most commonly deleted regions of chromosome 6q in human T-ALL are conserved in the mouse genome at chromosome 4q and chromosome 9q. The UCSC genome browser (genome.ucsc.edu) was used to determine the conserved regions in the mouse genome.

List of primers

Table A.1 Primers for ChIP-qPCR

Target locus	Direction	Primer sequence (5' to 3')
ChIP-mNMe	For	AACCCTGAACCTGGTGATTG
	Rev	AGTGCTGGTGCCAAGAACTC
ChIP-mNMe H	For	CCCAACGTATTCCTCAACTGC
	Rev	AATGAAGTCACCTGCCCACT
ChIP-mMyb+15	For	CTGTGTCTGGGGAAGGGGGT
	Rev	TCTTGCCTCCAACAGCATCT
ChIP-mMyb-92	For	TGGTTTCCAGGGACCGTTAG
	Rev	GCAAACCACAGAGACTTGCA
ChIP-mMyb-92 H	For	TGGATCCACTGAGCAGAACA
	Rev	TGGCTTCCCTACTGAGCTGT
N.control (Gene desert)	For	AACCTCACACACAACAAGCTG
	Rev	TGTGATAGGGAGAATGCTTGC
ChIP-mHes1pro	For	GACCTTGTGCCTAGCGGCCA
	Rev	AGACAGGGGATTCCGCTGTT

Table A.2. Primers for ATAC-qPCR

Target Locus	Direction	Primer sequence (5' to 3')
mNMe	For	AGAGGAGTTCTTGGCACCAG
	Rev	TTAGGCAGACTGCAGGGAAC
Gene Desert 1	For	AACCTCACACACAACAAGCTG
	Rev	TGTGATAGGGAGAATGCTTGC
Gene Desert 2	For	GCTACAAAAGAGTGAGGTCGT
	Rev	TTCCTACCCAGAAGTGTGCC

REFERENCES

1. Hunger SP, Mullighan CG. Acute Lymphoblastic Leukemia in Children. Longo DL, editor. N Engl J Med. 2015 Oct 15;373(16):1541–52.

2. Terwilliger T, Abdul-Hay M. Acute lymphoblastic leukemia: a comprehensive review and 2017 update. Blood Cancer J. 2017 Jun 30;7(6):e577.

3. Rossi L, Challen GA, Sirin O, Lin KK-Y, Goodell MA. Hematopoietic Stem Cell Characterization and Isolation. In: Methods in molecular biology . 2011. p. 47–59.

4. Ye F, Huang W, Guo G. Studying hematopoiesis using single-cell technologies. Vol. 10, Journal of Hematology and Oncology. BioMed Central; 2017. p. 27.

5. Birbrair A, Frenette PS. Niche heterogeneity in the bone marrow. Ann N Y Acad Sci. 2016 Apr 1;1370(1):82–96.

6. Osawa M, Hanada K, Hamada H, Nakauchi H. Long-term lymphohematopoietic reconstitution by a single CD34-low/negative hematopoietic stem cell. Science. 1996 Jul 12;273(5272):242–55.

7. Morrison SJ, Weissman IL. The long-term repopulating subset of hematopoietic stem cells is deterministic and isolatable by phenotype. Immunity. 1994 Nov 1;1(8):661–73.

8. Guenechea G, Gan OI, Dorrell C, Dick JE. Distinct classes of human stem cells that differ in proliferative and self-renewal potential. Nat Immunol. 2001 Jan 1;2(1):75–82.

9. Ema H, Sudo K, Seita J, Matsubara A, Morita Y, Osawa M, et al. Quantification of Self-Renewal Capacity in Single Hematopoietic Stem Cells from Normal and Lnk-Deficient Mice. Dev Cell. 2005 Jun;8(6):907–14.

10. Yang L, Bryder D, Adolfsson J, Nygren J, Månsson R, Sigvardsson M, et al. Identification of Lin(-)Sca1(+)kit(+)CD34(+)Flt3- short-term hematopoietic stem cells capable of rapidly reconstituting and rescuing myeloablated transplant recipients. Blood. 2005 Apr 1;105(7):2717–23.

11. Adolfsson J, Borge OJ, Bryder D, Theilgaard-Mönch K, Astrand-Grundström I, Sitnicka E, et al. Upregulation of Flt3 expression within the bone marrow Lin(-)Sca1(+)c-kit(+) stem cell compartment is accompanied by loss of self-renewal capacity. Immunity. 2001 Oct;15(4):659–69.

12. Christensen JL, Weissman IL. Flk-2 is a marker in hematopoietic stem cell differentiation: a simple method to isolate long-term stem cells. Proc Natl Acad Sci U S A. 2001 Dec 4;98(25):14541–6.

13. Kiel MJ, Yilmaz ÖH, Iwashita T, Yilmaz OH, Terhorst C, Morrison SJ. SLAM Family Receptors Distinguish Hematopoietic Stem and Progenitor Cells and Reveal Endothelial Niches for Stem Cells. Cell. 2005 Jul 1;121(7):1109–21.

14. Oguro H, Ding L, Morrison SJ. SLAM Family Markers Resolve Functionally Distinct Subpopulations of Hematopoietic Stem Cells and Multipotent Progenitors. Cell Stem Cell. 2013 Jul 3;13(1):102–16.

15. Akashi K, Traver D, Miyamoto T, Weissman IL. A clonogenic common myeloid progenitor that gives rise to all myeloid lineages. Nature. 2000 Mar 9;404(6774):193–7.

16. Kondo M, Weissman IL, Akashi K. Identification of Clonogenic Common Lymphoid Progenitors in Mouse Bone Marrow. Cell. 1997 Nov 28;91(5):661–72.

17. Fathman JW, Bhattacharya D, Inlay MA, Seita J, Karsunky H, Weissman IL. Identification of the earliest natural killer cell-committed progenitor in murine bone marrow. Blood. 2011 Nov 17;118(20):5439–47.

18. Adolfsson J, Månsson R, Buza-Vidas N, Hultquist A, Liuba K, Jensen CT, et al. Identification of Flt3+ Lympho-Myeloid Stem Cells Lacking Erythro-Megakaryocytic Potential: A Revised Road Map for Adult Blood Lineage Commitment. Cell. 2005 Apr 22;121(2):295–306.

19. Månsson R, Hultquist A, Luc S, Yang L, Anderson K, Kharazi S, et al. Molecular Evidence for Hierarchical Transcriptional Lineage Priming in Fetal and Adult Stem Cells and Multipotent Progenitors. Immunity. 2007 Apr;26(4):407–19.

20. Rothenberg E V., Moore JE, Yui MA. Launching the T-cell-lineage developmental programme. Nat Rev Immunol. 2008 Jan 1;8(1):9–21.

21. Allman D, Sambandam A, Kim S, Miller JP, Pagan A, Well D, et al. Thymopoiesis independent of common lymphoid progenitors. Nat Immunol.

2003 Feb 6;4(2):168–74.

22. Porritt HE, Rumfelt LL, Tabrizifard S, Schmitt TM, Zúñiga-Pflücker JC, Petrie HT. Heterogeneity among DN1 Prothymocytes Reveals Multiple Progenitors with Different Capacities to Generate T Cell and Non-T Cell Lineages. Immunity. 2004 Jun;20(6):735–45.

23. Paganin M, Ferrando A. Molecular pathogenesis and targeted therapies for NOTCH1-induced T-cell acute lymphoblastic leukemia. Blood Rev. 2011 Mar 1;25(2):83–90.

24. Petrie HT, Zúñiga-Pflücker JC. Zoned Out: Functional Mapping of Stromal Signaling Microenvironments in the Thymus. Annu Rev Immunol. 2007 Apr;25(1):649–79.

25. Lind EF, Prockop SE, Porritt HE, Petrie HT. Mapping precursor movement through the postnatal thymus reveals specific microenvironments supporting defined stages of early lymphoid development. J Exp Med. 2001 Jul 16;194(2):127–34.

26. Masuda K, Kakugawa K, Nakayama T, Minato N, Katsura Y, Kawamoto H. T cell lineage determination precedes the initiation of TCR beta gene rearrangement. J Immunol . 2007 Sep 15;179(6):3699–706.

27. Livák F, Tourigny M, Schatz DG, Petrie HT. Characterization of TCR gene rearrangements during adult murine T cell development. J Immunol . 1999 Mar 1;162(5):2575–80.

28. Saint-Ruf C, Ungewiss K, Groettrup M, Bruno L, Fehling HJ, von Boehmer H. Analysis and expression of a cloned pre-T cell receptor gene. Sci . 1994 Nov 18;266(5188):1208–12.

29. Taghon T, Yui MA, Pant R, Diamond RA, Rothenberg E V. Developmental and Molecular Characterization of Emerging β- and γδ-Selected Pre-T Cells in the Adult Mouse Thymus. Immunity. 2006 Jan 1;24(1):53–64.

30. Dudley EC, Petrie HT, Shah LM, Owen MJ, Hayday AC. T cell receptor β chain gene rearrangement and selection during thymocyte development in adult mice. Immunity. 1994 May 1;1(2):83–93.

31. Hoffman ES, Passoni L, Crompton T, Leu TM, Schatz DG, Koff A, et al. Productive T-cell receptor beta-chain gene rearrangement: coincident regulation of cell cycle and clonality during development in vivo. Genes Dev. 1996 Apr 15;10(8):948–62.

32. Kisielow P, Miazek A. Positive selection of T cells: rescue from programmed cell death and differentiation require continual engagement of the T cell receptor. J Exp Med. 1995 Jun 1;181(6):1975–84.

33. Blyth K, Cameron ER, Neil JC. The runx genes: gain or loss of function in cancer. Nat Rev Cancer. 2005 May 20;5(5):376–87.

34. Fukushima-Nakase Y, Naoe Y, Taniuchi I, Hosoi H, Sugimoto T, Okuda T, et al. Shared and distinct roles mediated through C-terminal subdomains of acute myeloid leukemia/Runt-related transcription factor molecules in murine development. Blood. 2005 Jun 1;105(11):4298–307.

35. Wang S, Wang Q, Crute BE, Melnikova IN, Keller SR, Speck NA. Cloning and characterization of subunits of the T-cell receptor and murine leukemia virus enhancer core-binding factor. Mol Cell Biol. 1993 Jun;13(6):3324–39.

36. Ogawa E, Inuzuka M, Maruyama M, Satake M, Naito-Fujimoto M, Ito Y, et al. Molecular Cloning and Characterization of PEBP2β, the Heterodimeric Partner of a Novel Drosophila runt-Related DNA Binding Protein PEBP2α. Virology. 1993 May;194(1):314–31.

37. Lutterbach B, Hiebert S. Role of the transcription factor AML-1 in acute leukemia and hematopoietic differentiation. Gene. 2000 Mar 21;245(2):223–35.

38. Lutterbach B, Westendorf JJ, Linggi B, Isaac S, Seto E, Hiebert SW. A mechanism of repression by acute myeloid leukemia-1, the target of multiple chromosomal translocations in acute leukemia. J Biol Chem. 2000 Jan 7;275(1):651–6.

39. Kitabayashi I, Yokoyama A, Shimizu K, Ohki M. Interaction and functional cooperation of the leukemia-associated factors AML1 and p300 in myeloid cell differentiation. EMBO J. 1998 Jun 1;17(11):2994–3004.

40. Yu M, Mazor T, Huang H, Huang H-T, Kathrein KL, Woo AJ, et al. Direct Recruitment of Polycomb Repressive Complex 1 to Chromatin by Core Binding Transcription Factors. Mol Cell. 2012 Feb 10;45(3):330–43.

41. Guo H, Friedman AD. Phosphorylation of RUNX1 by cyclin-dependent kinase reduces direct interaction with HDAC1 and HDAC3. J Biol Chem. 2011 Jan 7;286(1):208–15.

42. Huang G, Zhao X, Wang L, Elf S, Xu H, Zhao X, et al. The ability of MLL to bind RUNX1 and methylate H3K4 at PU.1 regulatory regions is impaired by MDS/AML-associated RUNX1/AML1 mutations. Blood. 2011 Dec

15;118(25):6544–52.

43. Bakshi R, Hassan MQ, Pratap J, Lian JB, Montecino MA, van Wijnen AJ, et al. The human SWI/SNF complex associates with RUNX1 to control transcription of hematopoietic target genes. J Cell Physiol. 2010 Nov 1;225(2):569–76.

44. Tanaka T, Kurokawa M, Ueki K, Tanaka K, Imai Y, Mitani K, et al. The extracellular signal-regulated kinase pathway phosphorylates AML1, an acute myeloid leukemia gene product, and potentially regulates its transactivation ability. Mol Cell Biol. 1996 Jul;16(7):3967–79.

45. Yamaguchi Y, Kurokawa M, Imai Y, Izutsu K, Asai T, Ichikawa M, et al. AML1 is functionally regulated through p300-mediated acetylation on specific lysine residues. J Biol Chem. 2004 Apr 9;279(15):15630–8.

46. Jin Y-H, Jeon E-J, Li Q-L, Lee YH, Choi J-K, Kim W-J, et al. Transforming growth factor-beta stimulates p300-dependent RUNX3 acetylation, which inhibits ubiquitination-mediated degradation. J Biol Chem. 2004 Jul 9;279(28):29409–17.

47. Wee H-J, Huang G, Shigesada K, Ito Y. Serine phosphorylation of RUNX2 with novel potential functions as negative regulatory mechanisms. EMBO Rep. 2002 Oct 1;3(10):967–74.

48. Okuda T, van Deursen J, Hiebert SW, Grosveld G, Downing JR. AML1, the Target of Multiple Chromosomal Translocations in Human Leukemia, Is Essential for Normal Fetal Liver Hematopoiesis. Cell. 1996 Jan 26;84(2):321–30.

49. Wang Q, Stacy T, Binder M, Marin-Padilla M, Sharpe AH, Speck NA. Disruption of the Cbfa2 gene causes necrosis and hemorrhaging in the central nervous system and blocks definitive hematopoiesis. Proc Natl Acad Sci U S A. 1996 Apr 16;93(8):3444–9.

50. Ducy P, Zhang R, Geoffroy V, Ridall AL, Karsenty G. Osf2/Cbfa1: a transcriptional activator of osteoblast differentiation. Cell. 1997 May 30;89(5):747–54.

51. Komori T, Yagi H, Nomura S, Yamaguchi A, Sasaki K, Deguchi K, et al. Targeted disruption of Cbfa1 results in a complete lack of bone formation owing to maturational arrest of osteoblasts. Cell. 1997 May 30;89(5):755–64.

52. Levanon D, Bettoun D, Harris-Cerruti C, Woolf E, Negreanu V, Eilam R, et

al. The Runx3 transcription factor regulates development and survival of TrkC dorsal root ganglia neurons. EMBO J. 2002;21(13):3454–63.

53. Woolf E, Xiao C, Fainaru O, Lotem J, Rosen D, Negreanu V, et al. Runx3 and Runx1 are required for CD8 T cell development during thymopoiesis. Proc Natl Acad Sci. 2003 Jun 24;100(13):7731–6.

54. Inoue K, Ozaki S, Shiga T, Ito K, Masuda T, Okado N, et al. Runx3 controls the axonal projection of proprioceptive dorsal root ganglion neurons. Nat Neurosci. 2002 Sep 23;5(10):946–54.

55. Li QL, Ito K, Sakakura C, Fukamachi H, Inoue K ichi, Chi XZ, et al. Causal relationship between the loss of RUNX3 expression and gastric cancer. Cell. 2002 Apr 5;109(1):113–24.

56. Ichikawa M, Asai T, Saito T, Seo S, Yamazaki I, Yamagata T, et al. AML-1 is required for megakaryocytic maturation and lymphocytic differentiation, but not for maintenance of hematopoietic stem cells in adult hematopoiesis. Nat Med. 2004 Mar;10(3):299–304.

57. Growney JD, Shigematsu H, Li Z, Lee BH, Adelsperger J, Rowan R, et al. Loss of Runx1 perturbs adult hematopoiesis and is associated with a myeloproliferative phenotype. Blood. 2005 Jul 15;106(2):494–504.

58. Cai X, Gaudet JJ, Mangan JK, Chen MJ, De Obaldia ME, Oo Z, et al. Runx1 loss minimally impacts long-term hematopoietic stem cells. PLoS One. 2011 Jan;6(12):e28430.

59. Elagib KE, Racke FK, Mogass M, Khetawat R, Delehanty LL, Goldfarb AN. RUNX1 and GATA-1 coexpression and cooperation in megakaryocytic differentiation. Blood. 2003 Jun 1;101(11):4333–41.

60. Lorsbach RB, Moore J, Ang SO, Sun W, Lenny N, Downing JR. Role of RUNX1 in adult hematopoiesis: analysis of RUNX1-IRES-GFP knock-in mice reveals differential lineage expression. Blood. 2004 Apr 1;103(7):2522–9.

61. Putz G, Rosner A, Nuesslein I, Schmitz N, Buchholz F. AML1 deletion in adult mice causes splenomegaly and lymphomas. Oncogene. 2006 Feb 10;25(6):929–39.

62. Taniuchi I, Osato M, Egawa T, Sunshine MJ, Bae SC, Komori T, et al. Differential requirements for Runx proteins in CD4 repression and epigenetic silencing during T lymphocyte development. Cell. 2002 Nov 27;111(5):621–33.

63. Sato T, Ohno SI, Hayashi T, Sato C, Kohu K, Satake M, et al. Dual functions of runx proteins for reactivating CD8 and silencing CD4 at the commitment process into CD8 thymocytes. Immunity. 2005 Mar;22(3):317–28.

64. Egawa T, Tillman RE, Naoe Y, Taniuchi I, Littman DR. The role of the Runx transcription factors in thymocyte differentiation and in homeostasis of naive T cells. J Exp Med. 2007 Aug 6;204(8):1945–57.

65. Wotton D, Ghysdael J, Wang S, Speck NA, Owen MJ. Cooperative binding of Ets-1 and core binding factor to DNA. Mol Cell Biol. 1994 Jan;14(1):840–50.

66. Zhao J-Y, Osipovich O, Koues OI, Majumder K, Oltz EM. Activation of Mouse Tcrb: Uncoupling RUNX1 Function from Its Cooperative Binding with ETS1. J Immunol. 2017 Aug 1;199(3):1131–41.

67. Cieslak A, Le Noir S, Trinquand A, Lhermitte L, Franchini D-M, Villarese P, et al. RUNX1-dependent RAG1 deposition instigates human TCR-δ locus rearrangement. J Exp Med. 2014 Aug 25;211(9):1821–32.

68. Sawada S, Scarborough JD, Killeen N, Littman DR. A lineage-specific transcriptional silencer regulates CD4 gene expression during T lymphocyte development. Cell. 1994 Jun 17;77(6):917–29.

69. Siu G, Wurster AL, Duncan DD, Soliman TM, Hedrick SM. A transcriptional silencer controls the developmental expression of the CD4 gene. EMBO J. 1994 Aug 1;13(15):3570–9.

70. Setoguchi R, Tachibana M, Naoe Y, Muroi S, Akiyama K, Tezuka C, et al. Repression of the Transcription Factor Th-POK by Runx Complexes in Cytotoxic T Cell Development. Science. 2008 Feb 8;319(5864):822–5.

71. Steinke FC, Yu S, Zhou X, He B, Yang W, Zhou B, et al. TCF-1 and LEF-1 act upstream of Th-POK to promote the CD4(+) T cell fate and interact with Runx3 to silence Cd4 in CD8(+) T cells. Nat Immunol. 2014 Jul 18;15(7):646–56.

72. Begley CG, Aplan PD, DAVEY MP, Nakahara K, Tchorz K, Kurtzberg J, et al. Chromosomal translocation in a human leukemic stem-cell line disrupts the T-cell antigen receptor 6-chain diversity region and results in a previously unreported fusion transcript. Proc Natl Acad Sci. 1989;86:2031–5.

73. Shivdasani RA, Mayer EL, Orkin SH. Absence of blood formation in mice

lacking the T-cell leukaemia oncoprotein tal-1/SCL. Nature. 1995 Feb 2;373(6513):432–4.

74. Robb L, Lyons I, Li R, Hartley L, Kontgen F, Harvey RP, et al. Absence of yolk sac hematopoiesis from mice with a targeted disruption of the sci gene. Proc Natl Acad Sci. 1995;92:7075–9.

75. Robb L, Elwood NJ, Elefanty AG, Köntgen F, Li R, Barnett LD, et al. The scl gene product is required for the generation of all hematopoietic lineages in the adult mouse. EMBO J. 1996 Aug 15;15(16):4123–9.

76. Porcher C, Swat W, Rockwell K, Fujiwara Y, Alt FW, Orkin SH. The T Cell Leukemia Oncoprotein SCL/tal-1 Is Essential for Development of All Hematopoietic Lineages. Cell. 1996;86:47–57.

77. Mikkola HKA, Klintman J, Yang H, Hock H, Schlaeger TM, Fujiwara Y, et al. Haematopoietic stem cells retain long-term repopulating activity and multipotency in the absence of stem-cell leukaemia SCL/tal-1 gene. Nature. 2003 Jan 30;421(6922):547–51.

78. Curtis DJ, Hall MA, Van Stekelenburg LJ, Robb L, Jane SM, Begley CG. SCL is required for normal function of short-term repopulating hematopoietic stem cells. Blood. 2004 May 1;103(9):3342–8.

79. Hsu HL, Huang L, Tsan JT, Funk W, Wright WE, Hu JS, et al. Preferred sequences for DNA recognition by the TAL1 helix-loop-helix proteins. Mol Cell Biol. 1994 Feb;14(2):1256–65.

80. Huang S, Qiu Y, Stein RW, Brandt SJ. p300 functions as a transcriptional coactivator for the TAL1/SCL oncoprotein. Oncogene. 1999 Sep 13;18(35):4958–67.

81. Huang S, Qiu Y, Shi Y, Xu Z, Brandt SJ. P/CAF-mediated acetylation regulates the function of the basic helix-loop-helix transcription factor TAL1/SCL. EMBO J. 2000 Dec 15;19(24):6792–803.

82. Huang S, Brandt SJ. mSin3A regulates murine erythroleukemia cell differentiation through association with the TAL1 (or SCL) transcription factor. Mol Cell Biol. 2000 Mar;20(6):2248–59.

83. Wadman IA, Osada H, Grütz GG, Agulnick AD, Westphal H, Forster A, et al. The LIM-only protein Lmo2 is a bridging molecule assembling an erythroid, DNA-binding complex which includes the TAL1, E47, GATA-1 and Ldb1/NLI proteins. EMBO J. 1997 Jun 2;16(11):3145–57.

84. Visvader JE, Mao X, Fujiwara Y, Hahm K, Orkin SH. The LIM-domain binding protein Ldb1 and its partner LMO2 act as negative regulators of erythroid differentiation. Proc Natl Acad Sci U S A. 1997 Dec 9;94(25):13707–12.

85. Kassouf MT, Chagraoui H, Vyas P, Porcher C. Differential use of SCL/TAL-1 DNA-binding domain in developmental hematopoiesis. Blood. 2008 Aug 15;112(4):1056–67.

86. Porcher C, Liao EC, Fujiwara Y, Zon LI, Orkin SH. Specification of hematopoietic and vascular development by the bHLH transcription factor SCL without direct DNA binding. Development. 1999 Oct;126(20):4603–15.

87. Draheim KM, Hermance N, Yang Y, Arous E, Calvo J, Kelliher MA. A DNA-binding mutant of TAL1 cooperates with LMO2 to cause T cell leukemia in mice. Oncogene. 2011 Mar 10;30(10):1252–60.

88. Mouthon M, Bernard O, Mitjavila M, Romeo P, Vainchenker W, Mathieu-Mahul D. Expression of tal-1 and GATA-binding proteins during human hematopoiesis. Blood. 1993;81(3):647–55.

89. Herblot S, Steff A-M, Hugo P, Aplan PD, Hoang T. SCL and LMO1 alter thymocyte differentiation: inhibition of E2A-HEB functionand pre-Tα chain expression. Nat Immunol. 2000 Aug 1;1(2):138–44.

90. Elefanty AG, Begley CG, Metcalf D, Barnett L, Köntgen F, Robb L. Characterization of hematopoietic progenitor cells that express the transcription factor SCL, using a lacZ "knock-in" strategy. Proc Natl Acad Sci U S A. 1998 Sep 29;95(20):11897–902.

91. Elwood NJ, Zogos H, Pereira DS, Dick JE, Begley CG. Enhanced megakaryocyte and erythroid development from normal human CD34(+) cells: consequence of enforced expression of SCL. Blood. 1998 May 15;91(10):3756–65.

92. Kassouf MT, Hughes JR, Taylor S, McGowan SJ, Soneji S, Green AL, et al. Genome-wide identification of TAL1's functional targets: insights into its mechanisms of action in primary erythroid cells. Genome Res. 2010 Aug 1;20(8):1064–83.

93. Palii CG, Perez-Iratxeta C, Yao Z, Cao Y, Dai F, Davison J, et al. Differential genomic targeting of the transcription factor TAL1 in alternate haematopoietic lineages. EMBO J. 2011 Feb 2;30(3):494–509.

94. Kuvardina ON, Herglotz J, Kolodziej S, Kohrs N, Herkt S, Wojcik B, et al.

RUNX1 represses the erythroid gene expression program during megakaryocytic differentiation. Blood. 2015 Jun 4;125(23):3570–9.

95. Lecuyer E, Hoang T. SCL: From the origin of hematopoiesis to stem cells and leukemia. Exp Hematol. 2004 Jan 1;32(1):11–24.

96. Aster JC, Pear WS, Blacklow SC. Notch Signaling in Leukemia. Annu Rev Pathol Mech Dis. 2008;3:587–613.

97. Brou C, Logeat F, Gupta N, Bessia C, LeBail O, Doedens JR, et al. A Novel Proteolytic Cleavage Involved in Notch Signaling: The Role of the Disintegrin-Metalloprotease TACE. Mol Cell. 2000 Feb 1;5(2):207–16.

98. Mumm JS, Schroeter EH, Saxena MT, Griesemer A, Tian X, Pan D., et al. A Ligand-Induced Extracellular Cleavage Regulates γ-Secretase-like Proteolytic Activation of Notch1. Mol Cell. 2000 Feb 1;5(2):197–206.

99. van Tetering G, van Diest P, Verlaan I, van der Wall E, Kopan R, Vooijs M. Metalloprotease ADAM10 is required for Notch1 site 2 cleavage. J Biol Chem. 2009 Nov 6;284(45):31018–27.

100. Bozkulak EC, Weinmaster G. Selective use of ADAM10 and ADAM17 in activation of Notch1 signaling. Mol Cell Biol. 2009 Nov 1;29(21):5679–95.

101. De La Coste A, Freitas AA. Notch signaling: Distinct ligands induce specific signals during lymphocyte development and maturation. Immunol Lett. 2006;102(1):1–9.

102. Hasserjian R, Aster J, Davi F, Weinberg D, Sklar J. Modulated expression of notch1 during thymocyte development. Blood. 1996;88(3):970–6.

103. Koyanagi A, Sekine C, Yagita H. Expression of Notch receptors and ligands on immature and mature T cells. Biochem Biophys Res Commun. 2012 Feb 24;418(4):799–805.

104. Radtke F, Wilson A, Stark G, Bauer M, van Meerwijk J, MacDonald HR, et al. Deficient T Cell Fate Specification in Mice with an Induced Inactivation of Notch1. Immunity. 1999 May 1;10(5):547–58.

105. Saito T, Chiba S, Ichikawa M, Kunisato A, Asai T, Shimizu K, et al. Notch2 Is Preferentially Expressed in Mature B Cells and Indispensable for Marginal Zone B Lineage Development. Immunity. 2003 May 1;18(5):675–85.

106. Shi J, Fallahi M, Luo J-L, Petrie HT. Nonoverlapping functions for Notch1

and Notch3 during murine steady-state thymic lymphopoiesis. Blood. 2011 Sep 1;118(9):2511–9.

107. Wolfer A, Wilson A, Nemir M, MacDonald HR, Radtke F. Inactivation of Notch1 Impairs VDJβ Rearrangement and Allows pre-TCR-Independent Survival of Early αβ Lineage Thymocytes. Immunity. 2002 Jun 1;16(6):869–79.

108. Tanigaki K, Tsuji M, Yamamoto N, Han H, Tsukada J, Inoue H, et al. Regulation of αβ/γδ T Cell Lineage Commitment and Peripheral T Cell Responses by Notch/RBP-J Signaling. Immunity. 2004 May 1;20(5):611–22.

109. Maillard I, Fang T, Pear WS. REGULATION OF LYMPHOID DEVELOPMENT, DIFFERENTIATION, AND FUNCTION BY THE NOTCH PATHWAY. Annu Rev Immunol. 2005 Apr 27;23(1):945–74.

110. Ikawa T, Kawamoto H, Goldrath AW, Murre C. E proteins and Notch signaling cooperate to promote T cell lineage specification and commitment. J Exp Med. 2006 May 15;203(5):1329–42.

111. Reizis B, Leder P. Direct induction of T lymphocyte-specific gene expression by the mammalian Notch signaling pathway. Genes Dev. 2002 Feb 1;16(3):295–300.

112. Taghon TN, David E-S, Zúñiga-Pflücker JC, Rothenberg E V. Delayed, asynchronous, and reversible T-lineage specification induced by Notch/Delta signaling. Genes Dev. 2005;19:965–78.

113. Carlos Zúñiga-Pflücker Michie JM, Çuburu N, Aublin A, Maria Ciofani JL, Schmitt TM, Ciofani A, et al. Obligatory Role for Cooperative Signaling by Pre-TCR and Notch during Thymocyte Differentiation. J Immunol. 2004;172:5230–9.

114. Ciofani M, Zúñiga-Pflücker JC. Notch promotes survival of pre–T cells at the β-selection checkpoint by regulating cellular metabolism. Nat Immunol. 2005 Sep;6(9):881–8.

115. Schmitt TM, Zúñiga-Pflücker JC. Induction of T cell development from hematopoietic progenitor cells by delta-like-1 in vitro. Immunity. 2002 Dec;17(6):749–56.

116. Litzow MR, Ferrando AA. How I treat T-cell acute lymphoblastic leukemia in adults. Blood. 2015 Aug 13;126(7):833–41.

117. Hunger SP, Lu X, Devidas M, Camitta BM, Gaynon PS, Winick NJ, et al. Improved Survival for Children and Adolescents With Acute Lymphoblastic Leukemia Between 1990 and 2005: A Report From the Children's Oncology Group. J Clin Oncol. 2012 May 10;30(14):1663–9.

118. Marks DI, Rowntree C. Management of adults with T-cell lymphoblastic leukemia. Blood. 2017 Mar 2;129(9):1134–42.

119. Marks DI, Paietta EM, Moorman A V, Richards SM, Buck G, DeWald G, et al. T-cell acute lymphoblastic leukemia in adults: clinical features, immunophenotype, cytogenetics, and outcome from the large randomized prospective trial (UKALL XII/ECOG 2993). Blood. 2009 Dec 10;114(25):5136–45.

120. Einsiedel HG, von Stackelberg A, Hartmann R, Fengler R, Schrappe M, Janka-Schaub G, et al. Long-Term Outcome in Children With Relapsed ALL by Risk-Stratified Salvage Therapy: Results of Trial Acute Lymphoblastic Leukemia-Relapse Study of the Berlin-Frankfurt-Münster Group 87. J Clin Oncol. 2005 Nov 1;23(31):7942–50.

121. Goldberg JM, Silverman LB, Levy DE, Dalton VK, Gelber RD, Lehmann L, et al. Childhood T-cell acute lymphoblastic leukemia: the Dana-Farber Cancer Institute acute lymphoblastic leukemia consortium experience. J Clin Oncol. 2003 Oct 1;21(19):3616–22.

122. Blanco E, Beyene J, Maloney AM, Almeida R, Ethier M-C, Winick N, et al. Non-relapse mortality in pediatric acute lymphoblastic leukemia: a systematic review and meta-analysis. Leuk Lymphoma. 2012 May 3;53(5):878–85.

123. Rubnitz JE, Lensing S, Zhou Y, Sandlund JT, Razzouk BI, Ribeiro RC, et al. Death during induction therapy and first remission of acute leukemia in childhood. Cancer. 2004 Oct 1;101(7):1677–84.

124. Te Winkel ML, Pieters R, Wind E-JD, Bessems JHJMG, van den Heuvel-Eibrink MM, Chiesa R, et al. Management and treatment of osteonecrosis in children and adolescents with acute lymphoblastic leukemia. Haematologica. 2014 Mar 1;99(3):430–6.

125. Inaba H, Pui C-H. Glucocorticoid use in acute lymphoblastic leukaemia. Lancet Oncol. 2010 Nov 1;11(11):1096–106.

126. Krull KR, Brinkman TM, Li C, Armstrong GT, Ness KK, Srivastava DK, et al. Neurocognitive outcomes decades after treatment for childhood acute lymphoblastic leukemia: a report from the St Jude lifetime cohort study. J

Clin Oncol . 2013 Dec 10;31(35):4407–15.

127. Maule M, Scelo G, Pastore G, Brennan P, Hemminki K, Tracey E, et al. Risk of Second Malignant Neoplasms After Childhood Leukemia and Lymphoma: An International Study. JNCI J Natl Cancer Inst. 2007 May 16;99(10):790–800.

128. Belver L, Ferrando A. The genetics and mechanisms of T cell acute lymphoblastic leukaemia. Nat Rev Cancer. 2016;16(8):494–507.

129. Ferrando AA, Neuberg DS, Staunton J, Loh ML, Huard C, Raimondi SC, et al. Gene expression signatures define novel oncogenic pathways in T cell acute lymphoblastic leukemia. Cancer Cell. 2002 Feb 1;1(1):75–87.

130. Coustan-Smith E, Mullighan CG, Onciu M, Behm FG, Raimondi SC, Pei D, et al. Early T-cell precursor leukaemia: a subtype of very high-risk acute lymphoblastic leukaemia. Lancet Oncol. 2009 Feb 1;10(2):147–56.

131. Zhang J, Ding L, Holmfeldt L, Wu G, Heatley SL, Payne-Turner D, et al. The genetic basis of early T-cell precursor acute lymphoblastic leukaemia. Nature. 2012 Jan 11;481(7380):157–63.

132. Van Vlierberghe P, Ambesi-Impiombato A, De Keersmaecker K, Hadler M, Paietta E, Tallman MS, et al. Prognostic relevance of integrated genetic profiling in adult T-cell acute lymphoblastic leukemia. Blood. 2013 Jul 4;122(1):74–82.

133. Niehues T, Kapaun P, Harms DO, Burdach S, Kramm C, Körholz D, et al. A classification based on T cell selection-related phenotypes identifies a subgroup of childhood T-ALL with favorable outcome in the COALL studies. Leukemia. 1999 Apr;13(4):614–7.

134. Aifantis I, Raetz E, Buonamici S. Molecular pathogenesis of T-cell leukaemia and lymphoma. Nat Rev Immunol. 2008 May;8(5):380–90.

135. Cauwelier B, Dastugue N, Cools J, Poppe B, Herens C, De Paepe A, et al. Molecular cytogenetic study of 126 unselected T-ALL cases reveals high incidence of TCRβ locus rearrangements and putative new T-cell oncogenes. Leukemia. 2006 Jul 4;20(7):1238–44.

136. Chen Q, Cheng JT, Tasi LH, Schneider N, Buchanan G, Carroll A, et al. The tal gene undergoes chromosome translocation in T cell leukemia and potentially encodes a helix-loop-helix protein. EMBO J. 1990 Feb;9(2):415–24.

137. Fitzgerald TJ, Neale GA, Raimondi SC, Goorha RM. c-tal, a helix-loop-helix protein, is juxtaposed to the T-cell receptor-beta chain gene by a reciprocal chromosomal translocation: t(1;7)(p32;q35). Blood. 1991 Nov 15;78(10):2686–95.

138. Xia Y, Brown L, Yang YC, TSAN TJ, SICILIANO MJ, Espinosa Iii R, et al. TAL2, a helix-loop-helix gene activated by the (7;9)(q34;q32) translocation in human T-cell leukemia. Proc Natl Acad Sci USA. 1991;88:11416–20.

139. Mellentin JD, Smith SD, Cleary ML. lyl-1, a novel gene altered by chromosomal translocation in T cell leukemia, codes for a protein with a helix-loop-helix DNA binding motif. Cell. 1989 Jul 14;58(1):77–83.

140. Wang J, Jani-Sait SN, Escalon EA, Carroll AJ, de Jong PJ, Kirsch IR, et al. The t(14;21)(q11.2;q22) chromosomal translocation associated with T-cell acute lymphoblastic leukemia activates the BHLHB1 gene. Proc Natl Acad Sci U S A. 2000 Mar 28;97(7):3497–502.

141. Hatano M, Roberts CW, Minden M, Crist WM, Korsmeyer SJ. Deregulation of a homeobox gene, HOX11, by the t(10;14) in T cell leukemia. Sci . 1991 Jul 5;253(5015):79–82.

142. Kennedy MA, Gonzalez-Sarmiento R, Kees UR, Lampert F, Dear N, Boehm T, et al. HOX11, a homeobox-containing T-cell oncogene on human chromosome 10q24. Proc Natl Acad Sci U S A. 1991 Oct 15;88(20):8900–4.

143. Hansen-Hagge TE, Schäfer M, Kiyoi H, Morris SW, Whitlock JA, Koch P, et al. Disruption of the RanBP17/Hox11L2 region by recombination with the TCRδ locus in acute lymphoblastic leukemias with t(5;14)(q34;q11). Leukemia. 2002 Nov 6;16(11):2205–12.

144. McGuire EA, Hockett RD, Pollock KM, Bartholdi MF, O'Brien SJ, Korsmeyer SJ. The t(11;14)(p15;q11) in a T-cell acute lymphoblastic leukemia cell line activates multiple transcripts, including Ttg-1, a gene encoding a potential zinc finger protein. Mol Cell Biol. 1989 May;9(5):2124–32.

145. Royer-Pokora B, Loos U, Ludwig WD. TTG-2, a new gene encoding a cysteine-rich protein with the LIM motif, is overexpressed in acute T-cell leukaemia with the t(11;14)(p13;q11). Oncogene. 1991 Oct;6(10):1887–93.

146. Clappier E, Cuccuini W, Kalota A, Crinquette A, Cayuela J-M, Dik WA, et al. The C-MYB locus is involved in chromosomal translocation and genomic duplications in human T-cell acute leukemia (T-ALL), the translocation

defining a new T-ALL subtype in very young children. Blood. 2007 Aug 15;110(4):1251–61.

147. Erikson J, Finger L, Sun L, ar-Rushdi A, Nishikura K, Minowada J, et al. Deregulation of c-myc by translocation of the alpha-locus of the T-cell receptor in T-cell leukemias. Science. 1986 May 16;232(4752):884–6.

148. Shima EA, Le Beau MM, McKeithan TW, Minowada J, Showe LC, Mak TW, et al. Gene encoding the alpha chain of the T-cell receptor is moved immediately downstream of c-myc in a chromosomal 8;14 translocation in a cell line from a human T-cell leukemia. Proc Natl Acad Sci U S A. 1986 May;83(10):3439–43.

149. Hebert J, Cayuela J, Berkeley J, Sigaux F. Candidate tumor-suppressor genes MTS1 (p16INK4A) and MTS2 (p15INK4B) display frequent homozygous deletions in primary cells from T- but not from B-cell lineage acute lymphoblastic leukemias. Blood. 1994;84(12):4038–44.

150. Liu Y, Easton J, Shao Y, Maciaszek J, Wang Z, Wilkinson MR, et al. The genomic landscape of pediatric and young adult T-lineage acute lymphoblastic leukemia. Nat Genet. 2017 Jul 3;49(8):1211–8.

151. Weng AP, Ferrando AA, Lee W, Morris JP, Silverman LB, Sanchez-Irizarry C, et al. Activating mutations of NOTCH1 in human T cell acute lymphoblastic leukemia. Science. 2004 Oct 8;306(5694):269–71.

152. bar-eli M, Ahuja H, and AF, Cline MJ. N-RAS mutations in T-cell acute lymphocytic leukaemia: analysis by direct sequencing detects a novel mutation. Br J Haematol. 1989 May 1;72(1):36–9.

153. Balgobind B V, Van Vlierberghe P, van den Ouweland AMW, Beverloo HB, Terlouw-Kromosoeto JNR, van Wering ER, et al. Leukemia-associated NF1 inactivation in patients with pediatric T-ALL and AML lacking evidence for neurofibromatosis. Blood. 2008 Apr 15;111(8):4322–8.

154. Palomero T, Sulis ML, Cortina M, Real PJ, Barnes K, Ciofani M, et al. Mutational loss of PTEN induces resistance to NOTCH1 inhibition in T-cell leukemia. Nat Med. 2007 Nov 16;13(10):1203–10.

155. Van Vlierberghe P, Palomero T, Khiabanian H, Van der Meulen J, Castillo M, Van Roy N, et al. PHF6 mutations in T-cell acute lymphoblastic leukemia. Nat Genet. 2010 Apr 14;42(4):338–42.

156. Ntziachristos P, Tsirigos A, Vlierberghe P Van, Nedjic J, Trimarchi T, Flaherty MS, et al. Genetic inactivation of the polycomb repressive

complex 2 in T cell acute lymphoblastic leukemia. Nat Med. 2012 Feb 6;18(2):298–303.

157. Ntziachristos P, Tsirigos A, Welstead GG, Trimarchi T, Bakogianni S, Xu L, et al. Contrasting roles of histone 3 lysine 27 demethylases in acute lymphoblastic leukaemia. Nature. 2014 Aug 17;514(7523):513–7.

158. Van der Meulen J, Sanghvi V, Mavrakis K, Durinck K, Fang F, Matthijssens F, et al. The H3K27me3 demethylase UTX is a gender-specific tumor suppressor in T-cell acute lymphoblastic leukemia. Blood. 2015 Jan 1;125(1):13–21.

159. Zuurbier L, Homminga I, Calvert V, Winkel M te, Buijs-Gladdines JGCAM, Kooi C, et al. NOTCH1 and/or FBXW7 mutations predict for initial good prednisone response but not for improved outcome in pediatric T-cell acute lymphoblastic leukemia patients treated on DCOG or COALL protocols. Leukemia. 2010 Dec 23;24(12):2014–22.

160. Ellisen LW, Bird J, West DC, Soreng AL, Reynolds TC, Smith SD, et al. TAN-1, the human homolog of the Drosophila Notch gene, is broken by chromosomal translocations in T lymphoblastic neoplasms. Cell. 1991 Aug 23;66(4):649–61.

161. Pear WS, Aster JC, Scott ML, Hasserjian RP, Soffer B, Sklar J, et al. Exclusive development of T cell neoplasms in mice transplanted with bone marrow expressing activated Notch alleles. J Exp Med. 1996 May 1;183(5):2283–91.

162. Malecki MJ, Sanchez-Irizarry C, Mitchell JL, Histen G, Xu ML, Aster JC, et al. Leukemia-Associated Mutations within the NOTCH1 Heterodimerization Domain Fall into at Least Two Distinct Mechanistic Classes. Mol Cell Biol. 2006 Jun 15;26(12):4642–51.

163. Oberg C, Li J, Pauley A, Wolf E, Gurney M, Lendahl U. The Notch intracellular domain is ubiquitinated and negatively regulated by the mammalian Sel-10 homolog. J Biol Chem. 2001 Sep 21;276(38):35847–53.

164. Wu G, Lyapina S, Das I, Li J, Gurney M, Pauley A, et al. SEL-10 is an inhibitor of notch signaling that targets notch for ubiquitin-mediated protein degradation. Mol Cell Biol. 2001 Nov 1;21(21):7403–15.

165. Fryer CJ, White JB, Jones KA. Mastermind Recruits CycC:CDK8 to Phosphorylate the Notch ICD and Coordinate Activation with Turnover. Mol Cell. 2004 Nov 19;16(4):509–20.

166. Sulis ML, Williams O, Palomero T, Tosello V, Pallikuppam S, Real PJ, et al. NOTCH1 extracellular juxtamembrane expansion mutations in T-ALL. Blood. 2008 Aug 1;112(3):733–40.

167. O'Neil J, Grim J, Strack P, Rao S, Tibbitts D, Winter C, et al. FBW7 mutations in leukemic cells mediate NOTCH pathway activation and resistance to gamma-secretase inhibitors. J Exp Med. 2007 Aug 6;204(8):1813–24.

168. Thompson BJ, Buonamici S, Sulis ML, Palomero T, Vilimas T, Basso G, et al. The SCFFBW7 ubiquitin ligase complex as a tumor suppressor in T cell leukemia. J Exp Med. 2007 Aug 6;204(8):1825–35.

169. Minella AC, Clurman BE. Mechanisms of tumor suppression by the SCF(Fbw7). Cell Cycle. 2005 Oct 23;4(10):1356–9.

170. Fujii Y, Yada M, Nishiyama M, Kamura T, Takahashi H, Tsunematsu R, et al. Fbxw7 contributes to tumor suppression by targeting multiple proteins for ubiquitin-dependent degradation. Cancer Sci. 2006 Aug;97(8):729–36.

171. Mao J-H, Kim I-J, Wu D, Climent J, Kang HC, DelRosario R, et al. FBXW7 targets mTOR for degradation and cooperates with PTEN in tumor suppression. Sci . 2008 Sep 12;321(5895):1499–502.

172. Girard L, Hanna Z, Beaulieu N, Hoemann CD, Simard C, Kozak CA, et al. Frequent provirus insertional mutagenesis of Notch1 in thymomas of MMTVD/myc transgenic mice suggests a collaboration of c-myc and Notch1 for oncogenesis. Genes Dev. 1996 Aug 1;10(15):1930–44.

173. O'Neil J, Calvo J, McKenna K, Krishnamoorthy V, Aster JC, Bassing CH, et al. Activating Notch1 mutations in mouse models of T-ALL. Blood. 2006 Jan 15;107(2):781–5.

174. Ashworth TD, Pear WS, Chiang MY, Blacklow SC, Mastio J, Xu L, et al. Deletion-based mechanisms of Notch1 activation in T-ALL: key roles for RAG recombinase and a conserved internal translational start site in Notch1. Blood. 2010 Dec 16;116(25):5455–64.

175. Tatarek J, Cullion K, Ashworth T, Gerstein R, Aster JC, Kelliher MA. Notch1 inhibition targets the leukemia-initiating cells in a Tal1/Lmo2 mouse model of T-ALL. Blood. 2011;118(6):1579–90.

176. Tremblay M, Tremblay CS, Herblot S, Aplan PD, Hébert J, Perreault C, et al. Modeling T-cell acute lymphoblastic leukemia induced by the SCL and LMO1 oncogenes. Genes Dev. 2010 Jun 1;24(11):1093–105.

177. Chiang MY, Xu L, Shestova O, Histen G, L'heureux S, Romany C, et al. Leukemia-associated NOTCH1 alleles are weak tumor initiators but accelerate K-ras-initiated leukemia. J Clin Invest. 2008 Sep 2;118(9):3181–94.

178. Cullion K, Draheim KM, Hermance N, Tammam J, Sharma VM, Ware C, et al. Targeting the Notch1 and mTOR pathways in a mouse T-ALL model. Blood. 2009 Jun 11;113(24):6172–81.

179. Palomero T, Lim WK, Odom DT, Sulis ML, Real PJ, Margolin A, et al. NOTCH1 directly regulates c-MYC and activates a feed-forward-loop transcriptional network promoting leukemic cell growth. Proc Natl Acad Sci U S A. 2006;103(48):18261–6.

180. Sharma VM, Calvo JA, Draheim KM, Cunningham LA, Hermance N, Beverly L, et al. Notch1 contributes to mouse T-cell leukemia by directly inducing the expression of c-myc. Mol Cell Biol. 2006 Nov 1;26(21):8022–31.

181. Weng AP, Millholland JM, Yashiro-Ohtani Y, Arcangeli ML, Lau A, Wai C, et al. c-Myc is an important direct target of Notch1 in T-cell acute lymphoblastic leukemia/lymphoma. Genes Dev. 2006 Aug 1;20(15):2096–109.

182. Klinakis A, Szabolcs M, Politi K, Kiaris H, Artavanis-Tsakonas S, Efstratiadis A. Myc is a Notch1 transcriptional target and a requisite for Notch1-induced mammary tumorigenesis in mice. Proc Natl Acad Sci U S A. 2006 Jun 13;103(24):9262–7.

183. Margolin AA, Palomero T, Sumazin P, Califano A, Ferrando AA, Stolovitzky G. ChIP-on-chip significance analysis reveals large-scale binding and regulation by human transcription factor oncogenes. Proc Natl Acad Sci U S A. 2009 Jan 6;106(1):244–9.

184. Coller HA, Grandori C, Tamayo P, Colbert T, Lander ES, Eisenman RN, et al. Expression analysis with oligonucleotide microarrays reveals that MYC regulates genes involved in growth, cell cycle, signaling, and adhesion. Proc Natl Acad Sci U S A. 2000 Mar 28;97(7):3260–5.

185. Guo QM, Malek RL, Kim S, Chiao C, He M, Ruffy M, et al. Identification of c-myc responsive genes using rat cDNA microarray. Cancer Res. 2000 Nov 1;60(21):5922–8.

186. van Riggelen J, Yetil A, Felsher DW. MYC as a regulator of ribosome biogenesis and protein synthesis. Nat Rev Cancer. 2010 Apr 1;10(4):301–9.

187. Douglas NC, Jacobs H, Bothwell ALM, Hayday AC. Defining the specific physiological requirements for c-Myc in T cell development. Nat Immunol. 2001 Apr 1;2(4):307–15.

188. Dose M, Khan I, Guo Z, Kovalovsky D, Krueger A, von Boehmer H, et al. c-Myc mediates pre-TCR-induced proliferation but not developmental progression. Blood. 2006 Oct 15;108(8):2669–77.

189. Dalla-Favera R, Bregni M, Erikson J, Patterson D, Gallo RC, Croce CM. Human c-myc onc gene is located on the region of chromosome 8 that is translocated in Burkitt lymphoma cells. Proc Natl Acad Sci U S A. 1982 Dec;79(24):7824–7.

190. Dang CV. MYC on the Path to Cancer. Cell. 2012 Mar 30;149(1):22–35.

191. Stine ZE, Walton ZE, Altman BJ, Hsieh AL, Dang C V. MYC, Metabolism, and Cancer. Cancer Discov. 2015 Oct 1;5(10):1024–39.

192. Gabay M, Li Y, Felsher DW. MYC activation is a hallmark of cancer initiation and maintenance. Cold Spring Harb Perspect Med. 2014 Jun 2;4(6):a014241.

193. Sears R, Nuckolls F, Haura E, Taya Y, Tamai K, Nevins JR. Multiple Ras-dependent phosphorylation pathways regulate Myc protein stability. Genes Dev. 2000 Oct 1;14(19):2501–14.

194. He TC, Sparks AB, Rago C, Hermeking H, Zawel L, da Costa LT, et al. Identification of c-MYC as a target of the APC pathway. Science. 1998 Sep 4;281(5382):1509–12.

195. Bernard O, Larsen CJ, Hampe A, Mauchauffé M, Berger R, Mathieu-Mahul D. Molecular mechanisms of a t(8;14)(q24;q11) translocation juxtaposing c-myc and TcR-alpha genes in a T-cell leukaemia: involvement of a V alpha internal heptamer. Oncogene. 1988 Feb;2(2):195–200.

196. King B, Trimarchi T, Reavie L, Xu L, Mullenders J, Ntziachristos P, et al. The ubiquitin ligase FBXW7 modulates leukemia-initiating cell activity by regulating MYC stability. Cell. 2013 Jun 20;153(7):1552–66.

197. Bonnet M, Loosveld M, Montpellier B, Navarro J-M, Quilichini B, Picard C, et al. Posttranscriptional deregulation of MYC via PTEN constitutes a major alternative pathway of MYC activation in T-cell acute lymphoblastic leukemia. Blood. 2011 Jun 16;117(24):6650–9.

198. Hann SR. Role of post-translational modifications in regulating c-Myc

proteolysis, transcriptional activity and biological function. Semin Cancer Biol. 2006 Aug 1;16(4):288–302.

199. De Strooper B, Annaert W, Cupers P, Saftig P, Craessaerts K, Mumm JS, et al. A presenilin-1-dependent γ-secretase-like protease mediates release of Notch intracellular domain. Nature. 1999 Apr 8;398(6727):518–22.

200. LaVoie MJ, Selkoe DJ. The Notch Ligands, Jagged and Delta, Are Sequentially Processed by α-Secretase and Presenilin/γ-Secretase and Release Signaling Fragments. J Biol Chem. 2003 Sep 5;278(36):34427–37.

201. Marambaud P, Shioi J, Serban G, Georgakopoulos A, Sarner S, Nagy V, et al. A presenilin-1/gamma-secretase cleavage releases the E-cadherin intracellular domain and regulates disassembly of adherens junctions. EMBO J. 2002 Apr 15;21(8):1948–56.

202. Marambaud P, Wen PH, Dutt A, Shioi J, Takashima A, Siman R, et al. A CBP Binding Transcriptional Repressor Produced by the PS1/ϵ-Cleavage of N-Cadherin Is Inhibited by PS1 FAD Mutations. Cell. 2003 Sep 5;114(5):635–45.

203. Kindler T, Cornejo MG, Scholl C, Liu J, Leeman DS, Haydu JE, et al. K-RasG12D-induced T-cell lymphoblastic lymphoma/leukemias harbor Notch1 mutations and are sensitive to gamma-secretase inhibitors. Blood. 2008 Oct 15;112(8):3373–82.

204. Armstrong F, Brunet de la Grange P, Gerby B, Rouyez M-C, Calvo J, Fontenay M, et al. NOTCH is a key regulator of human T-cell acute leukemia initiating cell activity. Blood. 2009 Feb 19;113(8):1730–40.

205. Roderick JE, Tesell J, Shultz LD, Brehm MA, Greiner DL, Harris MH, et al. c-Myc inhibition prevents leukemia initiation in mice and impairs the growth of relapsed and induction failure pediatric T-ALL cells. Blood. 2014 Feb 13;123(7):1040–50.

206. Filippakopoulos P, Qi J, Picaud S, Shen Y, Smith WB, Fedorov O, et al. Selective inhibition of BET bromodomains. Nature. 2010 Dec 23;468(7327):1067–73.

207. Knoechel B, Roderick JE, Williamson KE, Zhu J, Lohr JG, Cotton MJ, et al. An epigenetic mechanism of resistance to targeted therapy in T cell acute lymphoblastic leukemia. Nat Genet. 2014 Mar 2;46(4):364–70.

208. Yashiro-Ohtani Y, Wang H, Zang C, Arnett KL, Bailis W, Ho Y, et al. Long-range enhancer activity determines Myc sensitivity to Notch inhibitors in T

cell leukemia. Proc Natl Acad Sci U S A. 2014 Nov 18;111(46):E4946–53.

209. Silva A, Yunes JA, Cardoso BA, Martins LR, Jotta PY, Abecasis M, et al. PTEN posttranslational inactivation and hyperactivation of the PI3K/Akt pathway sustain primary T cell leukemia viability. J Clin Invest. 2008 Nov 3;118(11):3762–74.

210. Gutierrez A, Sanda T, Grebliunaite R, Carracedo A, Salmena L, Ahn Y, et al. High frequency of PTEN, PI3K, and AKT abnormalities in T-cell acute lymphoblastic leukemia. Blood. 2009 Jul 16;114(3):647–50.

211. Medyouf H, Gao X, Armstrong F, Gusscott S, Liu Q, Gedman AL, et al. Acute T-cell leukemias remain dependent on Notch signaling despite PTEN and INK4A/ARF loss. Blood. 2010 Feb 11;115(6):1175–84.

212. Silva A, Jotta PY, Silveira AB, Ribeiro D, Brandalise SR, Yunes JA, et al. Regulation of PTEN by CK2 and Notch1 in primary T-cell acute lymphoblastic leukemia: rationale for combined use of CK2- and gamma-secretase inhibitors. Haematologica. 2010 Apr 1;95(4):674–8.

213. González-García S, García-Peydró M, Martín-Gayo E, Ballestar E, Esteller M, Bornstein R, et al. CSL-MAML-dependent Notch1 signaling controls T lineage-specific IL-7R{alpha} gene expression in early human thymopoiesis and leukemia. J Exp Med. 2009 Apr 13;206(4):779–91.

214. Medyouf H, Gusscott S, Wang H, Tseng J-C, Wai C, Nemirovsky O, et al. High-level IGF1R expression is required for leukemia-initiating cell activity in T-ALL and is supported by Notch signaling. J Exp Med. 2011 Aug 29;208(9):1809–22.

215. Sade H, Krishna S, Sarin A. The Anti-apoptotic Effect of Notch-1 Requires p56 ^{lck} -dependent, Akt/PKB-mediated Signaling in T Cells. J Biol Chem. 2004 Jan 23;279(4):2937–44.

216. Mansour MR, Reed C, Eisenberg AR, Tseng J-C, Twizere J-C, Daakour S, et al. Targeting oncogenic interleukin-7 receptor signalling with *N* -acetylcysteine in T cell acute lymphoblastic leukaemia. Br J Haematol. 2015 Jan 1;168(2):230–8.

217. Chan SM, Weng AP, Tibshirani R, Aster JC, Utz PJ. Notch signals positively regulate activity of the mTOR pathway in T-cell acute lymphoblastic leukemia. Blood. 2007 Jul 1;110(1):278–86.

218. Shepherd C, Banerjee L, Cheung CW, Mansour MR, Jenkinson S, Gale RE, et al. PI3K/mTOR inhibition upregulates NOTCH-MYC signalling

leading to an impaired cytotoxic response. Leukemia. 2013 Mar 5;27(3):650–60.

219. Hales EC, Orr SM, Larson Gedman A, Taub JW, Matherly LH. Notch1 Receptor Regulates AKT Protein Activation Loop (Thr ^{308}) Dephosphorylation through Modulation of the PP2A Phosphatase in Phosphatase and Tensin Homolog (PTEN)-null T-cell Acute Lymphoblastic Leukemia Cells. J Biol Chem. 2013 Aug 2;288(31):22836–48.

220. Vilimas T, Mascarenhas J, Palomero T, Mandal M, Buonamici S, Meng F, et al. Targeting the NF-κB signaling pathway in Notch1-induced T-cell leukemia. Nat Med. 2007 Jan 17;13(1):70–7.

221. Espinosa L, Cathelin S, D'Altri T, Trimarchi T, Statnikov A, Guiu J, et al. The Notch/Hes1 pathway sustains NF-κB activation through CYLD repression in T cell leukemia. Cancer Cell. 2010 Sep 14;18(3):268–81.

222. Joshi I, Minter LM, Telfer J, Demarest RM, Capobianco AJ, Aster JC, et al. Notch signaling mediates G1/S cell-cycle progression in T cells via cyclin D3 and its dependent kinases. Blood. 2009 Feb 19;113(8):1689–98.

223. Rao SS, O'Neil J, Liberator CD, Hardwick JS, Dai X, Zhang T, et al. Inhibition of NOTCH signaling by gamma secretase inhibitor engages the RB pathway and elicits cell cycle exit in T-cell acute lymphoblastic leukemia cells. Cancer Res. 2009 Apr 1;69(7):3060–8.

224. Sicinska E, Aifantis I, Le Cam L, Swat W, Borowski C, Yu Q, et al. Requirement for cyclin D3 in lymphocyte development and T cell leukemias. Cancer Cell. 2003 Dec 1;4(6):451–61.

225. Cayuela J, Hebert J, Sigaux F. Homozygous MTS1 (p16INK4A) deletion in primary tumor cells of 163 leukemic patients [letter; comment]. Blood. 1995;85(3).

226. Iravani M, Dhat R, Price CM. Methylation of the multi tumor suppressor gene-2 (MTS2, CDKN1, p15INK4B) in childhood acute lymphoblastic leukemia. Oncogene. 1997 Dec 18;15(21):2609–14.

227. Sawai CM, Freund J, Oh P, Ndiaye-Lobry D, Bretz JC, Strikoudis A, et al. Therapeutic Targeting of the Cyclin D3:CDK4/6 Complex in T Cell Leukemia. Cancer Cell. 2012 Oct 16;22(4):452–65.

228. Choi YJ, Li X, Hydbring P, Sanda T, Stefano J, Christie AL, et al. The Requirement for Cyclin D Function in Tumor Maintenance. Cancer Cell. 2012 Oct 16;22(4):438–51.

229. Deangelo DJ, Stone RM, Silverman LB, Stock W, Attar EC, Fearen I, et al. A phase I clinical trial of the notch inhibitor MK-0752 in patients with T-cell acute lymphoblastic leukemia/lymphoma (T-ALL) and other leukemias. Journal of Clinical Oncology. 2006. p. 6585.

230. Lee SM, Moon J, Redman BG, Chidiac T, Flaherty LE, Zha Y, et al. Phase 2 study of RO4929097, a gamma-secretase inhibitor, in metastatic melanoma: SWOG 0933. Cancer. 2015 Feb 1;121(3):432–40.

231. O'Neil J, Look AT. Mechanisms of transcription factor deregulation in lymphoid cell transformation. Oncogene. 2007;26(47):6838–49.

232. Aplan PD, Lombardi DP, Reaman GH, Sather HN, Hammond GD, Kirsch IR. Involvement of the putative hematopoietic transcription factor SCL in T-cell acute lymphoblastic leukemia. Blood. 1992;79(5):1327–33.

233. Brown L, Cheng JT, Chen Q, Siciliano MJ, Crist W, Buchanan G, et al. Site-specific recombination of the tal-1 gene is a common occurrence in human T cell leukemia. EMBO J. 1990 Oct;9(10):3343–51.

234. Mansour MR, Abraham BJ, Anders L, Berezovskaya A, Gutierrez A, Durbin AD, et al. An oncogenic super-enhancer formed through somatic mutation of a noncoding intergenic element. Science. 2014 Dec 12;346(6215):1373–7.

235. O'Neil J, Shank J, Cusson N, Murre C, Kelliher M. TAL1/SCL induces leukemia by inhibiting the transcriptional activity of E47/HEB. Cancer Cell. 2004 Jun;5(6):587–96.

236. Palomero T, Odom DT, O'Neil J, Ferrando AA, Margolin A, Neuberg DS, et al. Transcriptional regulatory networks downstream of TAL1/SCL in T-cell acute lymphoblastic leukemia. Blood. 2006 Aug 1;108(3):986–92.

237. Sanda T, Lawton LN, Barrasa MI, Fan ZP, Kohlhammer H, Gutierrez A, et al. Core Transcriptional Regulatory Circuit Controlled by the TAL1 Complex in Human T Cell Acute Lymphoblastic Leukemia. Cancer Cell. 2012 Aug 14;22(2):209–21.

238. Larson RC, Lavenir I, Larson TA, Baer R, Warren AJ, Wadman I, et al. Protein dimerization between Lmo2 (Rbtn2) and Tall alters thymocyte development and potentiates T cell tumorigenesis in transgenic mice. EMBO J. 1996;15(5):1021–7.

239. Robb L, Rasko JE, Bath ML, Strasser A, Begley CG. scl, a gene frequently activated in human T cell leukaemia, does not induce lymphomas in

transgenic mice. Oncogene. 1995 Jan 5;10(1):205–9.

240. Elwood NJ, Begley CG. Reconstitution of mice with bone marrow cells expressing the SCL gene is insufficient to cause leukemia. Cell growth Differ. 1995 Jan;6(1):19–25.

241. Aplan PD, Jones CA, Chervinsky DS, Zhao X, Ellsworth M, Wu C, et al. An scl gene product lacking the transactivation domain induces bony abnormalities and cooperates with LMO1 to generate T-cell malignancies in transgenic mice. EMBO J. 1997 May 1;16(9):2408–19.

242. Cheng Y, Zhang Z, Slape C, Aplan PD. Cre-loxP-mediated recombination between the SIL and SCL genes leads to a block in T-cell development at the CD4- CD8- to CD4+ CD8+ transition. Neoplasia. 2007 Apr;9(4):315–21.

243. Kelliher MA, Seldin DC, Leder P. Tal-1 induces T cell acute lymphoblastic leukemia accelerated by casein kinase IIalpha. EMBO J. 1996 Oct 1;15(19):5160–6.

244. Chervinsky DS, Zhao XF, Lam DH, Ellsworth M, Gross KW, Aplan PD. Disordered T-cell development and T-cell malignancies in SCL LMO1 double-transgenic mice: parallels with E2A-deficient mice. Mol Cell Biol. 1999 Jul 1;19(7):5025–35.

245. Shank-Calvo JA, Draheim K, Bhasin M, Kelliher MA. p16Ink4a or p19Arf loss contributes to Tal1-induced leukemogenesis in mice. Oncogene. 2006 May 9;25(21):3023–31.

246. Fasseu M, Aplan PD, Chopin M, Boissel N, Bories J-C, Soulier J, et al. p16INK4A tumor suppressor gene expression and CD3epsilon deficiency but not pre-TCR deficiency inhibit TAL1-linked T-lineage leukemogenesis. Blood. 2007 Oct 1;110(7):2610–9.

247. Boehm T, Foroni L, Kaneko Y, Perutz MF, Rabbitts TH. The rhombotin family of cysteine-rich LIM-domain oncogenes: distinct members are involved in T-cell translocations to human chromosomes 11p15 and 11p13. Proc Natl Acad Sci U S A. 1991 May 15;88(10):4367–71.

248. Van Vlierberghe P, van Grotel M, Beverloo HB, Lee C, Helgason T, Buijs-Gladdines J, et al. The cryptic chromosomal deletion del(11)(p12p13) as a new activation mechanism of LMO2 in pediatric T-cell acute lymphoblastic leukemia. Blood. 2006 Nov 15;108(10):3520–9.

249. Hacein-Bey-Abina S, Garrigue A, Wang GP, Soulier J, Lim A, Morillon E, et al. Insertional oncogenesis in 4 patients after retrovirus-mediated gene

therapy of SCID-X1. J Clin Invest. 2008 Sep 2;118(9):3132–42.

250. Hacein-Bey-Abina S, Von Kalle C, Schmidt M, McCormack MP, Wulffraat N, Leboulch P, et al. LMO2-Associated Clonal T Cell Proliferation in Two Patients after Gene Therapy for SCID-X1. Science. 2003 Oct 17;302(5644):415–9.

251. Howe SJ, Mansour MR, Schwarzwaelder K, Bartholomae C, Hubank M, Kempski H, et al. Insertional mutagenesis combined with acquired somatic mutations causes leukemogenesis following gene therapy of SCID-X1 patients. J Clin Invest. 2008 Sep 2;118(9):3143–50.

252. Fisch P, Boehm T, Lavenir I, Larson T, Arno J, Forster A, et al. T-cell acute lymphoblastic lymphoma induced in transgenic mice by the RBTN1 and RBTN2 LIM-domain genes. Oncogene. 1992 Dec;7(12):2389–97.

253. McGuire EA, Rintoul CE, Sclar GM, Korsmeyer SJ. Thymic overexpression of Ttg-1 in transgenic mice results in T-cell acute lymphoblastic leukemia/lymphoma. Mol Cell Biol. 1992 Sep;12(9):4186–96.

254. Larson RC, Osada H, Larson TA, Lavenir I, Rabbitts TH. The oncogenic LIM protein Rbtn2 causes thymic developmental aberrations that precede malignancy in transgenic mice. Oncogene. 1995 Sep 7;11(5):853–62.

255. Neale GA, Rehg JE, Goorha RM. Ectopic expression of rhombotin-2 causes selective expansion of CD4-CD8- lymphocytes in the thymus and T-cell tumors in transgenic mice. Blood. 1995 Oct 15;86(8):3060–71.

256. Warren AJ, Colledge WH, Carlton MBL, Evans MJ, Smith AJH, Rabbitts TH. The Oncogenic Cysteine-rich LIM domain protein Rbtn2 is essential for erythroid development. Cell. 1994 Jul 15;78(1):45–57.

257. El Omari K, Hoosdally SJ, Tuladhar K, Karia D, Hall-Ponselé E, Platonova O, et al. Structural Basis for LMO2-Driven Recruitment of the SCL:E47bHLH Heterodimer to Hematopoietic-Specific Transcriptional Targets. Cell Rep. 2013 Jul 11;4(1):135–47.

258. Boyer LA, Lee TI, Cole MF, Johnstone SE, Levine SS, Zucker JP, et al. Core transcriptional regulatory circuitry in human embryonic stem cells. Cell. 2005 Sep 23;122(6):947–56.

259. Novershtern N, Subramanian A, Lawton LN, Mak RH, Haining WN, McConkey ME, et al. Densely Interconnected Transcriptional Circuits Control Cell States in Human Hematopoiesis. Cell. 2011 Jan;144(2):296–309.

260. Ramsay RG, Gonda TJ. MYB function in normal and cancer cells. Nat Rev Cancer. 2008;8(7):523–34.

261. Westin EH, Gallo RC, Arya SK, Eva A, Souza LM, Baluda MA, et al. Differential expression of the amv gene in human hematopoietic cells. Proc Natl Acad Sci U S A. 1982 Apr;79(7):2194–8.

262. Bender TP, Kremer CS, Kraus M, Buch T, Rajewsky K. Critical functions for c-Myb at three checkpoints during thymocyte development. Nat Immunol. 2004 Jul 13;5(7):721–9.

263. Shen-Ong GL, Morse HC, Potter M, Mushinski JF. Two modes of c-myb activation in virus-induced mouse myeloid tumors. Mol Cell Biol. 1986 Feb;6(2):380–92.

264. Weinstein Y, Ihle JN, Lavu S, Reddy EP. Truncation of the c-myb gene by a retroviral integration in an interleukin 3-dependent myeloid leukemia cell line. Proc Natl Acad Sci U S A. 1986;83:5010–4.

265. O'Neil J, Tchinda J, Gutierrez A, Moreau L, Maser RS, Wong K-K, et al. Alu elements mediate MYB gene tandem duplication in human T-ALL. J Exp Med. 2007 Dec 24;204(13):3059–66.

266. Lahortiga I, De Keersmaecker K, Van Vlierberghe P, Graux C, Cauwelier B, Lambert F, et al. Duplication of the MYB oncogene in T cell acute lymphoblastic leukemia. Nat Genet. 2007 May 15;39(5):593–5.

267. Badiani PA, Kioussis D, Swirsky DM, Lampert IA, Weston K. T-cell lymphomas in v-Myb transgenic mice. Oncogene. 1996 Nov 21;13(10):2205–12.

268. Miyoshi H, Shimizu K, Kozu T, Maseki N, Kaneko Y, Ohki M. t(8;21) breakpoints on chromosome 21 in acute myeloid leukemia are clustered within a limited region of a single gene, AML1. Proc Natl Acad Sci U S A. 1991 Dec 1;88(23):10431–4.

269. Sood R, Kamikubo Y, Liu P. Role of RUNX1 in hematological malignancies. Blood. 2017 Apr 13;129(15):2070–82.

270. Osato M, Asou N, Abdalla E, Hoshino K, Yamasaki H, Okubo T, et al. Biallelic and heterozygous point mutations in the runt domain of the AML1/PEBP2alphaB gene associated with myeloblastic leukemias. Blood. 1999 Mar 15;93(6):1817–24.

271. Preudhomme C, Warot-Loze D, Roumier C, Grardel-Duflos N, Garand R,

Lai JL, et al. High incidence of biallelic point mutations in the Runt domain of the AML1/PEBP2 alpha B gene in Mo acute myeloid leukemia and in myeloid malignancies with acquired trisomy 21. Blood. 2000 Oct 15;96(8):2862–929.

272. Carnicer MJ, Nomdedéu JF, Lasa A, Bellido M, Aventín A, Baiget M, et al. AML-1 mutations outside the RUNT domain: description of two cases in myeloid malignancies. Leukemia. 2002 Nov 6;16(11):2329–32.

273. Harada H, Harada Y, Niimi H, Kyo T, Kimura A, Inaba T, et al. High incidence of somatic mutations in the AML1/RUNX1 gene in myelodysplastic syndrome and low blast percentage myeloid leukemia with myelodysplasia. Blood. 2004 Mar 15;103(6):2316–24.

274. Meyers S, Lenny N, Hiebert SW. The t(8;21) fusion protein interferes with AML-1B-dependent transcriptional activation. Mol Cell Biol. 1995 Apr;15(4):1974–82.

275. Gelmetti V, Zhang J, Fanelli M, Minucci S, Pelicci PG, Lazar MA. Aberrant recruitment of the nuclear receptor corepressor-histone deacetylase complex by the acute myeloid leukemia fusion partner ETO. Mol Cell Biol. 1998 Dec;18(12):7185–91.

276. Lutterbach B, Westendorf JJ, Linggi B, Patten A, Moniwa M, Davie JR, et al. ETO, a target of t(8;21) in acute leukemia, interacts with the N-CoR and mSin3 corepressors. Mol Cell Biol. 1998 Dec;18(12):7176–84.

277. Song W-J, Sullivan MG, Legare RD, Hutchings S, Tan X, Kufrin D, et al. Haploinsufficiency of CBFA2 causes familial thrombocytopenia with propensity to develop acute myelogenous leukaemia. Nat Genet. 1999 Oct 1;23(2):166–75.

278. Preudhomme C, Renneville A, Bourdon V, Philippe N, Roche-Lestienne C, Boissel N, et al. High frequency of RUNX1 biallelic alteration in acute myeloid leukemia secondary to familial platelet disorder. Blood. 2009 May 28;113(22):5583–7.

279. Jongmans MCJ, Kuiper RP, Carmichael CL, Wilkins EJ, Dors N, Carmagnac A, et al. Novel RUNX1 mutations in familial platelet disorder with enhanced risk for acute myeloid leukemia: clues for improved identification of the FPD/AML syndrome. Leukemia. 2010 Jan 15;24(1):242–6.

280. Li J, Shen H, Himmel KL, Dupuy AJ, Largaespada DA, Nakamura T, et al. Leukaemia disease genes: large-scale cloning and pathway predictions.

Nat Genet. 1999 Nov 1;23(3):348–53.

281. Mikkers H, Allen J, Knipscheer P, Romeyn L, Hart A, Vink E, et al. High-throughput retroviral tagging to identify components of specific signaling pathways in cancer. Nat Genet. 2002 Sep 19;32(1):153–9.

282. Suzuki T, Shen H, Akagi K, Morse HC, Malley JD, Naiman DQ, et al. New genes involved in cancer identified by retroviral tagging. Nat Genet. 2002 Sep 19;32(1):166–74.

283. Wotton S, Stewart M, Blyth K, Vaillant F, Kilbey A, Neil JC, et al. Proviral insertion indicates a dominant oncogenic role for Runx1/AML-1 in T-cell lymphoma. Cancer Res. 2002 Dec 15;62(24):7181–5.

284. Niini T, Kanerva J, Vettenranta K, Saarinen-Pihkala UM, Knuutila S. AML1 gene amplification: a novel finding in childhood acute lymphoblastic leukemia. Haematologica. 2000 Apr 1;85(4):362–6.

285. Harewood L, Robinson H, Harris R, Al-Obaidi MJ, Jalali GR, Martineau M, et al. Amplification of AML1 on a duplicated chromosome 21 in acute lymphoblastic leukemia: a study of 20 cases. Leukemia. 2003 Mar 19;17(3):547–53.

286. Robinson HM, Broadfield ZJ, Cheung KL, Harewood L, Harris RL, Jalali GR, et al. Amplification of AML1 in acute lymphoblastic leukemia is associated with a poor outcome. Leukemia. 2003 Nov 18;17(11):2249–50.

287. Roumier C, Fenaux P, Lafage M, Imbert M, Eclache V, Preudhomme C. New mechanisms of AML1 gene alteration in hematological malignancies. Leukemia. 2003 Jan 3;17(1):9–16.

288. Streubel B, Valent P, Lechner K, Fonatsch C. Amplification of the AML1(CBFA2) gene on ring chromosomes in a patient with acute myeloid leukemia and a constitutional ring chromosome 21. Cancer Genet Cytogenet. 2001 Jan 1;124(1):42–6.

289. Niini T, Vettenranta K, Hollmén J, Larramendy ML, Aalto Y, Wikman H, et al. Expression of myeloid-specific genes in childhood acute lymphoblastic leukemia – a cDNA array study. Leukemia. 2002 Nov 6;16(11):2213–21.

290. Fenske TS, Pengue G, Mathews V, Hanson PT, Hamm SE, Riaz N, et al. Stem cell expression of the AML1/ETO fusion protein induces a myeloproliferative disorder in mice. Proc Natl Acad Sci U S A. 2004 Oct 19;101(42):15184–9.

291. de Guzman CG, Warren AJ, Zhang Z, Gartland L, Erickson P, Drabkin H, et al. Hematopoietic stem cell expansion and distinct myeloid developmental abnormalities in a murine model of the AML1-ETO translocation. Mol Cell Biol. 2002 Aug 1;22(15):5506–17.

292. Yuan Y, Zhou L, Miyamoto T, Iwasaki H, Harakawa N, Hetherington CJ, et al. AML1-ETO expression is directly involved in the development of acute myeloid leukemia in the presence of additional mutations. Proc Natl Acad Sci U S A. 2001 Aug 28;98(18):10398–403.

293. Nucifora G, Begy CR, Kobayashi H, Roulston D, Claxtont D, Pedersen-Bjergaardt J, et al. Consistent intergenic splicing and production of multiple transcripts between AMLl at 21q22 and unrelated genes at 3q26 in (3;21)(q26;q22) translocations. Med Sci. 1994;91:4004–8.

294. Jamil A, Theil KS, Kahwash S, Ruymann FB, Klopfenstein KJ. TEL/AML-1 fusion gene: its frequency and prognostic significance in childhood acute lymphoblastic leukemia. Cancer Genet Cytogenet. 2000 Oct 15;122(2):73–8.

295. Romana S, Mauchauffe M, Le Coniat M, Chumakov I, Le Paslier D, Berger R, et al. The t(12;21) of acute lymphoblastic leukemia results in a tel-AML1 gene fusion. Blood. 1995;85(12):3662–70.

296. Golub TR, Barker GF, Bohlandert SK, Hiebert SW, Wards DC, Bray-Wards P, et al. Fusion of the TEL gene on 12pl3 to the AML1 gene on 21q22 in acute lymphoblastic leukemia. Med Sci. 1995;92:4917–21.

297. Li Y, Wang H, Wang X, Jin W, Tan Y, Fang H, et al. Genome-wide studies identify a novel interplay between AML1 and AML1/ETO in t(8;21) acute myeloid leukemia. Blood. 2016 Jan 14;127(2):233–42.

298. Shia W-J, Okumura AJ, Yan M, Sarkeshik A, Lo M-C, Matsuura S, et al. PRMT1 interacts with AML1-ETO to promote its transcriptional activation and progenitor cell proliferative potential. Blood. 2012 May 24;119(21):4953–62.

299. Wang J, Hoshino T, Redner RL, Kajigaya S, Liu JM. ETO, fusion partner in t(8;21) acute myeloid leukemia, represses transcription by interaction with the human N-CoR/mSin3/HDAC1 complex. Proc Natl Acad Sci U S A. 1998 Sep 1;95(18):10860–5.

300. Vangala RK, Heiss-Neumann MS, Rangatia JS, Singh SM, Schoch C, Tenen DG, et al. The myeloid master regulator transcription factor PU.1 is inactivated by AML1-ETO in t(8;21) myeloid leukemia. Blood. 2003 Jan

1;101(1):270–7.

301. Pabst T, Mueller BU, Harakawa N, Schoch C, Haferlach T, Behre G, et al. AML1–ETO downregulates the granulocytic differentiation factor C/EBPα in t(8;21) myeloid leukemia. Nat Med. 2001 Apr 1;7(4):444–51.

302. Ptasinska A, Assi SA, Martinez-Soria N, Imperato MR, Piper J, Cauchy P, et al. Identification of a Dynamic Core Transcriptional Network in t(8;21) AML that Regulates Differentiation Block and Self-Renewal. Cell Rep. 2014 Sep 25;8(6):1974–88.

303. Christiansen DH, Andersen MK, Pedersen-Bjergaard J, Hangaishi A, Takeuchi K, Maki K, et al. Mutations of AML1 are common in therapy-related myelodysplasia following therapy with alkylating agents and are significantly associated with deletion or loss of chromosome arm 7q and with subsequent leukemic transformation. Blood. 2004 Sep 1;104(5):1474–81.

304. Chen C-Y, Lin L-I, Tang J-L, Ko B-S, Tsay W, Chou W-C, et al. RUNX1 gene mutation in primary myelodysplastic syndrome - the mutation can be detected early at diagnosis or acquired during disease progression and is associated with poor outcome. Br J Haematol. 2007 Oct 1;139(3):405–14.

305. Tang J-L, Hou H-A, Chen C-Y, Liu C-Y, Chou W-C, Tseng M-H, et al. AML1/RUNX1 mutations in 470 adult patients with de novo acute myeloid leukemia: prognostic implication and interaction with other gene alterations. Blood. 2009 Dec 17;114(26):5352–61.

306. Schnittger S, Dicker F, Kern W, Wendland N, Sundermann J, Alpermann T, et al. RUNX1 mutations are frequent in de novo AML with noncomplex karyotype and confer an unfavorable prognosis. Blood. 2011 Feb 24;117(8):2348–57.

307. Greif PA, Konstandin NP, Metzeler KH, Herold T, Pasalic Z, Ksienzyk B, et al. RUNX1 mutations in cytogenetically normal acute myeloid leukemia are associated with a poor prognosis and up-regulation of lymphoid genes. Haematologica. 2012 Dec 1;97(12):1909–15.

308. Tsai S-C, Shih L-Y, Liang S-T, Huang Y-J, Kuo M-C, Huang C-F, et al. Biological Activities of RUNX1 Mutants Predict Secondary Acute Leukemia Transformation from Chronic Myelomonocytic Leukemia and Myelodysplastic Syndromes. Clin cancer Res. 2015 Aug 1;21(15):3541–51.

309. Mendler JH, Maharry K, Radmacher MD, Mrózek K, Becker H, Metzeler KH, et al. RUNX1 mutations are associated with poor outcome in younger

and older patients with cytogenetically normal acute myeloid leukemia and with distinct gene and MicroRNA expression signatures. J Clin Oncol . 2012 Sep 1;30(25):3109–18.

310. Gaidzik VI, Bullinger L, Schlenk RF, Zimmermann AS, Röck J, Paschka P, et al. RUNX1 mutations in acute myeloid leukemia: results from a comprehensive genetic and clinical analysis from the AML study group. J Clin Oncol . 2011 Apr 1;29(10):1364–72.

311. Micol J-B, Duployez N, Boissel N, Petit A, Geffroy S, Nibourel O, et al. Frequent ASXL2 mutations in acute myeloid leukemia patients with t(8;21)/RUNX1-RUNX1T1 chromosomal translocations. Blood. 2014 Aug 28;124(9):1445–9.

312. Krauth M-T, Eder C, Alpermann T, Bacher U, Nadarajah N, Kern W, et al. High number of additional genetic lesions in acute myeloid leukemia with t(8;21)/RUNX1-RUNX1T1: frequency and impact on clinical outcome. Leukemia. 2014 Jul 9;28(7):1449–58.

313. Cuenco GM, Nucifora G, Ren R. Human AML1/MDS1/EVI1 fusion protein induces an acute myelogenous leukemia (AML) in mice: a model for human AML. Proc Natl Acad Sci U S A. 2000 Feb 15;97(4):1760–5.

314. Watanabe-Okochi N, Kitaura J, Ono R, Harada H, Harada Y, Komeno Y, et al. AML1 mutations induced MDS and MDS/AML in a mouse BMT model. Blood. 2008 Apr 15;111(8):4297–308.

315. Mulloy JC, Cammenga J, MacKenzie KL, Berguido FJ, Moore MA, Nimer SD. The AML1-ETO fusion protein promotes the expansion of human hematopoietic stem cells. Blood. 2002;99(1):15–23.

316. Tonks A, Pearn L, Tonks AJ, Pearce L, Hoy T, Phillips S, et al. The AML1-ETO fusion gene promotes extensive self-renewal of human primary erythroid cells. Blood. 2003 Jan 15;101(2):624–32.

317. Liu P, Tarlé SA, Hajra A, Claxton DF, Marlton P, Freedman M, et al. Fusion between transcription factor CBF beta/PEBP2 beta and a myosin heavy chain in acute myeloid leukemia. Science. 1993 Aug 20;261(5124):1041–4.

318. Adya N, Stacy T, Speck NA, Liu PP. The leukemic protein core binding factor beta (CBFbeta)-smooth-muscle myosin heavy chain sequesters CBFalpha2 into cytoskeletal filaments and aggregates. Mol Cell Biol. 1998 Dec;18(12):7432–43.

319. Lutterbach B, Hou Y, Durst KL, Hiebert SW. The inv(16) encodes an acute

myeloid leukemia 1 transcriptional corepressor. Proc Natl Acad Sci U S A. 1999 Oct 26;96(22):12822–7.

320. Castilla LH, Wijmenga C, Wang Q, Stacy T, Speck NA, Eckhaus M, et al. Failure of Embryonic Hematopoiesis andLethal Hemorrhages in Mouse Embryos Heterozygousfor a Knocked-In Leukemia Gene CBFB–MYH11. Cell. 1996 Nov 15;87(4):687–96.

321. Grossmann V, Haferlach C, Weissmann S, Roller A, Schindela S, Poetzinger F, et al. The molecular profile of adult T-cell acute lymphoblastic leukemia: Mutations in *RUNX1* and *DNMT3A* are associated with poor prognosis in T-ALL. Genes, Chromosom Cancer. 2013 Apr 1;52(4):410–22.

322. Mok MMH, Du L, Wang CQ, Tergaonkar V, Liu TC, Yin Kham SK, et al. RUNX1 point mutations potentially identify a subset of early immature T-cell acute lymphoblastic leukaemia that may originate from differentiated T-cells. Gene. 2014 Jul 15;545(1):111–6.

323. Della Gatta G, Palomero T, Perez-Garcia A, Ambesi-Impiombato A, Bansal M, Carpenter ZW, et al. Reverse engineering of TLX oncogenic transcriptional networks identifies RUNX1 as tumor suppressor in T-ALL. Nat Med. 2012 Feb 26;18(3):436–40.

324. Wang H, Zang C, Taing L, Arnett KL, Wong YJ, Pear WS, et al. NOTCH1-RBPJ complexes drive target gene expression through dynamic interactions with superenhancers. Proc Natl Acad Sci U S A. 2014 Jan 14;111(2):705–10.

325. Wang H, Zou J, Zhao B, Johannsen E, Ashworth T, Wong H, et al. Genome-wide analysis reveals conserved and divergent features of Notch1/RBPJ binding in human and murine T-lymphoblastic leukemia cells. Proc Natl Acad Sci U S A. 2011 Sep 6;108(36):14908–13.

326. Fuda NJ, Ardehali MB, Lis JT. Defining mechanisms that regulate RNA polymerase II transcription in vivo. Nature. 2009 Sep 10;461(7261):186–92.

327. Li B, Carey M, Workman JL. The role of chromatin during transcription. Cell. 2007 Feb 23;128(4):707–19.

328. Takahashi K, Yamanaka S. Induction of Pluripotent Stem Cells from Mouse Embryonic and Adult Fibroblast Cultures by Defined Factors. Cell. 2006 Aug 25;126(4):663–76.

329. Takahashi K, Tanabe K, Ohnuki M, Narita M, Ichisaka T, Tomoda K, et al.

Induction of Pluripotent Stem Cells from Adult Human Fibroblasts by Defined Factors. Cell. 2007 Nov 30;131(5):861–72.

330. Buganim Y, Faddah DA, Jaenisch R. Mechanisms and models of somatic cell reprogramming. Nat Rev Genet. 2013 Jun 1;14(6):427–39.

331. Sancho-Martinez I, Baek SH, Izpisua Belmonte JC. Lineage conversion methodologies meet the reprogramming toolbox. Nat Cell Biol. 2012 Sep 1;14(9):892–9.

332. Laiosa C V., Stadtfeld M, Xie H, de Andres-Aguayo L, Graf T. Reprogramming of Committed T Cell Progenitors to Macrophages and Dendritic Cells by C/EBPα and PU.1 Transcription Factors. Immunity. 2006 Nov 1;25(5):731–44.

333. Soufi A, Donahue G, Zaret KS. Facilitators and Impediments of the Pluripotency Reprogramming Factors' Initial Engagement with the Genome. Cell. 2012 Nov 21;151(5):994–1004.

334. Lin CY, Lovén J, Rahl PB, Paranal RM, Burge CB, Bradner JE, et al. Transcriptional Amplification in Tumor Cells with Elevated c-Myc. Cell. 2012 Sep 28;151(1):56–67.

335. Nie Z, Hu G, Wei G, Cui K, Yamane A, Resch W, et al. c-Myc Is a Universal Amplifier of Expressed Genes in Lymphocytes and Embryonic Stem Cells. Cell. 2012 Sep 28;151(1):68–79.

336. Trompouki E, Bowman TV, Lawton LN, Fan ZP, Wu D-C, DiBiase A, et al. Lineage Regulators Direct BMP and Wnt Pathways to Cell-Specific Programs during Differentiation and Regeneration. Cell. 2011 Oct 28;147(3):577–89.

337. Mullen AC, Orlando DA, Newman JJ, Lovén J, Kumar RM, Bilodeau S, et al. Master Transcription Factors Determine Cell-Type-Specific Responses to TGF-β Signaling. Cell. 2011 Oct 28;147(3):565–76.

338. Barbieri CE, Baca SC, Lawrence MS, Demichelis F, Blattner M, Theurillat J-P, et al. Exome sequencing identifies recurrent SPOP, FOXA1 and MED12 mutations in prostate cancer. Nat Genet. 2012 Jun 20;44(6):685–9.

339. Makinen N, Mehine M, Tolvanen J, Kaasinen E, Li Y, Lehtonen HJ, et al. MED12, the Mediator Complex Subunit 12 Gene, Is Mutated at High Frequency in Uterine Leiomyomas. Science. 2011 Oct 14;334(6053):252–5.

340. Hnisz D, Abraham BJ, Lee TI, Lau A, Saint-Andr V, Sigova AA, et al.

Super-Enhancers in the Control of Cell Identity and Disease. Cell. 2013 Nov 7;155(4):934–47.

341. Dunham I, Kundaje A, Aldred SF, Collins PJ, Davis CA, Doyle F, et al. An integrated encyclopedia of DNA elements in the human genome. Nature. 2012 Sep 5;489(7414):57–74.

342. Whyte WA, Orlando DA, Hnisz D, Abraham BJ, Lin CY, Kagey MH, et al. Master transcription factors and mediator establish super-enhancers at key cell identity genes. Cell. 2013 Apr 11;153(2):307–19.

343. Li W, Notani D, Rosenfeld MG. Enhancers as non-coding RNA transcription units: recent insights and future perspectives. Nat Rev Genet. 2016 Apr 7;17(4):207–23.

344. Lai F, Orom UA, Cesaroni M, Beringer M, Taatjes DJ, Blobel GA, et al. Activating RNAs associate with Mediator to enhance chromatin architecture and transcription. Nature. 2013 Feb 17;494(7438):497–501.

345. Maurano MT, Humbert R, Rynes E, Thurman RE, Haugen E, Wang H, et al. Systematic Localization of Common Disease-Associated Variation in Regulatory DNA. Science. 2012;337(6099):1190–5.

346. Hindorff LA, Sethupathy P, Junkins HA, Ramos EM, Mehta JP, Collins FS, et al. Potential etiologic and functional implications of genome-wide association loci for human diseases and traits. Proc Natl Acad Sci U S A. 2009 Jun 9;106(23):9362–7.

347. Lovén J, Hoke HA, Lin CY, Lau A, Orlando DA, Vakoc CR, et al. Selective Inhibition of Tumor Oncogenes by Disruption of Super-Enhancers. Cell. 2013;153:320–34.

348. Drier Y, Cotton MJ, Williamson KE, Gillespie SM, Ryan RJH, Kluk MJ, et al. An oncogenic MYB feedback loop drives alternate cell fates in adenoid cystic carcinoma. Nat Genet. 2016 Mar 1;48(3):265–72.

349. Gröschel S, Sanders MA, Hoogenboezem R, de Wit E, Bouwman BAM, Erpelinck C, et al. A Single Oncogenic Enhancer Rearrangement Causes Concomitant EVI1 and GATA2 Deregulation in Leukemia. Cell. 2014 Apr 10;157(2):369–81.

350. Walker BA, Wardell CP, Brioli A, Boyle E, Kaiser MF, Begum DB, et al. Translocations at 8q24 juxtapose MYC with genes that harbor superenhancers resulting in overexpression and poor prognosis in myeloma patients. Blood Cancer J. 2014 Mar 14;4(3):e191.

351. Herranz D, Ambesi-Impiombato A, Palomero T, Schnell SA, Belver L, Wendorff AA, et al. A NOTCH1-driven MYC enhancer promotes T cell development, transformation and acute lymphoblastic leukemia. Nat Med. 2014 Sep 7;20(10):1130–7.

352. Shi J, Whyte WA, Zepeda-Mendoza CJ, Milazzo JP, Shen C, Roe JS, et al. Role of SWI/SNF in acute leukemia maintenance and enhancer-mediated Myc regulation. Genes Dev. 2013 Dec 15;27(24):2648–62.

353. Zhang X, Choi PS, Francis JM, Imielinski M, Watanabe H, Cherniack AD, et al. Identification of focally amplified lineage-specific super-enhancers in human epithelial cancers. Nat Genet. 2016 Feb 14;48(2):176–82.

354. Radtke I, Mullighan CG, Ishii M, Su X, Cheng J, Ma J, et al. Genomic analysis reveals few genetic alterations in pediatric acute myeloid leukemia. Proc Natl Acad Sci U S A. 2009 Aug 4;106(31):12944–9.

355. Kühn MWM, Radtke I, Bullinger L, Goorha S, Cheng J, Edelmann J, et al. High-resolution genomic profiling of adult and pediatric core-binding factor acute myeloid leukemia reveals new recurrent genomic alterations. Blood. 2012 Mar 8;119(10):e67-75.

356. Easton DF, Pooley KA, Dunning AM, Pharoah PDP, Thompson D, Ballinger DG, et al. Genome-wide association study identifies novel breast cancer susceptibility loci. Nature. 2007 Jun 28;447(7148):1087–93.

357. Kiemeney LA, Thorlacius S, Sulem P, Geller F, Aben KKH, Stacey SN, et al. Sequence variant on 8q24 confers susceptibility to urinary bladder cancer. Nat Genet. 2008 Nov 14;40(11):1307–12.

358. Ghoussaini M, Song H, Koessler T, Al Olama AA, Kote-Jarai Z, Driver KE, et al. Multiple Loci With Different Cancer Specificities Within the 8q24 Gene Desert. JNCI J Natl Cancer Inst. 2008 Jul 2;100(13):962–6.

359. Ahmadiyeh N, Pomerantz MM, Grisanzio C, Herman P, Jia L, Almendro V, et al. 8q24 prostate, breast, and colon cancer risk loci show tissue-specific long-range interaction with MYC. Proc Natl Acad Sci. 2010 May 25;107(21):9742–6.

360. Wright JB, Brown SJ, Cole MD. Upregulation of c-MYC in cis through a large chromatin loop linked to a cancer risk-associated single-nucleotide polymorphism in colorectal cancer cells. Mol Cell Biol. 2010 Mar 15;30(6):1411–20.

361. Dave K, Sur I, Yan J, Zhang J, Kaasinen E, Zhong F, et al. Mice deficient

of Myc super-enhancer region reveal differential control mechanism between normal and pathological growth. Elife. 2017 Jun 6;6:e23382.

362. Bellon T, Perrotti D, Calabretta B. Granulocytic differentiation of normal hematopoietic precursor cells induced by transcription factor PU.1 correlates with negative regulation of the c-myb promoter. Blood. 1997 Sep 1;90(5):1828–39.

363. Nicolaides NC, Gualdi R, Casadevall C, Manzella L, Calabretta B. Positive autoregulation of c-myb expression via Myb binding sites in the 5' flanking region of the human c-myb gene. Mol Cell Biol. 1991 Dec;11(12):6166–76.

364. Kwiatkowski N, Zhang T, Rahl PB, Abraham BJ, Reddy J, Ficarro SB, et al. Targeting transcription regulation in cancer with a covalent CDK7 inhibitor. Nature. 2014 Jun 22;511(7511):616–20.

365. Sato T, Ohno S, Hayashi T, Sato C, Kohu K, Satake M, et al. Dual Functions of Runx Proteins for Reactivating CD8 and Silencing CD4 at the Commitment Process into CD8 Thymocytes. Immunity. 2005 Mar;22(3):317–28.

366. Illendula A, Gilmour J, Grembecka J, Tirumala VSS, Boulton A, Kuntimaddi A, et al. Small Molecule Inhibitor of CBFbeta-RUNX Binding for RUNX Transcription Factor Driven Cancers. EBioMedicine. 2016;8:117–31.

367. Choi Ah, Illendula A, Pulikkan JA, Roderick JE, Tesell J, Yu J, et al. RUNX1 is required for oncogenic Myb and Myc enhancer activity in T-cell acute lymphoblastic leukemia. Blood. 2017 Oct 12;130(15):1722–33.

368. Giambra V, Jenkins CR, Wang H, Lam SH, Shevchuk OO, Nemirovsky O, et al. NOTCH1 promotes T cell leukemia-initiating activity by RUNX-mediated regulation of PKC-θ and reactive oxygen species. Nat Med. 2012 Oct 21;18(11):1693–8.

369. Kundu M, Compton S, Garrett-Beal L, Stacy T, Starost MF, Eckhaus M, et al. Runx1 deficiency predisposes mice to T-lymphoblastic lymphoma. Blood. 2005 Nov 15;106(10):3621–4.

370. Lelli KM, Slattery M, Mann RS. Disentangling the Many Layers of Eukaryotic Transcriptional Regulation. Annu Rev Genet. 2012 Dec 15;46(1):43–68.

371. Panne D. The enhanceosome. Curr Opin Struct Biol. 2008 Apr 1;18(2):236–42.

372. Spitz F, Furlong EEM. Transcription factors: from enhancer binding to developmental control. Nat Rev Genet. 2012 Aug 7;13(9):613–26.

373. Wilson NK, Foster SD, Wang X, Knezevic K, Schütte J, Kaimakis P, et al. Combinatorial Transcriptional Control In Blood Stem/Progenitor Cells: Genome-wide Analysis of Ten Major Transcriptional Regulators. Cell Stem Cell. 2010 Oct;7(4):532–44.

374. Wang H, Zou J, Zhao B, Johannsen E, Ashworth T, Wong H, et al. Genome-wide analysis reveals conserved and divergent features of Notch1/RBPJ binding in human and murine T-lymphoblastic leukemia cells. Proc Natl Acad Sci U S A. 2011 Sep 6;108(36):14908–13.

375. Vernimmen D, De Gobbi M, Sloane-Stanley JA, Wood WG, Higgs DR. Long-range chromosomal interactions regulate the timing of the transition between poised and active gene expression. EMBO J. 2007 Apr 18;26(8):2041–51.

376. Spilianakis CG, Flavell RA. Long-range intrachromosomal interactions in the T helper type 2 cytokine locus. Nat Immunol. 2004 Oct 19;5(10):1017–27.

377. Tolhuis B, Palstra R-J, Splinter E, Grosveld F, de Laat W. Looping and Interaction between Hypersensitive Sites in the Active β-globin Locus. Mol Cell. 2002 Dec 1;10(6):1453–65.

378. Jing H, Vakoc CR, Ying L, Mandat S, Wang H, Zheng X, et al. Exchange of GATA Factors Mediates Transitions in Looped Chromatin Organization at a Developmentally Regulated Gene Locus. Mol Cell. 2008 Feb 1;29(2):232–42.

379. Kagey MH, Newman JJ, Bilodeau S, Zhan Y, Orlando DA, van Berkum NL, et al. Mediator and cohesin connect gene expression and chromatin architecture. Nature. 2010 Sep 18;467(7314):430–5.

380. Yatim A, Benne C, Sobhian B, Laurent-Chabalier S, Deas O, Judde JG, et al. NOTCH1 Nuclear Interactome Reveals Key Regulators of Its Transcriptional Activity and Oncogenic Function. Mol Cell. 2012 Nov 9;48(3):445–58.

381. Zuber J, Shi J, Wang E, Rappaport AR, Herrmann H, Sison E a, et al. RNAi screen identifies Brd4 as a therapeutic target in acute myeloid leukaemia. Nature. 2011 Oct 27;478(7370):524–8.

382. Bolden JE, Tasdemir N, Dow LE, van Es JH, Wilkinson JE, Zhao Z, et al.

Inducible in vivo silencing of Brd4 identifies potential toxicities of sustained BET protein inhibition. Cell Rep. 2014 Sep 25;8(6):1919–29.

383. Lee TI, Johnstone SE, Young RA. Chromatin immunoprecipitation and microarray-based analysis of protein location. Nat Protoc. 2006 Jul 13;1(2):729–48.

384. Buenrostro JD, Wu B, Chang HY, Greenleaf WJ, Buenrostro JD, Wu B, et al. ATAC-seq: A Method for Assaying Chromatin Accessibility Genome-Wide. In: Current Protocols in Molecular Biology. Hoboken, NJ, USA: John Wiley & Sons, Inc.; 2015. p. 21.29.1-21.29.9.

385. Naumova N, Smith EM, Zhan Y. Analysis of long-range chromatin interactions using Chromosome Conformation Capture. Methods. 2012 Nov 1;58(3):192–203.

386. Bell JJ, Bhandoola A. The earliest thymic progenitors for T cells possess myeloid lineage potential. Nature. 2008 Apr 10;452(7188):764–7.

387. Fujii M, Hayashi K, Niki M, Chiba N, Meguro K, Endo K, et al. Overexpression of AML1 renders a T hybridoma resistant to T cell receptor-mediated apoptosis. Oncogene. 1998 Oct 9;17(14):1813–20.

388. Abe N, Kohu K, Ohmori H, Hayashi K, Watanabe T, Hozumi K, et al. Reduction of Runx1 transcription factor activity up-regulates Fas and Bim expression and enhances the apoptotic sensitivity of double positive thymocytes. J Immunol. 2005 Oct 1;175(7):4475–82.

389. Hnisz D, Weintraub AS, Day DS, Valton A-L, Bak RO, Li CH, et al. Activation of proto-oncogenes by disruption of chromosome neighborhoods. Science. 2016 Mar 25;351(6280):1454–8.

390. Nottingham WT, Jarratt A, Burgess M, Speck CL, Cheng J-F, Prabhakar S, et al. Runx1-mediated hematopoietic stem-cell emergence is controlled by a Gata/Ets/SCL-regulated enhancer. Blood. 2007 Dec 15;110(13):4188–97.

391. Kitabayashi I, Aikawa Y, Nguyen LA, Yokoyama A, Ohki M. Activation of AML1-mediated transcription by MOZ and inhibition by the MOZ-CBP fusion protein. EMBO J. 2001;20(24):7184–96.

392. Guo C, Morris SA. Engineering cell identity: establishing new gene regulatory and chromatin landscapes. Curr Opin Genet Dev. 2017 Oct 1;46:50–7.

393. Ramakrishnan V, Finch JT, Graziano V, Lee PL, Sweet RM. Crystal

structure of globular domain of histone H5 and its implications for nucleosome binding. Nature. 1993 Mar 18;362(6417):219–23.

394. Lichtinger M, Ingram R, Hannah R, Müller D, Clarke D, Assi SA, et al. RUNX1 reshapes the epigenetic landscape at the onset of haematopoiesis. EMBO J. 2012 Nov 14;31(22):4318–33.

395. Gibcus JH, Dekker J. The Hierarchy of the 3D Genome. Mol Cell. 2013 Mar 7;49(5):773–82.

396. Montavon T, Soshnikova N, Mascrez B, Joye E, Thevenet L, Splinter E, et al. A Regulatory Archipelago Controls Hox Genes Transcription in Digits. Cell. 2011 Nov 23;147(5):1132–45.

397. Carter D, Chakalova L, Osborne CS, Dai Y, Fraser P. Long-range chromatin regulatory interactions in vivo. Nat Genet. 2002 Nov 11;32(4):623–6.

398. Jiang H, Peterlin BM. Differential chromatin looping regulates CD4 expression in immature thymocytes. Mol Cell Biol. 2008 Feb 1;28(3):907–12.

399. Levantini E, Lee S, Radomska HS, Hetherington CJ, Alberich-Jorda M, Amabile G, et al. RUNX1 regulates the CD34 gene in haematopoietic stem cells by mediating interactions with a distal regulatory element. EMBO J. 2011;30:4059–70.

400. Barutcu AR, Hong D, Lajoie BR, McCord RP, van Wijnen AJ, Lian JB, et al. RUNX1 contributes to higher-order chromatin organization and gene regulation in breast cancer cells. Biochim Biophys Acta - Gene Regul Mech. 2016 Nov 1;1859(11):1389–97.

401. Dixon JR, Jung I, Selvaraj S, Shen Y, Antosiewicz-Bourget JE, Lee AY, et al. Chromatin architecture reorganization during stem cell differentiation. Nature. 2015 Feb 18;518(7539):331–6.

402. Dixon JR, Selvaraj S, Yue F, Kim A, Li Y, Shen Y, et al. Topological domains in mammalian genomes identified by analysis of chromatin interactions. Nature. 2012 Apr 11;485(7398):376–80.

403. Phillips-Cremins JE, Sauria MEG, Sanyal A, Gerasimova TI, Lajoie BR, Bell JSK, et al. Architectural Protein Subclasses Shape 3D Organization of Genomes during Lineage Commitment. Cell. 2013 Jun 6;153(6):1281–95.

404. Apostolou E, Ferrari F, Walsh RM, Bar-Nur O, Stadtfeld M, Cheloufi S, et al.

Genome-wide Chromatin Interactions of the Nanog Locus in Pluripotency, Differentiation, and Reprogramming. Cell Stem Cell. 2013 Jun 6;12(6):699–712.

405. Van de Walle I, De Smet G, De Smedt M, Vandekerckhove B, Leclercq G, Plum J, et al. An early decrease in Notch activation is required for human TCR-alphabeta lineage differentiation at the expense of TCR-gammadelta T cells. Blood. 2009 Mar 26;113(13):2988–98.

406. Peng Z, Tang H, Wang X, Zhou C, Fan J, Wang L, et al. Inhibition of the growth and metastasis of human colon cancer by restoration of RUNX3 expression in cancer cells. Int J Oncol. 2008 Nov;33(5):979–84.

407. Ito K, Inoue K, Bae S-C, Ito Y. Runx3 expression in gastrointestinal tract epithelium: resolving the controversy. Oncogene. 2009 Mar 26;28(10):1379–84.

408. Soong R, Shah N, Peh BK, Chong PY, Ng SS, Zeps N, et al. The expression of RUNX3 in colorectal cancer is associated with disease stage and patient outcome. Br J Cancer. 2009 Mar 17;100(5):676–9.

409. Whittle MC, Izeradjene K, Rani PG, Feng L, Carlson MA, DelGiorno KE, et al. RUNX3 Controls a Metastatic Switch in Pancreatic Ductal Adenocarcinoma. Cell. 2015 Jun 4;161(6):1345–60.

410. Klunker S, Chong MMW, Mantel P-Y, Palomares O, Bassin C, Ziegler M, et al. Transcription factors RUNX1 and RUNX3 in the induction and suppressive function of Foxp3+ inducible regulatory T cells. J Exp Med. 2009 Nov 23;206(12):2701–15.

411. Morita K, Suzuki K, Maeda S, Matsuo A, Mitsuda Y, Tokushige C, et al. Genetic regulation of the RUNX transcription factor family has antitumor effects. J Clin Invest. 2017 Jun 30;127(7):2815–28.

412. Kim WY, Sieweke M, Ogawa E, Wee HJ, Englmeier U, Graf T, et al. Mutual activation of Ets-1 and AML1 DNA binding by direct interaction of their autoinhibitory domains. EMBO J. 1999 Mar 15;18(6):1609–20.

413. Gu TL, Goetz TL, Graves BJ, Speck NA. Auto-inhibition and partner proteins, core-binding factor beta (CBFbeta) and Ets-1, modulate DNA binding by CBFalpha2 (AML1). Mol Cell Biol. 2000 Jan 1;20(1):91–103.

414. Soler E, Andrieu-Soler C, de Boer E, Bryne JC, Thongjuea S, Stadhouders R, et al. The genome-wide dynamics of the binding of Ldb1 complexes during erythroid differentiation. Genes Dev. 2010 Feb 1;24(3):277–89.

415. Goyama S, Schibler J, Cunningham L, Zhang Y, Rao Y, Nishimoto N, et al. Transcription factor RUNX1 promotes survival of acute myeloid leukemia cells. J Clin Invest. 2013 Sep 3;123(9):3876–88.

416. Ben-Ami O, Friedman D, Leshkowitz D, Goldenberg D, Orlovsky K, Pencovich N, et al. Addiction of t(8;21) and inv(16) Acute Myeloid Leukemia to Native RUNX1. CellReports. 2013;4:1131–43.

417. Wilkinson AC, Ballabio E, Geng H, North P, Tapia M, Kerry J, et al. RUNX1 Is a Key Target in t(4;11) Leukemias that Contributes to Gene Activation through an AF4-MLL Complex Interaction. Cell Rep. 2013 Jan 31;3(1):116–27.

418. Michaud JL, Wu F, Osato M, Cottles GM, Yanagida M, Asou N, et al. In vitro analyses of known and novel RUNX1/AML1 mutations in dominant familial platelet disorder with predisposition to acute myelogenous leukemia: implications for mechanisms of pathogenesis. Blood . 2002;99(4):1364–72.

419. Bluteau D, Gilles L, Hilpert M, Antony-Debré I, James C, Debili N, et al. Down-regulation of the RUNX1-target gene NR4A3 contributes to hematopoiesis deregulation in familial platelet disorder/acute myelogenous leukemia. Blood. 2011 Dec 8;118(24):6310–20.

420. Antony-Debré I, Duployez N, Bucci M, Geffroy S, Micol J-B, Renneville A, et al. Somatic mutations associated with leukemic progression of familial platelet disorder with predisposition to acute myeloid leukemia. Leukemia. 2016 Apr 28;30(4):999–1002.

421. Schmit JM, Turner DJ, Hromas RA, Wingard JR, Brown RA, Li Y, et al. Two novel RUNX1 mutations in a patient with congenital thrombocytopenia that evolved into a high grade myelodysplastic syndrome. Leuk Res Reports. 2015 Jan 1;4(1):24–7.

422. Sakurai M, Kunimoto H, Watanabe N, Fukuchi Y, Yuasa S, Yamazaki S, et al. Impaired hematopoietic differentiation of RUNX1-mutated induced pluripotent stem cells derived from FPD/AML patients. Leukemia. 2014 Dec 15;28(12):2344–54.

423. Iizuka H, Kagoya Y, Kataoka K, Yoshimi A, Miyauchi M, Taoka K, et al. Targeted gene correction of RUNX1 in induced pluripotent stem cells derived from familial platelet disorder with propensity to myeloid malignancy restores normal megakaryopoiesis. Exp Hematol. 2015 Oct 1;43(10):849–57.

424. Connelly JP, Kwon EM, Gao Y, Trivedi NS, Elkahloun AG, Horwitz MS, et al. Targeted correction of RUNX1 mutation in FPD patient-specific induced pluripotent stem cells rescues megakaryopoietic defects. Blood. 2014 Sep 18;124(12):1926–30.

425. Ouchi-Uchiyama M, Sasahara Y, Kikuchi A, Goi K, Nakane T, Ikeno M, et al. Analyses of Genetic and Clinical Parameters for Screening Patients With Inherited Thrombocytopenia with Small or Normal-Sized Platelets. Pediatr Blood Cancer. 2015 Dec 1;62(12):2082–8.

426. de Wit E, de Laat W. A decade of 3C technologies: insights into nuclear organization. Genes Dev. 2012 Jan 1;26(1):11–24.

427. Blackburn JS, Liu S, Wilder JL, Dobrinski KP, Lobbardi R, Moore FE, et al. Clonal Evolution Enhances Leukemia-Propagating Cell Frequency in T Cell Acute Lymphoblastic Leukemia through Akt/mTORC1 Pathway Activation. Cancer Cell. 2014 Mar 17;25(3):366–78.

428. Hoshii T, Kasada A, Hatakeyama T, Ohtani M, Tadokoro Y, Naka K, et al. Loss of mTOR complex 1 induces developmental blockage in early T-lymphopoiesis and eradicates T-cell acute lymphoblastic leukemia cells. Proc Natl Acad Sci U S A. 2014 Mar 11;111(10):3805–10.

429. Sarbassov DD, Guertin DA, Ali SM, Sabatini DM. Phosphorylation and Regulation of Akt/PKB by the Rictor-mTOR Complex. Science. 2005 Feb 18;307(5712):1098–101.

430. Hua C, Guo H, Bu J, Zhou M, Cheng H, He F, et al. Rictor/mammalian target of rapamycin 2 regulates the development of notch1 induced murine T-cell acute lymphoblastic leukemia via forkhead box O3. Exp Hematol. 2014 Dec 1;42(12):1031–1040.e4.

431. Hoogenkamp M, Lichtinger M, Krysinska H, Lancrin C, Clarke D, Williamson A, et al. Early chromatin unfolding by RUNX1: a molecular explanation for differential requirements during specification versus maintenance of the hematopoietic gene expression program. Blood. 2009 Jul 9;114(2):299–309.

432. Buenrostro JD, Giresi PG, Zaba LC, Chang HY, Greenleaf WJ. Transposition of native chromatin for fast and sensitive epigenomic profiling of open chromatin, DNA-binding proteins and nucleosome position. Nat Methods. 2013 Dec 6;10(12):1213–8.

433. Boyle AP, Davis S, Shulha HP, Meltzer P, Margulies EH, Weng Z, et al. High-Resolution Mapping and Characterization of Open Chromatin across

the Genome. Cell. 2008 Jan 25;132(2):311–22.

434. Kundaje A, Meuleman W, Ernst J, Bilenky M, Yen A, Heravi-Moussavi A, et al. Integrative analysis of 111 reference human epigenomes. Nature. 2015 Feb 18;518(7539):317–30.

435. Deng C, Zhang P, Wade Harper J, Elledge SJ, Leder P. Mice Lacking p21CIP1/WAF1 undergo normal development, but are defective in G1 checkpoint control. Cell. 1995 Aug 25;82(4):675–84.

436. Bai F, Pei X-H, Godfrey VL, Xiong Y. Haploinsufficiency of p18(INK4c) sensitizes mice to carcinogen-induced tumorigenesis. Mol Cell Biol. 2003 Feb 15;23(4):1269–77.

437. Cai X, Gao L, Teng L, Ge J, Oo ZM, Kumar AR, et al. Runx1 Deficiency Decreases Ribosome Biogenesis and Confers Stress Resistance to Hematopoietic Stem and Progenitor Cells. Cell Stem Cell. 2015 Aug 6;17(2):165–77.

438. Ali SA, Zaidi SK, Dacwag CS, Salma N, Young DW, Shakoori AR, et al. Phenotypic transcription factors epigenetically mediate cell growth control. Proc Natl Acad Sci. 2008 May 6;105(18):6632–7.

439. Young DW, Hassan MQ, Pratap J, Galindo M, Zaidi SK, Lee S, et al. Mitotic occupancy and lineage-specific transcriptional control of rRNA genes by Runx2. Nature. 2007 Jan 25;445(7126):442–6.

440. Rada-Iglesias A. Is H3K4me1 at enhancers correlative or causative? Nat Genet. 2018 Jan 22;50(1):4–5.

441. Creyghton MP, Cheng AW, Welstead GG, Kooistra T, Carey BW, Steine EJ, et al. Histone H3K27ac separates active from poised enhancers and predicts developmental state. Proc Natl Acad Sci U S A. 2010 Dec 14;107(50):21931–6.

442. Garnett MJ, Edelman EJ, Heidorn SJ, Greenman CD, Dastur A, Lau KW, et al. Systematic identification of genomic markers of drug sensitivity in cancer cells. Nature. 2012 Mar 29;483(7391):570–5.

443. Tse C, Shoemaker AR, Adickes J, Anderson MG, Chen J, Jin S, et al. ABT-263: A Potent and Orally Bioavailable Bcl-2 Family Inhibitor. Cancer Res. 2008 May 1;68(9):3421–8.

444. Chonghaile TN, Letai A. Mimicking the BH3 domain to kill cancer cells. Oncogene. 2008 Dec 30;27(S1):S149–57.

445. Iorio F, Knijnenburg TA, Vis DJ, Bignell GR, Menden MP, Schubert M, et al. A Landscape of Pharmacogenomic Interactions in Cancer. Cell. 2016 Jul 28;166(3):740–54.

446. Faber AC, Coffee EM, Costa C, Dastur A, Ebi H, Hata AN, et al. mTOR inhibition specifically sensitizes colorectal cancers with KRAS or BRAF mutations to BCL-2/BCL-XL inhibition by suppressing MCL-1. Cancer Discov. 2014 Jan 1;4(1):42–52.

447. Hsieh AC, Costa M, Zollo O, Davis C, Feldman ME, Testa JR, et al. Genetic dissection of the oncogenic mTOR pathway reveals druggable addiction to translational control via 4EBP-eIF4E. Cancer Cell. 2010 Mar 16;17(3):249–61.

448. Mills JR, Hippo Y, Robert F, Chen SMH, Malina A, Lin C-J, et al. mTORC1 promotes survival through translational control of Mcl-1. Proc Natl Acad Sci U S A. 2008 Aug 5;105(31):10853–8.

449. Faber AC, Li D, Song Y, Liang M-C, Yeap BY, Bronson RT, et al. Differential induction of apoptosis in HER2 and EGFR addicted cancers following PI3K inhibition. Proc Natl Acad Sci U S A. 2009 Nov 17;106(46):19503–8.

450. Neumann M, Heesch S, Gökbuget N, Schwartz S, Schlee C, Benlasfer O, et al. Clinical and molecular characterization of early T-cell precursor leukemia: a high-risk subgroup in adult T-ALL with a high frequency of FLT3 mutations. Blood Cancer J. 2012 Jan 27;2(1):e55–e55.

451. Ma M, Wang X, Tang J, Xue H, Chen J, Pan C, et al. Early T-cell precursor leukemia: a subtype of high risk childhood acute lymphoblastic leukemia. Front Med. 2012 Dec 12;6(4):416–20.

452. Inukai T, Kiyokawa N, Campana D, Coustan-Smith E, Kikuchi A, Kobayashi M, et al. Clinical significance of early T-cell precursor acute lymphoblastic leukaemia: results of the Tokyo Children's Cancer Study Group Study L99-15. Br J Haematol. 2012 Feb;156(3):358–65.

453. Allen A, Sireci A, Colovai A, Pinkney K, Sulis M, Bhagat G, et al. Early T-cell precursor leukemia/lymphoma in adults and children. Leuk Res. 2013 Sep;37(9):1027–34.

454. Schrappe M, Valsecchi MG, Bartram CR, Schrauder A, Panzer-Grümayer R, Möricke A, et al. Late MRD response determines relapse risk overall and in subsets of childhood T-cell ALL: results of the AIEOP-BFM-ALL 2000 study. Blood. 2011 Aug 25;118(8):2077–84.

455. Tarafdar A, Michie AM, O ’gorman P. Protein kinase C in cellular transformation: a valid target for therapy? Biochem Soc Trans. 2014;42(6):1556–62.

456. Garg R, Benedetti LG, Abera MB, Wang H, Abba M, Kazanietz MG. Protein kinase C and cancer: what we know and what we do not. Oncogene. 2014 Nov 16;33(45):5225–37.

457. Newton AC. Protein kinase C: structure, function, and regulation. J Biol Chem. 1995 Dec 1;270(48):28495–8.

458. Regala RP, Davis RK, Kunz A, Khoor A, Leitges M, Fields AP. Atypical protein kinase C{iota} is required for bronchioalveolar stem cell expansion and lung tumorigenesis. Cancer Res. 2009 Oct 1;69(19):7603–11.

459. Dann SG, Golas J, Miranda M, Shi C, Wu J, Jin G, et al. p120 catenin is a key effector of a Ras-PKCε oncogenic signaling axis. Oncogene. 2014 Mar 1;33(11):1385–94.

460. Kim J, Choi Y-L, Vallentin A, Hunrichs BS, Hellerstein MK, Peehl DM, et al. Centrosomal PKCbetaII and pericentrin are critical for human prostate cancer growth and angiogenesis. Cancer Res. 2008 Aug 15;68(16):6831–9.

461. Kirchhefer U, Heinick A, König S, Kristensen T, Mü FU, Seidl MD, et al. Protein Phosphatase 2A Is Regulated by Protein Kinase Ca (PKCa)-dependent Phosphorylation of Its Targeting Subunit B56a at Ser 41. J Biol Chem. 2013;289(1):163–76.

462. Wang Z-Y, Chen Z. Acute promyelocytic leukemia: from highly fatal to highly curable. Blood. 2008 Mar 1;111(5):2505–15.

463. Symonds JM, Ohm AM, Carter CJ, Heasley LE, Boyle TA, Franklin WA, et al. Protein kinase C δ is a downstream effector of oncogenic K-ras in lung tumors. Cancer Res. 2011 Mar 15;71(6):2087–97.

464. Regala RP, Weems C, Jamieson L, Khoor A, Edell ES, Lohse CM, et al. Atypical protein kinase C iota is an oncogene in human non-small cell lung cancer. Cancer Res. 2005 Oct 1;65(19):8905–11.

465. Cai H, Smola U, Wixler V, Eisenmann-Tappe I, Diaz-Meco MT, Moscat J, et al. Role of diacylglycerol-regulated protein kinase C isotypes in growth factor activation of the Raf-1 protein kinase. Mol Cell Biol. 1997 Feb;17(2):732–41.

466. Cacace AM, Ueffing M, Philipp A, Han EK, Kolch W, Weinstein IB. PKC

epsilon functions as an oncogene by enhancing activation of the Raf kinase. Oncogene. 1996 Dec 19;13(12):2517–26.

467. Christina L-N, Nikolaus T, Katarzyna W, Thomas G, Michael L, Gottfried B, et al. PKCα and PKCβ cooperate functionally in CD3-induced de novo IL-2 mRNA transcription. Immunol Lett. 2013 Mar;151(1–2):31–8.

468. Thuille N, Wachowicz K, Hermann-Kleiter N, Kaminski S, Fresser F, Lutz-Nicoladoni C, et al. PKCθ/β and CYLD Are Antagonistic Partners in the NFκB and NFAT Transactivation Pathways in Primary Mouse CD3+ T Lymphocytes. Combs C, editor. PLoS One. 2013 Jan 15;8(1):e53709.

469. Baier G. The PKC gene module: molecular biosystematics to resolve its T cell functions. Immunol Rev. 2003 Apr 1;192(1):64–79.

470. Hill KS, Erdogan E, Khoor A, Walsh MP, Leitges M, Murray NR, et al. Protein kinase Cα suppresses Kras-mediated lung tumor formation through activation of a p38 MAPK-TGFβ signaling axis. Oncogene. 2014 Apr 22;33(16):2134–44.

471. Fujii T, García-Bermejo ML, Bernabó JL, Caamaño J, Ohba M, Kuroki T, et al. Involvement of protein kinase C delta (PKCdelta) in phorbol ester-induced apoptosis in LNCaP prostate cancer cells. Lack of proteolytic cleavage of PKCdelta. J Biol Chem. 2000 Mar 17;275(11):7574–82.

472. DeVries TA, Neville MC, Reyland ME. Nuclear import of PKCdelta is required for apoptosis: identification of a novel nuclear import sequence. EMBO J. 2002 Nov 15;21(22):6050–60.

473. Antal CE, Hudson AM, Kang E, Zanca C, Wirth C, Stephenson NL, et al. Cancer-Associated Protein Kinase C Mutations Reveal Kinase's Role as Tumor Suppressor. Cell. 2015 Jan 29;160(3):489–502.

474. Bivona TG, Quatela SE, Bodemann BO, Ahearn IM, Soskis MJ, Mor A, et al. PKC Regulates a Farnesyl-Electrostatic Switch on K-Ras that Promotes its Association with Bcl-Xl on Mitochondria and Induces Apoptosis. Mol Cell. 2006 Feb 17;21(4):481–93.

475. Kamada N, Sakurai M, Miyamoto K, Sanada I, Sadamori N, Fukuhara S, et al. Chromosome abnormalities in adult T-cell leukemia/lymphoma: a karyotype review committee report. Cancer Res. 1992 Mar 15;52(6):1481–93.

476. Takeuchi S, Koike M, Seriu T, Bartram CR, Schrappe M, Reiter A, et al. Frequent loss of heterozygosity on the long arm of chromosome 6:

identification of two distinct regions of deletion in childhood acute lymphoblastic leukemia. Cancer Res. 1998 Jun 15;58(12):2618–23.

477. Hayashi Y, Raimondi S, Look A, Behm F, Kitchingman G, Pui C, et al. Abnormalities of the long arm of chromosome 6 in childhood acute lymphoblastic leukemia. Blood. 1990;76(8):1626–30.

478. Remke M, Pfister S, Kox C, Toedt G, Becker N, Benner A, et al. High-resolution genomic profiling of childhood T-ALL reveals frequent copy-number alterations affecting the TGF-beta and PI3K-AKT pathways and deletions at 6q15-16.1 as a genomic marker for unfavorable early treatment response. Blood. 2009 Jul 30;114(5):1053–62.

479. Sinclair PB, Sorour A, Martineau M, Harrison CJ, Mitchell WA, O'Neill E, et al. A Fluorescence ***in Situ*** Hybridization Map of 6q Deletions in Acute Lymphocytic Leukemia. Cancer Res. 2004 Jun 15;64(12):4089–98.

480. López-Nieva P, Vaquero C, Fernández-Navarro P, González-Sánchez L, Villa-Morales M, Santos J, et al. EPHA7 , a new target gene for 6q deletion in T-cell lymphoblastic lymphomas. Carcinogenesis. 2012 Feb 1;33(2):452–8.